

Supporting Information

Tuning the optical properties of spiro-centered charge-transfer dyes by extending the donor or acceptor Part

Jan S. Wössner, David C. Grenz, Daniel Kratzert and Birgit Esser*

1. Table of contents

1.	Table of contents	S1
2.	Materials and Methods	S4
	Chemicals and Solvents	S4
	Analytical Thin Layer Chromatography (TLC)	S4
	Flash Column Chromatography	S4
	Nuclear Magnetic Resonance Spectroscopy (NMR)	S5
	High-Resolution Mass Spectrometry (HRMS)	S5
	Absorption and Emission Spectroscopy	S5
	Infrared spectroscopy	S5
	Cyclic Voltammetry	S6
	Single Crystal X-Ray Analysis	S6
	Thermal Gravimetric Analysis (TGA) and Differential Scanning Calorimetry (DSC)	S6
3.	Synthetic Manipulations	S7
3.1	Synthesis of 1,3-dimethyl-1,3-dihydrospiro[benzo[<i>d</i>]imidazole-2,2'-indene]-1',3'-dione (3)	S7
3.2	Synthesis of diethyl naphthalene-1,8-diyl dicarbamate (30)	S8
3.3	Synthesis of <i>N</i> ¹ , <i>N</i> ⁸ -Dimethylnaphthalene-1,8-diamine (7)	S9
3.4	Synthesis of 1',3'-Dimethyl-1' <i>H</i> ,3' <i>H</i> -spiro[indene-2,2'-perimidine]-1,3-dione (4) and 1',3'-Dimethyl-1' <i>H</i> ,3' <i>H</i> -spiro[indene-1,2'-perimidine]-2,3-dione (9)	S10
3.5	Synthesis of [1,1'-Biphenyl]-2,2'-diamine (31)	S11
3.6	Synthesis of Diethyl [1,1'-biphenyl]-2,2'-diyl dicarbamate (32)	S12
3.7	Synthesis of <i>N</i> ² , <i>N</i> ^{2'} -Dimethyl-[1,1'-biphenyl]-2,2'-diamine (8)	S13
3.8	Synthesis of 5,7-Dimethyl-5,7-dihydrospiro[dibenzo[<i>d,f</i>][1,3]diazepine-6,2'-indene]-1',3'-dione (5)	S14
3.9	Synthesis of 2,2-dimethyl-1 <i>H</i> -indene-1,3(2 <i>H</i>)-dione (13)	S15
3.10	Synthesis of 2,2-Dimethyl-2,3-dihydro-1 <i>H</i> -perimidine (33)	S16
3.11	Synthesis of 1,2,2,3-Tetramethyl-2,3-dihydro-1 <i>H</i> -perimidine (12)	S17
3.12	Synthesis of 5-Bromo-2,2-dihydroxy-1 <i>H</i> -indene-1,3(2 <i>H</i>)-dione (19)	S18
3.13	Synthesis of 5-Bromo-1',3'-dimethyl-1' <i>H</i> ,3' <i>H</i> -spiro[indene-2,2'-perimidine]-1,3-dione (20)	S19
3.14	Synthesis of 5'-bromo-5,7-dimethyl-5,7-dihydrospiro[dibenzo[<i>d,f</i>][1,3]diazepine-6,2'-indene]-1',3'-dione (21)	S20

3.15	Synthesis of 1',3'-dimethyl-5-(4-(5-phenyl-1,3,4-oxadiazol-2-yl)phenyl)-1 <i>H</i> ,3' <i>H</i> -spiro[indene-2,2'-perimidine]-1,3-dione (14).....	S21
3.16	Synthesis of 4-(1',3'-dimethyl-1,3-dioxo-1,3-dihydro-1 <i>H</i> ,3' <i>H</i> -spiro[indene-2,2'-perimidin]-5-yl)benzotrile (15)	S22
3.17	Synthesis of 5,7-dimethyl-1',3'-dioxo-1',3',5,7-tetrahydrospiro[dibenzo[<i>d,f</i>][1,3]diazepine-6,2'-indene]-5'-carbonitrile (17).....	S23
3.18	Synthesis of 2,3-dihydro-1 <i>H</i> -cyclopenta[<i>b</i>]naphthalen-1-one (25).....	S24
3.19	Synthesis of 2,2-dihydroxy-1 <i>H</i> -cyclopenta[<i>b</i>]naphthalene-1,3(2 <i>H</i>)-dione (26) .	S25
3.20	Synthesis of 1',3'-dimethyl-1 <i>H</i> ,3' <i>H</i> -spiro[cyclopenta[<i>b</i>]naphthalene-2,2'-perimidine]-1,3-dione (16).....	S26
3.21	Synthesis of 2,10-dibromo-5,7-dimethyl-5,7-dihydrospiro[dibenzo[<i>d,f</i>][1,3]diazepine-6,2'-indene]-1',3'-dione (27)	S27
3.22	Synthesis of 2,10-bis(4-(diphenylamino)phenyl)-5,7-dimethyl-5,7-dihydrospiro[dibenzo[<i>d,f</i>][1,3]diazepine-6,2'-indene]-1',3'-dione (29)	S28
4.	Single Crystal X-Ray Diffraction.....	S29
4.1	Growing singles crystals by solvent layering	S29
4.2	Single-crystal structure and packing of 3.....	S30
4.3	Single-crystal structure and packing of 4.....	S33
4.4	Single-crystal structure and packing of 9.....	S36
4.5	Single-crystal structure and packing of 5.....	S39
4.6	Single-crystal structure and packing of 14.....	S42
4.7	Single-crystal structure and packing of 15.....	S45
4.8	Single-crystal structure and packing of 16.....	S48
4.9	Single-crystal structure and packing of 27.....	S51
5.	Photophysical Properties.....	S54
6.	Thermal Measurements	S57
7.	Cyclic Voltammograms	S60
8.	Infrared Spectra	S65
9.	DFT Calculations.....	S69
9.1	Frontier Orbitals.....	S70
9.2	TDDFT Calculations	S71
9.2.1	Charge transfer transitions	S71
9.2.2	Calculated Band gaps	S76

9.2.3	Calculated Absorption Spectra	S78
9.3	Excited State Geometry Optimization	S81
9.4	Total Energies.....	S82
9.5	Cartesian Coordinates of the Calculated Structures.....	S83
10.	NMR Spectra	S91
10.1	NMR Experiments	S91
10.2	Spectra	S92
11.	References	S146

2. Materials and Methods

Chemicals and Solvents

Chemicals and reagents were purchased from Acros-Organics, Alfa-Aesar, ChemPur, Merck, Sigma Aldrich or TCI and used directly without further purification unless otherwise specified. Moisture- or oxygen-sensitive reactions were carried out in dried glassware - heated under vacuum - using standard Schlenk techniques in an anhydrous argon atmosphere (Argon 5.0 from Sauerstoffwerke Friedrichshafen). Anhydrous solvents (THF, toluene, CH₂Cl₂) were obtained from an M. BRAUN solvent purification system (MB-SPS-800) and stored over activated molecular sieves (3 Å) for several days. Benzene and triethylamine were dried over activated molecular sieves (3 Å) for several days. Cyclohexane for column chromatography was purchased in technical grade and purified by distillation under reduced pressure. Other solvents were purchased and used in analytical grade. Neutral Al₂O₃ (Brockmann Activity I) was purchased from Machery-Nagel and used directly without further activation.

Analytical Thin Layer Chromatography (TLC)

Thin layer chromatography was carried out using silica gel-coated aluminium plates with a fluorescence indicator (Merck 60 F₂₅₄). The visualization of spots was achieved using UV light ($\lambda_{\text{max}} = 254 \text{ nm}$ and 366 nm) or a KMnO₄ staining solution (3.0 g KMnO₄, 20 g K₂CO₃, 5.0 mL (5.0%) NaOH, 300 mL H₂O).

Flash Column Chromatography

Column chromatography was carried out using silica gel 60 (grain size 40–63 μm) from Machery-Nagel. Some purifications were performed using a Reveleris X2 flash chromatography instrument by Grace.

Nuclear Magnetic Resonance Spectroscopy (NMR)

NMR spectra were recorded at 300 K using the following spectrometers:

Bruker Avance III HD [300.1 MHz (^1H)], Bruker Avance II [400.1 MHz (^1H), 101.6 MHz (^{13}C)], Bruker Avance III HD [500.3 MHz (^1H), 125.8 MHz (^{13}C)]. Chemical shifts are reported in parts per million (ppm, δ = scale) relative to the signal of tetramethylsilane (δ = 0.00 ppm). ^1H NMR spectra are referenced to tetramethylsilane as an internal standard or the residual solvent signal of the respective solvent: CDCl_3 : δ 7.26 ppm, CD_2Cl_2 : δ 5.32 ppm, $\text{DMSO-}d_6$: δ 2.50 ppm. ^{13}C NMR spectra are referenced to the following signals: CDCl_3 : δ 77.16 ppm, CD_2Cl_2 : δ 54.00 ppm, $\text{DMSO-}d_6$: δ 39.52 ppm.

The following abbreviations for multiplicities were used: singlet (s), broad singlet (br), doublet (d), triplet (t), quartet (q), multiplet (m) and combinations thereof, i.e. doublet of doublets (dd). Coupling constants (J) are given in Hertz [Hz].

High-Resolution Mass Spectrometry (HRMS)

HRMS spectra were measured on a Thermo Fisher Scientific inc. Exactive or LCQ Advantage via electron spray ionization (ESI) or atmospheric pressure chemical ionization (APCI) with an orbitrap analyser.

Absorption and Emission Spectroscopy

Ultraviolet-visible spectra were measured on a Tidas I diode array spectrometer (J&M Analytik) or a Perkin Elmer Lambda 950. Measurements were performed in a 10 mm quartz cuvette.

The emission spectra were measured on a PerkinElmer LS 55 Luminescence spectrometer.

UV/Vis reflectance spectra were recorded with a ThermoScientific Evolution 600 equipped with an integration sphere. The baseline was measured against SUPRASIL[®]. For the measurement, a powdered sample was pressed into a thick pellet inside the sample holder.

Infrared spectroscopy

IR spectra were recorded on a Thermo Scientific Nicolet iS10 FT-IR spectrometer equipped with a diamond ATR unit and are reported in frequency of absorption.

Cyclic Voltammetry

Cyclic voltammograms were measured in solution under an argon atmosphere using a Metrohm Autolab PGSTAT 128N. As working electrodes, a carbon paste electrode or a platinum electrode (2 mm diameter) was used. The spectra are referenced to the ferrocene/ferrocenium (Fc/Fc⁺) redox couple.

Single Crystal X-Ray Analysis

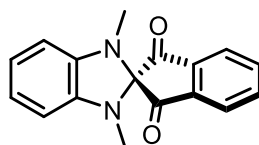
Single Crystal X-Ray Analysis was performed on a BRUKER APEX-II CCD diffractometer. A suitable crystal was selected and mounted on a MiTeGen holder in perfluoroether oil.

Thermal Gravimetric Analysis (TGA) and Differential Scanning Calorimetry (DSC)

For TGA an STA 409 by Netzsch and for DSC a Seiko 6200 by Seiko were used.

3. Synthetic Manipulations

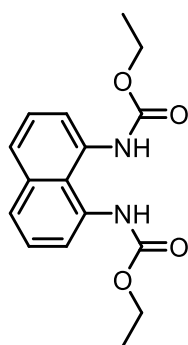
3.1 Synthesis of 1,3-dimethyl-1,3-dihydrospiro[benzo[*d*]imidazole-2,2'-indene]-1',3'-dione (**3**)



The synthesis was performed following a modified procedure by MASLAK *et al.*^[1]

A flame-dried flask was charged with ninhydrin (498 mg, 2.80 mmol, 1.0 eq.), *N*¹,*N*²-dimethylbenzene-1,2-diamine (**6**, 426 mg, 3.13 mmol, 1.1 eq.) and *p*-TsOH · H₂O (25.0 mg, 130 μmol, 11 mol%). The flask was evacuated and backfilled with argon, and degassed anhydrous toluene (50 mL) was added. The reaction mixture was refluxed for 20 h, during which water was azeotropically removed using a *Dean-Stark*-type apparatus. The reaction was allowed to cool to rt and quenched by addition of saturated aqueous NaHCO₃ (30 mL). The layers were separated, and the aqueous layer was extracted with CH₂Cl₂ (5 × 15 mL). The organic extracts were dried over MgSO₄, filtered, and the solvent was removed *in vacuo*. Column chromatography (silica gel, cyclohexane/EtOAc: 1/0 to 1/1) afforded **3** (521 mg, 67%) as a purple solid. *R*_f = 0.45 (cyclohexane/EtOAc: 3/2); ¹H NMR (500 MHz, CDCl₃): δ = 8.11–8.06 (m, 2H), 8.02–7.98 (m, 2H), 6.69–6.66 (m, 2H), 6.34–6.30 (m, 2H), 2.61 (s, 6H); ¹³C NMR (125 MHz, CDCl₃): δ = 198.4, 140.8, 140.8, 137.5, 123.7, 119.5, 104.7, 87.8, 30.9; HRMS (ESI⁺): *m/z* calcd. for C₁₇H₁₅O₂N₂ 279.1128⁺ [M+H]⁺, found 279.1130.

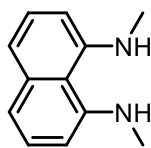
3.2 Synthesis of diethyl naphthalene-1,8-diylldicarbamate (**30**)



The synthesis was carried out following a modified procedure by *IANNUCCI et al.*^[2]

A solution of naphthalene-1,8-diamine (**10**, 1.28 g, 8.09 mmol, 1.0 eq.) in anhydrous CH₂Cl₂ (40 mL) and anhydrous pyridine (5.22 mL, 5.12 g, 64.7 mmol, 8.0 eq.) was cooled to 0 °C. Ethylchloroformate (1.62 mL, 1.84 g, 16.9 mmol, 2.1 eq.) in anhydrous CH₂Cl₂ (20 mL) was added dropwise and the mixture was stirred at rt for 2 h. The reaction mixture was cooled to 0 °C, and aqueous NaOH (1 M, 100 mL) was added. The organic layer was separated, and the aqueous layer was extracted with CH₂Cl₂ (5 × 20 mL). The organic extracts were filtered through a pad of silica gel, which was then rinsed with EtOAc. The filtrate was concentrated under reduced pressure. Recrystallization from CHCl₃ afforded **30** (2.14 g, 95%) as a white fibrous solid. *R*_f = 0.23 (cyclohexane/EtOAc: 1/1); ¹H NMR (500 MHz, DMSO-*d*₆): δ = 9.16 (s, 2H), 7.80 (dd, *J* = 8.0, 1.5 Hz, 2H), 7.51 (d, *J* = 7.4 Hz, 2H), 7.49–7.43 (m, 2H), 4.09 (q, *J* = 7.1 Hz, 4H), 1.23 (t, *J* = 7.1 Hz, 6H); ¹³C NMR (126 MHz, DMSO-*d*₆): δ = 154.6, 135.5, 132.9, 126.4, 125.5, 124.1, 123.8, 60.4, 14.5; HRMS (ESI⁺): *m/z* calcd. for C₁₆H₁₈O₄N₂Na⁺ 325.1159 [M+Na]⁺, found 303.1164.

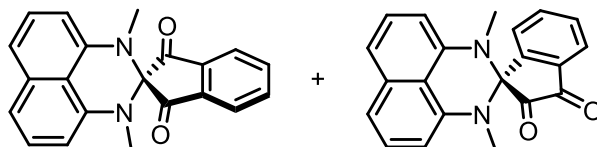
3.3 Synthesis of *N*¹,*N*⁸-Dimethylnaphthalene-1,8-diamine (**7**)



The synthesis was carried out following a modified procedure by *IANNUCCI et al.*^[2]

A suspension of diethyl naphthalene-1,8-diyldicarbamate (**30**, 4.98 g, 16.5 mmol, 1.0 eq.) in degassed and anhydrous THF (50 mL) was cooled to 0 °C. LiAlH₄ (3.75 g, 98.8 mmol, 6.0 eq.) was added in small portions. The suspension was refluxed for 5 h under an argon atmosphere. The reaction mixture was cooled to 0 °C and diluted by addition of CHCl₃ (60 mL). The reaction was quenched by the addition of H₂O (400 mL). The organic layer was separated, and the aqueous layer was extracted with CH₂Cl₂ (5 × 30 mL). The organic extracts were dried over MgSO₄, filtered, and the solvent was removed *in vacuo*. Column chromatography (silica gel, cyclohexane/EtOAc: 1/0 to 9/1) afforded **7** (2.51 g, 82%) as a white crystalline solid. *R*_f = 0.52 (cyclohexane/EtOAc: 9/1); ¹H NMR (400 MHz, CDCl₃): δ = 7.27 (dd, *J* = 8.2, 7.5 Hz, 2H), 7.21 (dd, *J* = 8.3, 1.2 Hz, 2H), 6.60 (dd, *J* = 7.5, 1.3 Hz, 2H), 5.76 (br, 2H), 2.87 (s, 6H); ¹³C NMR (101 MHz, CDCl₃): δ = 147.2, 136.7, 126.3, 117.1, 119.3, 107.1, 32.4; HRMS (APCI+): *m/z* calcd. for C₁₂H₁₅N₂⁺ 187.1230 [M+H]⁺, found 187.1229.

3.4 Synthesis of 1',3'-Dimethyl-1'H,3'H-spiro[indene-2,2'-perimidine]-1,3-dione (**4**) and 1',3'-Dimethyl-1'H,3'H-spiro[indene-1,2'-perimidine]-2,3-dione (**9**)



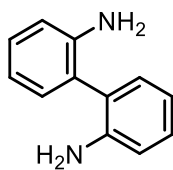
The synthesis was performed following a modified procedure by MASLAK *et al.*^[1]

A flame-dried flask was charged with ninhydrin (1.57 g, 8.43 mmol, 1.0 eq.), *N*¹,*N*⁸-dimethylnaphthalene-1,8-diamine (**7**, 1.65 g, 9.27 mmol, 1.1 eq.) and *p*-TsOH · H₂O (80.2 mg, 421 μmol, 5 mol%). The flask was evacuated and backfilled with argon, and degassed anhydrous toluene (60 mL) was added. The reaction mixture was refluxed for 20 h, during which water was azeotropically removed using a *Dean-Stark*-type apparatus. The reaction was allowed to cool to rt and quenched by addition of saturated aqueous NaHCO₃ (50 mL). The layers were separated, and the aqueous layer was extracted with CH₂Cl₂ (5 × 20 mL). The organic extracts were dried over MgSO₄, filtered, and the solvent was removed *in vacuo*. Column chromatography (silica gel, cyclohexane/EtOAc: 1/0 to 4/1) afforded **4** (2.05 g, 64%) as ruby-red and **9** (278 mg, 9%) as purple needles.

Analytical data for **4**: *R*_f = 0.54 (cyclohexane/EtOAc: 3/2); ¹H NMR (400 MHz, CDCl₃): δ = 8.06–7.95 (m, 4H), 7.41–7.27 (m, 4H), 6.64 (dd, *J* = 7.5, 1.2 Hz, 2H), 2.80 (s, 6H); ¹³C NMR (126 MHz, CD₂Cl₂): δ = 199.9, 141.6, 140.9, 137.9, 133.9, 127.3, 123.8, 119.3, 113.4, 105.4, 77.4, 34.8; HRMS (ESI⁺): *m/z* calcd. for C₂₁H₁₇O₂N₂⁺ 329.1285 [M+H]⁺, found 329.1286.

Analytical data for **9**: *R*_f = 0.62 (cyclohexane/EtOAc: 3/2); ¹H NMR (500 MHz, CDCl₃) δ = 8.08 (ddd, *J* = 7.7, 1.1, 1.1 Hz, 1H), 7.92 (ddd, *J* = 7.6, 7.6, 1.3 Hz, 1H), 7.74 (ddd, *J* = 8.6, 7.6, 1.0 Hz, 2H), 7.44–7.35 (m, 4H), 6.66 (dd, *J* = 7.4, 1.2 Hz, 2H), 2.63 (s, 6H); ¹³C NMR (126 MHz, CDCl₃): δ = 205.8, 184.4, 149.4, 141.2, 139.7, 139.1, 133.6, 131.3, 127.4, 127.0, 124.8, 119.6, 112.8, 105.6, 74.8, 34.9; HRMS (ESI⁺): *m/z* calcd. for C₂₁H₁₇O₂N₂⁺ 329.1285 [M+H]⁺, found 329.1286.

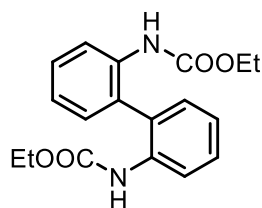
3.5 Synthesis of [1,1'-Biphenyl]-2,2'-diamine (**31**)



The synthesis was carried out following a modified procedure by *IANNUCCI et al.*^[2]

To a solution of 2,2'-dinitro-1,1'-biphenyl (**11**, 4.95 g, 20.2 mmol, 1.0 eq.) in EtOH (10 mL) was added conc. HCl (60 mL). Tin powder (16.7 g, 141 mmol, 6.9 eq.) was added in small portions. The reaction mixture was refluxed for 4 h and then allowed to cool to rt. The reaction mixture was cooled to 0 °C, diluted with CH₂Cl₂ (50 mL) and treated with sat. aq. NaOH until pH 7 was reached. The reaction mixture was extracted with CH₂Cl₂ (4 × 50 mL) and the combined organic layers were dried over MgSO₄ and filtered. The solvent was removed *in vacuo*. Column chromatography (silica gel, cyclohexane/EtOAc: 4/1 to 1/1) afforded **31** (3.59 g, 96%) as a light-yellow solid. *R_f* = 0.18 (cyclohexane/EtOAc: 4/1); ¹H NMR (400 MHz, CDCl₃): δ = 7.17 (ddd, *J* = 8.0, 7.3, 1.6 Hz, 2H), 7.11 (dd, *J* = 7.6, 1.4 Hz, 2H), 6.82 (ddd, *J* = 7.4, 7.4, 1.2 Hz, 2H), 6.76 (dd, *J* = 8.2, 0.9 Hz, 2H), 3.61 (br, 4H); ¹³C NMR (101 MHz, CDCl₃): δ = 144.1, 131.0, 128.8, 124.6, 118.8, 115.5; HRMS (ESI+): *m/z* calcd. for C₁₂H₁₃N₂ 185.1073⁺ [M+H]⁺, found 185.1073.

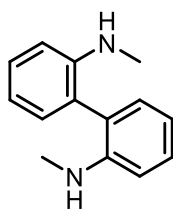
3.6 Synthesis of Diethyl [1,1'-biphenyl]-2,2'-diylidicarbamate (**32**)



The synthesis was carried out following a modified procedure by *IANNUCCI et al.*^[2]

A solution of [1,1'-biphenyl]-2,2'-diamine (**31**, 993 mg, 5.39 mmol, 1.0 eq.) in anhydrous CH₂Cl₂ (25 mL) and anhydrous pyridine (20 mL) was cooled to 0 °C. Ethylchloroformate (1.60 mL, 1.82 g, 16.8 mmol, 3.1 eq.) was added dropwise, and the mixture was stirred at rt for 26 h. The reaction mixture was cooled to 0 °C, and aqueous NaOH (2 M, 20 mL) was added. The organic layer was separated, and the aqueous layer was extracted with CH₂Cl₂ (4 × 10 mL). The organic extracts were dried over MgSO₄, filtered, and the solvent was removed *in vacuo*. Column chromatography (silica gel, cyclohexane/EtOAc: 9/1 to 4/1) afforded **32** (1.74 g, 98%) as a white solid. *R*_f = 0.71 (cyclohexane/EtOAc: 4/1); ¹H NMR (400 MHz, CDCl₃): δ = 8.20 (d, *J* = 8.4 Hz, 2H), 7.47–7.40 (m, 2H), 7.17–7.15 (m, 4H), 6.31 (br, 2H), 4.13 (q, *J* = 7.1 Hz, 4H), 1.23 (t, *J* = 7.1 Hz, 6H); ¹³C NMR (101 MHz, CDCl₃): δ = 153.5, 136.1, 130.4, 129.63, 126.4, 123.7, 120.1, 61.3, 14.4; HRMS (ESI+): *m/z* calcd. for C₁₈H₂₁O₄N₂⁺ 329.1496 [M+H]⁺, found 329.1495.

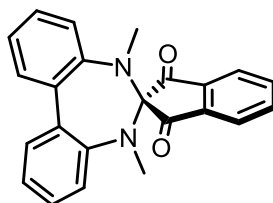
3.7 Synthesis of *N*²,*N*^{2'}-Dimethyl-[1,1'-biphenyl]-2,2'-diamine (**8**)



The synthesis was carried out following a modified procedure by *IANNUCCI et al.*^[2]

A solution of diethyl-[1,1'-biphenyl]-2,2'-diyldicarbamate (**32**, 1.07 g, 3.26 mmol, 1.0 eq.) in anhydrous THF (40 mL) was cooled to 0 °C. LiAlH₄ (1.87 g, 25.9 mmol, 15.1 eq.) was added in small portions. The suspension was refluxed for 5 h and then allowed to cool to rt. The suspension was stirred for 12 h. The reaction mixture was cooled to 0 °C and diluted by addition of CHCl₃ (40 mL). The reaction was quenched by the addition of H₂O (100 mL). The organic layer was separated, and the aqueous layer was extracted with CH₂Cl₂ (5 × 30 mL). The organic extracts were dried over MgSO₄, filtered, and the solvent was removed *in vacuo*. Column chromatography (silica gel, cyclohexane/EtOAc: 10/1) afforded **8** (617 mg, 89%) as a white solid. *R*_f = 0.75 (cyclohexane/EtOAc: 9/1); ¹H NMR (400 MHz, CDCl₃): δ = 7.38–7.32 (m, 2H), 7.14–7.12 (m, 2H), 6.86–6.81 (m, 2H), 6.77 (d, *J* = 8.1, 2H), 3.79 (br, 2H), 2.84 (s, 6H); ¹³C NMR (101 MHz, CDCl₃): δ = 147.1, 130.9, 129.2, 124.1, 117.1, 110.0, 30.8; HRMS (ESI+): *m/z* calcd. for C₁₄H₁₇N₂⁺ 213.1386 [M+H]⁺, found 213.1387.

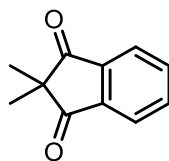
3.8 Synthesis of 5,7-Dimethyl-5,7-dihydrospiro[dibenzo[*d,f*][1,3]diazepine-6,2'-indene]-1',3'-dione (5)



The synthesis was performed following a modified procedure by MASLAK *et al.*^[1]

A flame-dried flask was charged with ninhydrin (675 mg, 3.79 mmol, 1.1 eq.), *N*²,*N*^{2'}-dimethyl-[1,1'-biphenyl]-2,2'-diamine (**8**, 732 mg, 3.45 mmol, 1.0 eq.) and *p*-TsOH · H₂O (26.2 mg, 13.8 μmol, 3 mol%). The flask was evacuated and backfilled with argon, and degassed anhydrous toluene (40 mL) was added. The reaction mixture was refluxed for 20 h, during which water was azeotropically removed using a *Dean-Stark*-type apparatus. The reaction was allowed to cool to rt and quenched by addition of sat. aq. NaHCO₃ (30 mL). The layers were separated, and the aqueous layer was extracted with CH₂Cl₂ (5 × 20 mL). The organic extracts were dried over MgSO₄, filtered, and the solvent was removed *in vacuo*. Column chromatography (silica gel, cyclohexane/EtOAc: 1/0 to 1/1) afforded **5** (991 mg, 81%) as an orange solid. *R*_f = 0.55 (cyclohexane/EtOAc: 3/2); ¹H NMR (400 MHz, DMSO-*d*₆): δ = 8.18–8.02 (m, 4H), 7.38–7.31 (m, 4H), 7.23 (ddd, *J* = 7.4, 7.4, 1.2 Hz, 2H), 7.11 (dd, *J* = 7.9, 1.2 Hz, 2H), 2.41 (s, 6H); ¹³C NMR (101 MHz, CDCl₃): δ = 200.8, 145.6, 139.5, 137.1, 136.6, 128.4, 128.2, 125.0, 123.1, 121.7, 91.0, 37.0; HRMS (ESI+): *m/z* calcd. for C₂₁H₁₉O₂N₂⁺ 355.1441 [M+H]⁺, found 355.1443.

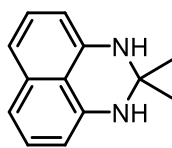
3.9 Synthesis of 2,2-dimethyl-1*H*-indene-1,3(2*H*)-dione (**13**)



The synthesis was performed following a modified procedure by KISTEMAKER *et al.*^[3]

To a solution of 1*H*-indene-1,3(2*H*)-dione (547 mg, 3.74 mmol, 1.0 eq.) and iodomethane (1.17 mL, 2.66 g, 18.7 mmol, 5.0 eq.) in anhydrous acetonitrile (20 mL) was added K₂CO₃ (2.07 g, 15.0 mmol, 4.0 eq.). The reaction mixture was stirred at rt for 2 d. H₂O (100 mL) and CH₂Cl₂ (20 mL) were added, and the reaction mixture was stirred for another 5 min. The organic layer was separated, and the aqueous layer was extracted with CH₂Cl₂ (4 × 15 mL). The combined organic layers were dried over MgSO₄, filtered and concentrated under reduced pressure. Column chromatography (silica gel, cyclohexane/CH₂Cl₂: 1/0 to 0/1) afforded **13** (627 mg, 96%) as a white solid. *R*_f = 0.21 (cyclohexane/CH₂Cl₂: 1/1); ¹H NMR (400 MHz, CDCl₃): δ = 8.01–7.95 (m, 2H), 7.88–7.82 (m, 2H), 1.29 (s, 6H); ¹³C NMR (101 MHz, CDCl₃): δ = 204.6, 140.5, 135.9, 123.8, 50.0, 20.4; HRMS (ESI⁺): *m/z* calcd. for C₁₁H₁₁O₂⁺ 175.0754 [M+H]⁺, found 175.0754.

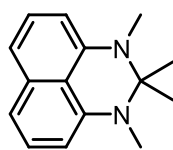
3.10 Synthesis of 2,2-Dimethyl-2,3-dihydro-1H-perimidine (33)



The synthesis was performed following a modified procedure by OZERYANSKII *et al.*^[4]

Neutral activated Al₂O₃ (31.5 g, 309 mmol, 16.1 eq.) was added in one portion to a solution of naphthalene-1,8-diamine (**10**; 3.05 g, 28.1 mmol, 1.0 eq.) in acetone (70 mL). The suspension was stirred at rt for 18 h. The reaction mixture was filtered through a pad of silica gel, which was then rinsed with acetone (5 × 50 mL), and the filtrate was concentrated under reduced pressure. Recrystallization from *n*-hexane/EtOAc afforded **33** (3.42 g, 90%) as a red solid. *R_f* = 0.23 (cyclohexane/EtOAc: 9/1); ¹H NMR (400 MHz, CDCl₃): δ = 7.21 (dd, *J* = 8.3, 7.3 Hz, 2H), 7.13 (dd, *J* = 8.4, 1.0 Hz, 2H), 6.43 (dd, *J* = 7.3, 1.0 Hz, 2H), 4.11 (br, 2H), 1.44 (s, 6H); ¹³C NMR (101 MHz, CDCl₃): δ = 140.3, 134.6, 127.0, 117.0, 113.0, 105.9, 64.5, 28.8; HRMS (ESI+): *m/z* calcd. for C₁₃H₁₅N₂⁺ 199.1230 [M+H]⁺, found 199.1231.

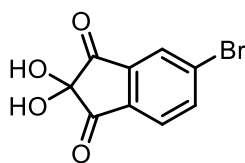
3.11 Synthesis of 1,2,2,3-Tetramethyl-2,3-dihydro-1H-perimidine (**12**)



The synthesis was performed following a modified procedure by OZERYANSKII *et al.*^[4]

To a solution of 2,2-dimethyl-2,3-dihydro-1H-perimidine (**33**, 149 mg, 730 μ mol, 1.0 eq.) in DMF (1 mL), K_2CO_3 (250 mg, 1.81 mmol, 2.4 eq.) and iodomethane (0.2 mL, 456 mg, 3.21 mmol, 4.3 eq.) were added. The reaction mixture was stirred at 75 $^{\circ}C$ for 1 h and then allowed to cool to rt. H_2O (20 mL) and CH_2Cl_2 (20 mL) were added, and the reaction mixture was stirred for a further 15 min. The organic layer was separated, and the aqueous layer was extracted with CH_2Cl_2 (4 \times 10 mL). The combined organic layers were dried over $MgSO_4$, filtered and concentrated under reduced pressure. Column chromatography (silica gel, cyclohexane/ CH_2Cl_2 : 1/0 to 1/1) afforded **12** (141 mg, 83%) as a colorless crystalline solid. R_f = 0.58 (CH_2Cl_2); 1H NMR (400 MHz, $CDCl_3$): δ = 7.32 (dd, J = 8.2, 7.6 Hz, 2H), 7.20 (dd, J = 8.2, 1.0 Hz, 2H), 6.59 (d, J = 7.6 Hz, 2H), 2.94 (s, 6H), 1.39 (s, 6H); ^{13}C NMR (101 MHz, $CDCl_3$): δ = 143.5, 134.2, 126.9, 117.7, 116.2, 106.3, 73.0, 33.5, 22.3; HRMS (ESI+): m/z calcd. for $C_{15}H_{19}N_2^+$ 227.1543 [M+H] $^+$, found 227.1545.

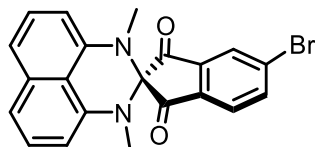
3.12 Synthesis of 5-Bromo-2,2-dihydroxy-1H-indene-1,3(2H)-dione (**19**)



The synthesis was performed following a modified procedure by MARMINON *et al.*^[5]

To a solution of 6-bromo-2,3-dihydro-1H-inden-1-one (**18**, 2.12 g, 10.1 mmol) in acetic acid (25 mL) was added SeO₂ (4.71 g, 42.4 mmol, 4.2 eq.). The yellow suspension was refluxed for 6 h and then allowed to cool to rt. The reaction mixture was filtered through a pad of silica gel, which was then rinsed with acetone (5 × 50 mL). The filtrate was dried over MgSO₄, filtered, and the solvent was removed *in vacuo*. Column chromatography (silica gel, cyclohexane/EtOAc: 20/1 to 3/1) afforded **19** (1.61 g, 62%) as a brown solid. *R*_f = 0.55 (cyclohexane/EtOAc: 1/1); ¹H NMR (400 MHz, DMSO-*d*₆): δ = 8.24–8.19 (m, 2H), 7.94 (dd, *J* = 8.0, 0.9 Hz, 1H), 7.59 (br, 2H); ¹³C NMR (101 MHz, DMSO-*d*₆): δ = 196.0, 195.7, 140.0, 139.8, 137.1, 131.4, 126.6, 125.8, 87.6; HRMS (ESI⁻): *m/z* calcd. for C₉H₄O₄⁸¹Br⁻ 256.9278 [M-H]⁻, found 256.9287.

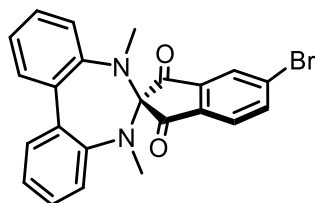
3.13 Synthesis of 5-Bromo-1',3'-dimethyl-1'H,3'H-spiro[indene-2,2'-perimidine]-1,3-dione (20)



The synthesis was performed following a modified procedure by MASLAK *et al.*^[1]

A flame-dried flask was charged with 5-bromo-2,2-dihydroxy-1*H*-indene-1,3(2*H*)-dione (**19**, 102 mg, 400 μ mol, 1.0 eq.), *N*¹,*N*⁸-dimethylnaphthalene-1,8-diamine (**7**, 107 mg, 570 μ mol, 1.5 eq.), and *p*-TsOH \cdot H₂O (12 mg, 60 μ mol, 16 mol%). The flask was evacuated and backfilled with argon, and degassed anhydrous toluene (10 mL) was added. The reaction mixture was refluxed for 7 h, during which water was azeotropically removed using a *Dean-Stark*-type apparatus. The reaction was allowed to cool to rt and quenched by addition of saturated aqueous NaHCO₃ (30 mL). The layers were separated, and the aqueous layer was extracted with CH₂Cl₂ (5 \times 20 mL). The organic extracts were dried over MgSO₄, filtered, and the solvent was removed *in vacuo*. Column chromatography (silica gel, cyclohexane/EtOAc: 1/0 to 2/1) propanol afforded **20** (103 mg, 64%) as a brown solid. R_f = 0.43 (cyclohexane/EtOAc: 4/1); ¹H NMR (400 MHz, DMSO-*d*₆): δ = 8.35 (dd, J = 8.1, 1.8 Hz, 1H), 8.28 (d, J = 1.9 Hz, 1H), 8.01 (d, J = 8.2 Hz, 1H), 7.36 (dd, J = 7.9, 7.9 Hz, 2H), 7.28 (d, J = 8.3 Hz, 2H), 6.67 (d, J = 7.6 Hz, 2H), 2.68 (s, 6H); ¹³C NMR (101 MHz, DMSO-*d*₆): δ = 198.4, 198.3, 140.9, 140.6, 140.4, 138.2, 132.7, 132.7, 126.8, 126.2, 125.2, 118.1, 111.8, 104.6, 76.3, 34.0; HRMS (ESI⁺): m/z calcd. for C₂₁H₁₆O₂N₂⁸¹Br⁺ 409.0369 [M+H]⁺, found 409.0370.

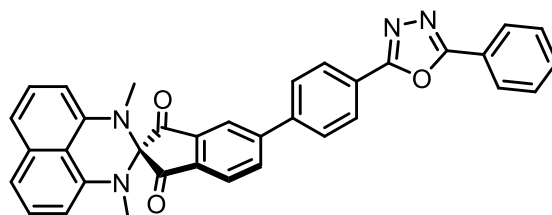
3.14 Synthesis of 5'-bromo-5,7-dimethyl-5,7-dihydrospiro[dibenzo[*d,f*][1,3]diazepine-6,2'-indene]-1',3'-dione (**21**)



The synthesis was performed following a modified procedure by MASLAK *et al.*^[1]

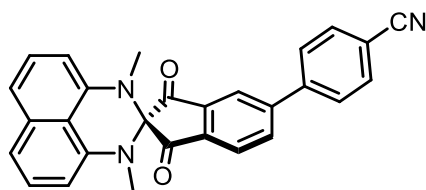
A flame-dried flask was charged with *N*²,*N*^{2'}-dimethyl-[1,1'-biphenyl]-2,2'-diamine (**8**, 473 mg, 2.23 mmol, 1.0 eq.), 5-bromo-2,2-dihydroxy-1*H*-indene-1,3(2*H*)-dione (**19**, 573 mg, 2.28 mmol, 1.0 eq.), and *p*-TsOH · H₂O (21.2 mg, 111 μmol, 5 mol%). The flask was evacuated and backfilled with argon, and degassed anhydrous toluene (15 mL) was added. The reaction mixture was refluxed for 20 h, during which water was azeotropically removed using a *Dean-Stark*-type apparatus. The reaction was allowed to cool to rt and quenched by addition of saturated aqueous NaHCO₃ (50 mL). The layers were separated, and the aqueous layer was extracted with CH₂Cl₂ (5 × 20 mL). The organic extracts were dried over MgSO₄, filtered, and the solvent was removed *in vacuo*. Column chromatography (silica gel, cyclohexane/EtOAc: 1/0 to 4/1) afforded **21** (693 mg, 72%) as a dark orange solid. *R*_f = 0.67 (cyclohexane/EtOAc: 4/1); ¹H NMR (300 MHz, CDCl₃): δ = 8.16 (dd, *J* = 1.8, 0.6 Hz, 1H), 8.07 (dd, *J* = 8.1, 1.8 Hz, 1H), 7.89 (dd, *J* = 8.2, 0.6 Hz, 1H), 7.43–7.34 (m, 4H), 7.31–7.24 (m, 2H), 7.15–7.08 (m, 2H), 2.56 (s, 6H); ¹³C NMR (126 MHz, CD₂Cl₂) δ = 200.6, 145.9, 140.9, 140.8, 138.2, 136.9, 133.3, 128.7, 128.5, 126.5, 125.4, 124.9, 122.0, 91.5, 37.1; HRMS (APCI+): *m/z* calcd. for C₂₃H₁₈O₂N₂⁸¹Br⁺ 435.0526 [M+H]⁺, found 435.0522.

3.15 Synthesis of 1',3'-dimethyl-5-(4-(5-phenyl-1,3,4-oxadiazol-2-yl)phenyl)-1'H,3'H-spiro[indene-2,2'-perimidine]-1,3-dione (**14**)



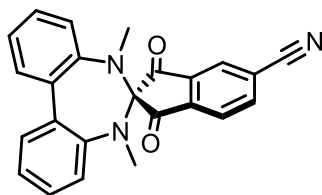
A flame-dried flask was charged with 5-bromo-1',3'-dimethyl-1'H,3'H-spiro[indene-2,2'-perimidine]-1,3-dione (**20**, 25.0 mg, 620 μmol , 1.0 eq.), 2-phenyl-5-(4-(4,4,5,5-tetramethyl-1,3,2-dioxaborolan-2-yl)phenyl)-1,3,4-oxadiazole (**22**, 25.7 mg, 73.9 μmol , 1.2 eq.), K_3PO_4 (41.8 mg, 246 μmol , 4.0 eq.), $\text{Pd}(\text{OAc})_2$ (6.91 mg, 30.8 μmol , 50 mol%) and SPhos (25.3 mg, 69.1 μmol , 1.0 eq.). The flask was evacuated and backfilled with argon and a mixture of degassed toluene (1.8 mL) and H_2O (0.2 mL) was added. The reaction mixture was stirred at 90 °C in a sealed flask for 14 h. After cooling to room temperature, the mixture was filtered over a silica plug and concentrated under reduced pressure. Column chromatography (silica gel, cyclohexane/EtOAc: 1/0 to 1/4) afforded **14** (27.1 mg, 80%) as a dark red solid. $R_f = 0.21$ (cyclohexane/EtOAc: 4/1); $^1\text{H NMR}$ (300 MHz, Chloroform-*d*) δ 8.35 – 8.24 (m, 4H), 8.21 – 8.13 (m, 3H), 7.91 – 7.82 (m, 2H), 7.61 – 7.52 (m, 3H), 7.42 – 7.30 (m, 4H), 6.66 (dd, $J = 7.3, 1.4$ Hz, 2H), 2.86 (s, 6H); HRMS (ESI+): m/z calcd. for $\text{C}_{35}\text{H}_{25}\text{O}_3\text{N}_4^+$ 549.1921 $[\text{M}+\text{H}]^+$, found 549.1923.

3.16 Synthesis of 4-(1',3'-dimethyl-1,3-dioxo-1,3-dihydro-1'H,3'H-spiro[indene-2,2'-perimidin]-5-yl)benzotrile (15)



A flame-dried flask was charged with 5-bromo-1',3'-dimethyl-1'H,3'H-spiro[indene-2,2'-perimidine]-1,3-dione (**20**, 35.0 mg, 86.2 μmol , 1.0 eq.), (4-cyanophenyl)boronic acid (25.3 mg, 172 μmol , 1.0 eq.), K_3PO_4 (54.9 mg, 259 μmol , 3.0 eq.), $\text{Pd}(\text{OAc})_2$ (3.87 mg, 17.2 μmol , 20 mol%) and SPhos (14.2 mg, 34.5 μmol , 40 mol%). The flask was evacuated and backfilled with argon and a mixture of degassed toluene (2 mL) and H_2O (0.5 mL) was added. The reaction mixture was stirred at 95 $^\circ\text{C}$ in a sealed flask for 14 h. After cooling to room temperature, the mixture was filtered over a silica plug and concentrated under reduced pressure. Column chromatography (silica gel, cyclohexane/EtOAc: 1/0 to 4/1) afforded **15** (27.1 mg, 73%) as a red solid. $R_f = 0.19$ (cyclohexane/EtOAc: 4/1); ^1H NMR (500 MHz, CD_2Cl_2) $\delta = 8.23\text{--}8.21$ (m, 2H), 8.16–8.13 (m, 1H), 7.87–7.82 (m, 4H), 7.39 (dd, $J = 8.3, 7.5$ Hz, 2H), 7.33 (dd, $J = 8.3, 1.0$ Hz, 2H), 6.66 (dd, $J = 7.6, 0.9$ Hz, 2H), 2.80 (s, 6H); ^{13}C NMR (126 MHz, CD_2Cl_2) δ 199.7, 199.1, 148.6, 143.1, 141.3, 141.3, 139.99, 140.0, 133.7, 133.5, 128.7, 127.2, 124.5, 122.0, 119.3, 118.6, 113.6, 113.2, 105.3, 77.6, 34.7; HRMS (ESI+): m/z calcd. for $\text{C}_{28}\text{H}_{20}\text{O}_2\text{N}_3^+$ 430.1550 $[\text{M}+\text{H}]^+$, found 430.1550.

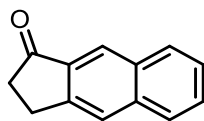
3.17 Synthesis of 5,7-dimethyl-1',3'-dioxo-1',3',5,7-tetrahydrospiro[dibenzo[*d,f*][1,3]diazepine-6,2'-indene]-5'-carbonitrile (**17**)



The synthesis was performed following a modified procedure by *Hahn et al.*^[6]

A flame-dried flask was charged with 5'-bromo-5,7-dimethyl-5,7-dihydrospiro[dibenzo[*d,f*][1,3]diazepine-6,2'-indene]-1',3'-dione (**21**, 394 mg, 0.91 mmol, 1.0 eq.) and copper(I) cyanide (1.63 g, 18.2 mmol, 20 eq.). The flask was evacuated and backfilled with argon and degassed 1-methylpyrrolidin-2-one (6 mL) was added. The reaction mixture was stirred at 95 °C in a sealed flask for 6 d. After cooling to room temperature, the mixture was filtered over a silica plug, which was then rinsed with EtOAc. The solvent was removed *in vacuo*. Column chromatography (silica gel, cyclohexane/EtOAc: 1/0 to 1/1) afforded **17** (232 mg, 67%) as a red solid. $R_f = 0.72$ (cyclohexane/EtOAc: 1/1); $^1\text{H NMR}$ (500 MHz, CD_2Cl_2) $\delta = 8.32$ (dd, $J = 1.4, 0.8$ Hz, 1H), 8.22 (dd, $J = 7.9, 1.5$ Hz, 1H), 8.13 (dd, $J = 7.9, 0.8$ Hz, 1H), 7.44–7.36 (m, 4H), 7.32–7.26 (m, 2H), 7.15–7.06 (m, 2H), 2.53 (s, 6H); $^{13}\text{C NMR}$ (126 MHz, CD_2Cl_2): $\delta = 200.7, 199.8, 145.6, 141.2, 140.5, 139.4, 136.9, 128.8, 128.7, 127.7, 125.6, 124.3, 122.2, 121.0, 117.3, 91.4, 37.1$; HRMS (APCI+): m/z calcd. for $\text{C}_{24}\text{H}_{18}\text{O}_2\text{N}_3^+$ 380.1394 [M+H] $^+$, found 380.1396.

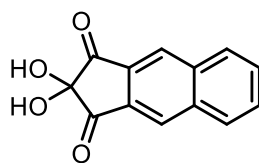
3.18 Synthesis of 2,3-dihydro-1H-cyclopenta[b]naphthalen-1-one (**25**)



The synthesis was performed following a modified procedure by SANDERS *et al.*^[7]

To a solution of 1,2-bis(dibromomethyl)benzene (**24**, 24.7 g, 58.5 mmol, 1.2 eq.) and cyclopent-2-en-1-one (**23**, 4.08 mL, 4.00 g, 48.7 mmol, 1.0 eq.) in anhydrous degassed DMF (150 mL) was added potassium iodide (56.6 g, 341 mmol, 7.0 eq.) in one portion. The reaction mixture was stirred at 85 °C for 20 h under an argon atmosphere. The reaction mixture was allowed to cool to rt and was poured into H₂O (1 L). The reaction mixture was extracted with CH₂Cl₂ (5 × 100 mL). The organic extracts were dried over MgSO₄, filtered, and the solvent was removed *in vacuo*. Column chromatography (silica gel, cyclohexane/EtOAc: 1/0 to 9/1) afforded **25** (6.92 g, 78%) as a slightly yellow solid. *R*_f = 0.42 (cyclohexane/EtOAc: 9/1); ¹H NMR (400 MHz, CDCl₃): δ = 8.33–8.32 (m, 1H), 8.00–7.97 (m, 1H), 7.90–7.83 (m, 2H), 7.58 (ddd, *J* = 8.3, 6.8, 1.3 Hz, 1H), 7.49 (ddd, *J* = 8.2, 6.8, 1.3 Hz, 1H), 3.35–3.28 (m, 2H), 2.84–2.77 (m, 2H); ¹³C NMR (101 MHz, CDCl₃): δ = 207.4, 148.0, 137.3, 134.9, 132.5, 130.5, 128.7, 127.9, 126.2, 125.0, 124.5, 37.1, 25.5; HRMS (APCI+): *m/z* calcd. for C₁₃H₁₁O⁺ 183.0804 [M+H]⁺, found 183.0805.

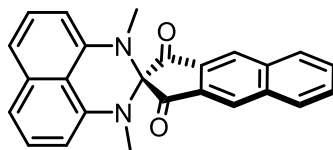
3.19 Synthesis of 2,2-dihydroxy-1H-cyclopenta[*b*]naphthalene-1,3(2*H*)-dione (**26**)



The synthesis was performed following a modified procedure by MARMINON *et al.*^[5]

To a suspension of SeO₂ (4.21 g, 37.9 mmol, 2.2 eq.) in acetic acid (25 mL) was added 2,3-dihydro-1*H*-cyclopenta[*b*]naphthalen-1-one (**25**, 3.14 g, 17.2 mmol, 1.0 eq.). The reaction mixture was refluxed for 4 h and then allowed to cool to rt. The suspension was filtered through a pad of silica gel, which was then rinsed with EtOAc. The solvent was removed *in vacuo*. Column chromatography (silica gel, cyclohexane/EtOAc: 1/0 to 1/1) afforded **26** (2.01 g, 51%) as a dark red solid. *R*_f = 0.47 (cyclohexane/EtOAc: 1/1); ¹H NMR (500 MHz, DMSO-*d*₆): δ = 8.72 (s, 2H), 8.39–8.30 (m, 2H), 7.88–7.81 (m, 2H), 7.54 (s, 2H); ¹³C NMR (126 MHz, DMSO-*d*₆): δ = 197.1, 136.5, 133.5, 130.6, 130.1, 125.3, 88.1; HRMS (APCI⁻): *m/z* calcd. for C₁₃H₆O₃ 210.0322 [M–H₂O]⁻, found 210.0322.

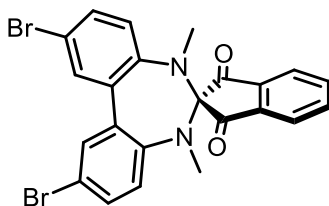
3.20 Synthesis of 1',3'-dimethyl-1'H,3'H-spiro[cyclopenta[*b*]naphthalene-2,2'-perimidine]-1,3-dione (**16**)



The synthesis was performed following a modified procedure by MASLAK *et al.*^[1]

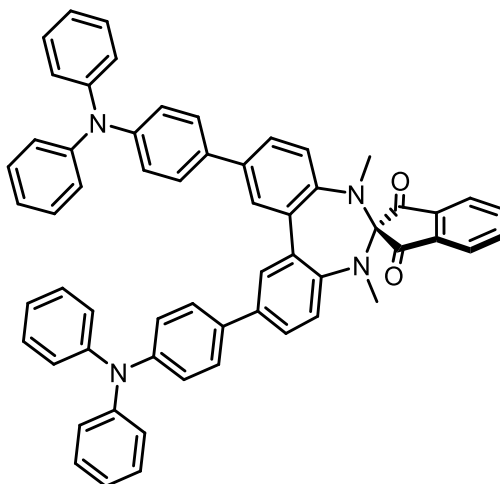
A flame-dried flask was charged with 2,2-dihydroxy-1*H*-cyclopenta[*b*]naphthalene-1,3(2*H*)-dione (**26**, 205 mg, 1.10 mmol, 1.0 eq.), *N*¹,*N*⁸-dimethylnaphthalene-1,8-diamine (**7**, 264 mg, 1.16 mmol, 1.05 eq.), and *p*-TsOH · H₂O (4.01 mg, 44.0 μmol, 4 mol%). The flask was evacuated and backfilled with argon, and degassed anhydrous toluene (20 mL) was added. The reaction mixture was refluxed for 5 h, during which water was azeotropically removed using a *Dean-Stark*-type apparatus. The reaction was allowed to cool to rt and quenched by addition of saturated aqueous NaHCO₃ (30 mL). The layers were separated, and the aqueous layer was extracted with CH₂Cl₂ (5 × 20 mL). The organic extracts were dried over MgSO₄, filtered, and the solvent was removed *in vacuo*. Column chromatography (silica gel, cyclohexane/CH₂Cl₂: 1/0 to 0/1) afforded **16** (263 mg, 63%) as a dark red solid. *R*_f = 0.67 (CH₂Cl₂); ¹H NMR (500 MHz, CDCl₃): δ = 8.59 (s, 2H), 8.20–8.16 (m, 2H), 7.82–7.77 (m, 2H), 7.38 (dd, *J* = 8.3, 7.4 Hz, 2H), 7.32 (dd, *J* = 8.3, 1.1 Hz, 2H), 6.65 (dd, *J* = 7.5, 1.0 Hz, 2H), 2.84 (s, 6H); ¹³C NMR (126 MHz, CDCl₃): δ = 199.6, 141.1, 137.3, 135.3, 133.5, 131.1, 130.6, 126.9, 124.8, 119.3, 113.3, 105.3, 77.7, 34.6; HRMS (ESI+): *m/z* calcd. for C₂₅H₁₉O₂N₂⁺ 379.1441 [M+H]⁺, found 379.1446.

3.21 Synthesis of 2,10-dibromo-5,7-dimethyl-5,7-dihydrospiro[dibenzo[*d,f*][1,3]diazepine-6,2'-indene]-1',3'-dione (**27**)



To a solution of spiro-N-CO compound, **5** (650 mg, 1.83 mmol, 1.0 eq.) in CHCl_3 (10 mL) was added *N*-bromosuccinimide (718 mg, 4.03 mmol, 2.2 eq.) in one portion. The reaction mixture was refluxed for 20 min and then allowed to cool to rt. The reaction was quenched by the addition of H_2O (80 mL). The organic layer was separated, and the aqueous layer was extracted with CH_2Cl_2 (3×20 mL). The organic extracts were dried over MgSO_4 , filtered, and the solvent was removed *in vacuo*. Column chromatography (silica gel, cyclohexane/EtOAc: 1/0 to 4/1) afforded **27** (852 mg, 91%) as a bright orange solid. $R_f = 0.39$ (cyclohexane/EtOAc: 4/1); ^1H NMR (500 MHz, CDCl_3): $\delta = 8.09\text{--}7.91$ (m, 4H), $7.59\text{--}7.40$ (m, 4H), $7.02\text{--}6.98$ (m, 2H), 2.52 (s, 6H); ^{13}C NMR (126 MHz, CDCl_3): $\delta = 200.4, 144.6, 139.4, 137.4, 137.1, 131.6, 131.0, 123.4, 123.2, 118.3, 90.5, 36.9$; HRMS (APCI+): m/z calcd. for $\text{C}_{23}\text{H}_{17}\text{O}_2\text{N}_2^{81}\text{Br}_2^+$ 514.9610 $[\text{M}+\text{H}]^+$, found 514.9608.

3.22 Synthesis of 2,10-bis(4-(diphenylamino)phenyl)-5,7-dimethyl-5,7-dihydrospiro[dibenzo[d,f][1,3]diazepine-6,2'-indene]-1',3'-dione (**29**)



A flame-dried flask was charged with dibromospiro-N-CO compound **27** (223 mg, 440 μ mol, 1.0 eq.), *N,N*-diphenyl-4-(4,4,5,5-tetramethyl-1,3,2-dioxaborolan-2-yl)aniline (649 mg, 1.75 mmol, 4.0 eq.), K_3PO_4 (557 mg, 2.62 mmol, 6.0 eq.), $Pd(OAc)_2$ (9.82 mg, 43.7 μ mol, 10 mol%) and SPhos (35.9 mg, 87.6 μ mol, 20 mol%). The flask was evacuated and backfilled with argon and a mixture of degassed 1,4-dioxane (6 mL) and H_2O (3 mL) was added. The reaction mixture was stirred at 95 $^{\circ}C$ in a sealed flask for 3 d. After cooling to room temperature, the mixture was filtered over a silica plug, which was then rinsed with CH_2Cl_2 . The solvent was removed *in vacuo*. Column chromatography (silica gel, cyclohexane/ CH_2Cl_2 : 1/0 to 1/3) afforded **29** (284 mg, 77%) as an orange-yellow solid. $R_f = 0.53$ ($CHCl_3$); 1H NMR (500 MHz, $CDCl_3$): $\delta = 8.07$ – 8.02 (m, 2H), 7.99–7.94 (m, 2H), 7.65 (d, $J = 2.3$ Hz, 2H), 7.58 (dd, $J = 8.2, 2.3$ Hz, 2H), 7.55–7.49 (m, 4H), 7.29–7.23 (m, 8H), 7.20 (d, $J = 8.3$ Hz, 2H), 7.17–7.10 (m, 12H), 7.02 (m, 4H), 2.62 (s, 6H); ^{13}C NMR (126 MHz, $CDCl_3$): $\delta = 201.1, 147.9, 147.0, 144.5, 139.5, 137.4, 137.2, 136.7, 135.1, 129.4, 127.9, 126.9, 126.5, 124.5, 124.0, 123.1, 123.0, 121.8, 90.9, 37.1$; HRMS (ESI $^-$): m/z calcd. for $C_{59}H_{45}O_4N_4^-$ 873.3446 $[M+H]^-$, found 873.3450.

4. Single Crystal X-Ray Diffraction

4.1 Growing singles crystals by solvent layering



Figure S1: A solution of the spiro compound of **16** in CH_2Cl_2 was layered with methanol or *n*-hexane. The crystals were grown at 268 K.

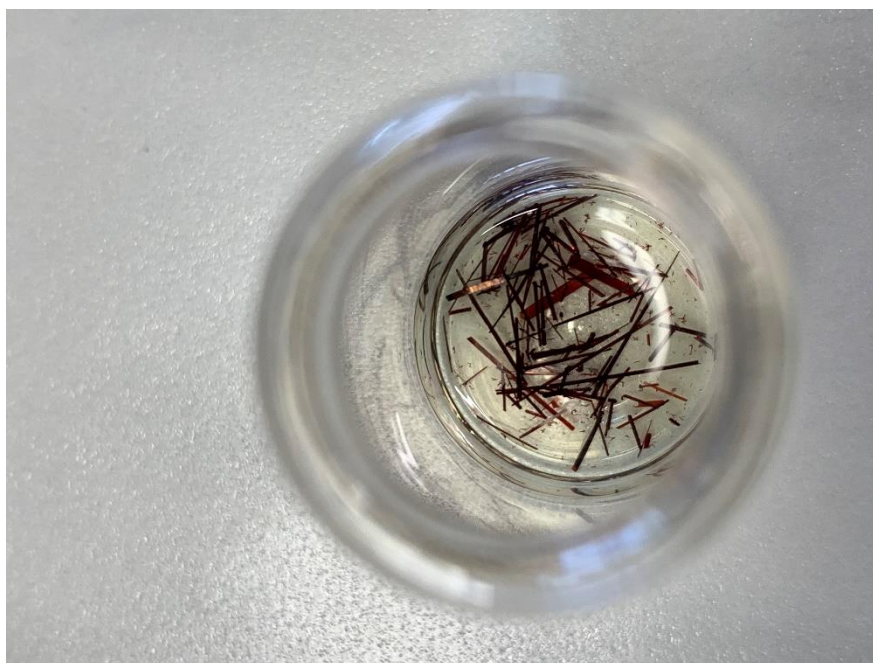
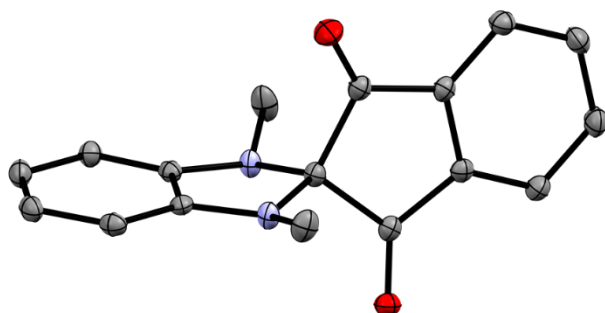


Figure S2: Crystals of **4**.

4.2 Single-crystal structure and packing of **3**

Crystal Data and Experimental



Experimental. Single dark brown block-shaped crystals of **3** were recrystallised from benzene by slow evaporation. A suitable crystal (0.33×0.30×0.14) mm³ was selected and mounted on a MITIGEN holder in perfluoroether oil on a Bruker APEX-II CCD diffractometer. The crystal was kept at $T = 100(2)$ K during data collection. Using **Olex2** (Dolomanov *et al.*, 2009)^[8], the structure was solved with the ShelXT 2014/5 (Sheldrick, 2014) structure solution program, using the direct solution method. The model was refined with version 2016/6 of **XL** (Sheldrick, 2008) using Least Squares minimisation.^[9,10]

Compound	3
CCDC	1570449
Formula	C ₁₇ H ₁₄ N ₂ O ₂
$D_{calc.}/\text{g cm}^{-3}$	1.380
μ/mm^{-1}	0.092
Formula Weight	278.30
Colour	dark brown
Shape	block
Size/mm ³	0.33×0.30×0.14
T/K	100(2)
Crystal System	monoclinic
Space Group	$P2_1/c$
$a/\text{Å}$	8.4028(2)
$b/\text{Å}$	8.4685(2)
$c/\text{Å}$	18.8231(5)
$\alpha/^\circ$	90
$\beta/^\circ$	91.121(2)
$\gamma/^\circ$	90
$V/\text{Å}^3$	1339.18(6)
Z	4
Z'	1
Wavelength/Å	0.710730
Radiation type	MoK α
$\theta_{min}/^\circ$	2.164
$\theta_{max}/^\circ$	27.127
Measured Refl.	19413
Independent Refl.	2963
Reflections Used	2572
R_{int}	0.0273
Parameters	192
Restraints	0
Largest Peak	0.334
Deepest Hole	-0.216
GooF	1.030
wR_2 (all data)	0.0926
wR_2	0.0881
R_1 (all data)	0.0432
R_1	0.0365

A dark brown block-shaped crystal with dimensions $0.33 \times 0.30 \times 0.14 \text{ mm}^3$ was mounted on a MITIGEN holder in perfluoroether oil. X-ray diffraction data were collected using a Bruker APEX-II CCD diffractometer equipped with an Oxford Cryosystems 800 low-temperature device, operating at $T = 100(2) \text{ K}$.

Data were measured using ω and ϕ scans scans of 0.50° per frame for 50.00 s using $\text{MoK}\alpha$ radiation (sealed tube, 0.6 kV, 50 mA). The total number of runs and images was based on the strategy calculation from the program Bruker AKEX2. The maximum resolution achieved was $\Theta = 27.127^\circ$.

Cell parameters were retrieved using the **SAINT** (Bruker, V8.38A, after 2013) software and refined using **SAINT** (Bruker, V8.38A, after 2013) on 8559 reflections, 44 % of the observed reflections. Data reduction was performed using the **SAINT** (Bruker, V8.38A, after 2013) software which corrects for Lorentz polarisation. The final completeness is 100.00 % out to 27.127° in Θ .

A multi-scan absorption correction was performed using SADABS-2016/2 (Bruker,2016/2) was used for absorption correction. $wR_2(\text{int})$ was 0.1494 before and 0.0380 after correction. The Ratio of minimum to maximum transmission is 0.9391. The $\lambda/2$ correction factor is Not present. The absorption coefficient μ of this material is 0.092 mm^{-1} at this wavelength ($\lambda = 0.71073 \text{ \AA}$) and the minimum and maximum transmissions are 0.7001 and 0.7455.

The structure was solved in the space group $P2_1/c$ (# 14) by direct using the ShelXT 2014/5 (Sheldrick, 2014) structure solution program and refined by Least Squares using version 2016/6 of **XL** (Sheldrick, 2008). All non-hydrogen atoms were refined anisotropically. Hydrogen atom positions were calculated geometrically and refined using the riding model.

There is a single molecule in the asymmetric unit, which is represented by the reported sum formula. In other words: Z is 4 and Z' is 1.

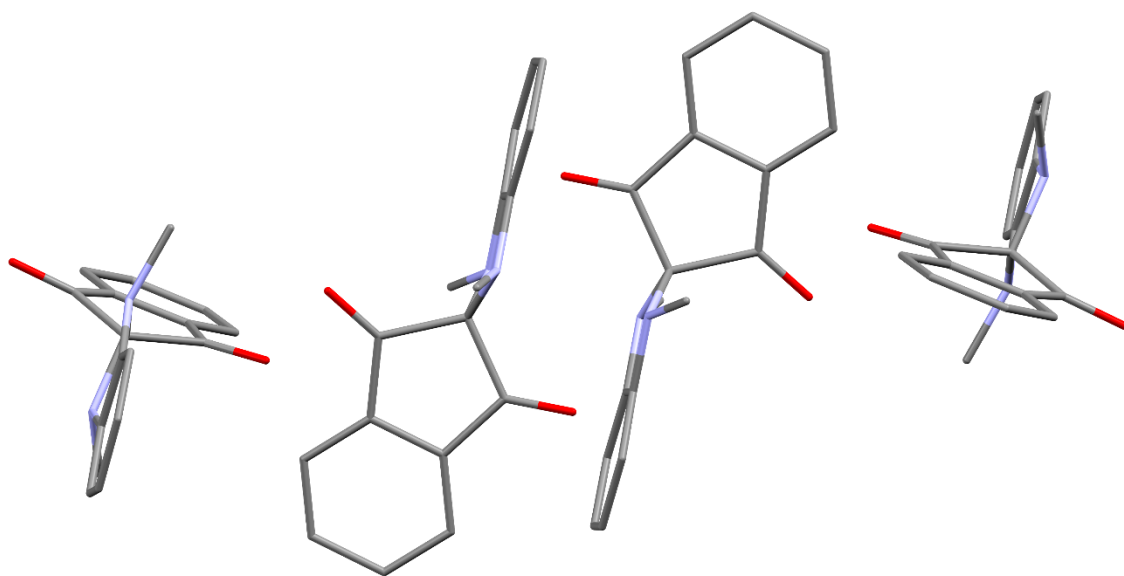
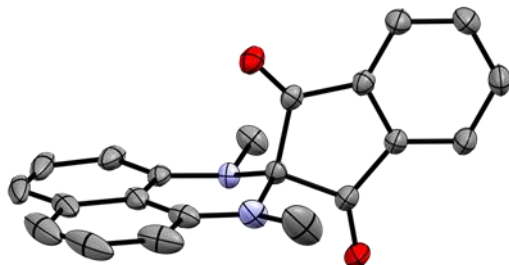


Figure S3: Packing model of **3**.

4.3 Single-crystal structure and packing of **4**

Crystal Data and Experimental



Experimental. Single brown block-shaped crystals of **4** were recrystallised from a mixture of chloroform and *n*-hexane by solvent layering. A suitable crystal (0.37×0.33×0.10) mm³ was selected and mounted on a MITIGEN holder in perfluoroether oil on a Bruker SMART APEX2 area detector diffractometer. The crystal was kept at *T* = 100 K during data collection. Using **Olex2** (Dolomanov et al., 2009), the structure was solved with the **ShelXT** (Sheldrick, 2015) structure solution program, using the Intrinsic Phasing solution method. The model was refined with version 2016/6 of **XL** (Sheldrick, 2008) using Least Squares minimisation.

Compound	4
CCDC	1582940
Formula	C ₂₁ H ₁₆ N ₂ O ₂
<i>D</i> _{calc.} / g cm ⁻³	1.415
μ /mm ⁻¹	0.092
Formula Weight	328.36
Colour	brown
Shape	block
Size/mm ³	0.37×0.33×0.10
<i>T</i> /K	100
Crystal System	orthorhombic
Space Group	Pbca
<i>a</i> /Å	16.5350(7)
<i>b</i> /Å	8.4288(4)
<i>c</i> /Å	22.1228(9)
α /°	90
β /°	90
γ /°	90
<i>V</i> /Å ³	3083.3(2)
<i>Z</i>	8
<i>Z</i> '	1
Wavelength/Å	0.710730
Radiation type	MoK α
θ _{min} /°	1.841
θ _{max} /°	26.458
Measured Refl.	31576
Independent Refl.	3177
Reflections Used	2513
<i>R</i> _{int}	0.0579
Parameters	228
Restraints	261
Largest Peak	0.362
Deepest Hole	-0.420
Goof	1.061
<i>wR</i> ₂ (all data)	0.1519
<i>wR</i> ₂	0.1381
<i>R</i> ₁ (all data)	0.0729
<i>R</i> ₁	0.0557

A brown block-shaped crystal with dimensions 0.37×0.33×0.10 mm³ was mounted on a MITIGEN holder in perfluoroether oil. X-ray diffraction data were collected using a Bruker SMART APEX2 area detector diffractometer equipped with an Oxford Cryosystems 800 low-temperature device, operating at $T = 100$ K.

Data were measured using ω and ϕ scans scans of 0.50 ° per frame for 100.00 s using MoK α radiation (microfocus sealed X-ray tube, 0.6 kV, 50 mA). The total number of runs and images was based on the strategy calculation from the program Bruker APEXII. The maximum resolution achieved was $\theta = 26.458^\circ$.

Cell parameters were retrieved using the **SAINT** (Bruker, V8.38A, after 2013) software and refined using **SAINT** (Bruker, V8.38A, after 2013) on 7705 reflections, 24 % of the observed reflections. Data reduction was performed using the **SAINT** (Bruker, V8.38A, after 2013) software which corrects for Lorentz polarisation. The final completeness is 100.00 % out to 26.458° in θ .

A multi-scan absorption correction was performed using SADABS-2016/2 (Bruker,2016/2) was used for absorption correction. $wR_2(\text{int})$ was 0.1620 before and 0.0701 after correction. The Ratio of minimum to maximum transmission is 0.8273. The $\lambda/2$ correction factor is Not present. The absorption coefficient μ of this material is 0.092 mm⁻¹ at this wavelength ($\lambda = 0.71073\text{\AA}$) and the minimum and maximum transmissions are 0.6167 and 0.7454.

The structure was solved in the space group Pbca (# 61) by Intrinsic Phasing using the **ShelXT** (Sheldrick, 2015) structure solution program and refined by Least Squares using version 2016/6 of **XL** (Sheldrick, 2008). All non-hydrogen atoms were refined anisotropically. Hydrogen atom positions were calculated geometrically and refined using the riding model.

There is a single molecule in the asymmetric unit, which is represented by the reported sum formula. In other words: Z is 8 and Z' is 1.

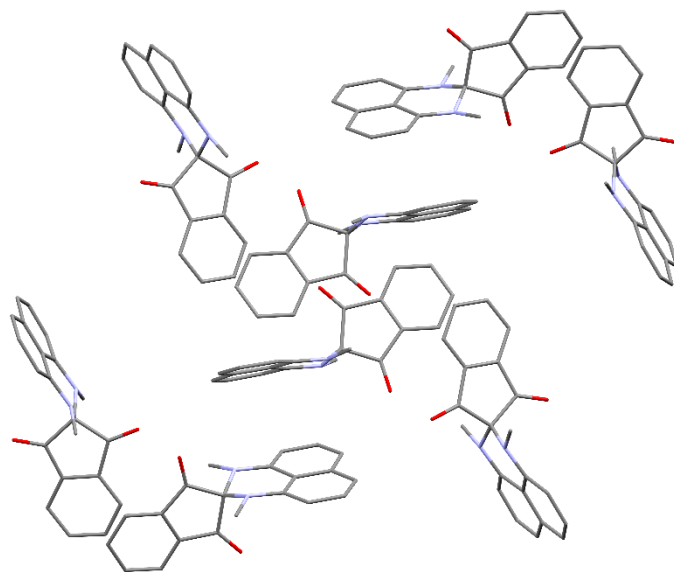
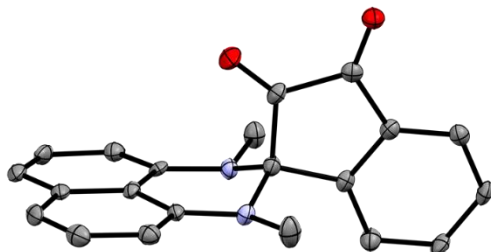


Figure S4: Packing model of **4**.

4.4 Single-crystal structure and packing of **9**

Crystal Data and Experimental



Experimental. Single brown needle-shaped crystals of **9** were recrystallised from CHCl_3 by slow evaporation. A suitable crystal $0.11 \times 0.07 \times 0.03 \text{ mm}^3$ was selected and mounted on a MITIGEN holder in perfluoroether oil on an Bruker SMART APEX2 area detector diffractometer. The crystal was kept at a steady $T = 100(2) \text{ K}$ during data collection. The structure was solved with the **ShelXT** (Sheldrick, 2015) structure solution program using the Intrinsic Phasing solution method and by using **Olex2** (Dolomanov et al., 2009) as the graphical interface. The model was refined with version 2018/3 of **ShelXL** (Sheldrick, 2015) using Least Squares minimisation.

Compound	9
CCDC	1900309
Formula	$\text{C}_{21}\text{H}_{16}\text{N}_2\text{O}_2$
$D_{\text{calc.}} / \text{g cm}^{-3}$	1.405
μ / mm^{-1}	0.092
Formula Weight	328.36
Colour	brown
Shape	needle
Size/ mm^3	$0.11 \times 0.07 \times 0.03$
T / K	100(2)
Crystal System	orthorhombic
Space Group	<i>Pbca</i>
$a / \text{\AA}$	8.899(8)
$b / \text{\AA}$	16.027(13)
$c / \text{\AA}$	21.774(19)
$\alpha / ^\circ$	90
$\beta / ^\circ$	90
$\gamma / ^\circ$	90
$V / \text{\AA}^3$	3105(5)
Z	8
Z'	1
Wavelength/ \AA	0.710730
Radiation type	$\text{MoK}\alpha$
$\theta_{\text{min}} / ^\circ$	1.871
$\theta_{\text{max}} / ^\circ$	25.131
Measured Refl.	58408
Independent Refl.	2769
Reflections with $I > 2\sigma(I)$	>2017
R_{int}	0.1943
Parameters	228
Restraints	0
Largest Peak	0.203
Deepest Hole	-0.292
Goof	1.104
wR_2 (all data)	0.1376
wR_2	0.1251
R_1 (all data)	0.1027
R_1	0.0676

A brown needle-shaped crystal with dimensions 0.11×0.07×0.03 mm³ was mounted on a MITIGEN holder in perfluoroether oil. Data were collected using an Bruker SMART APEX2 area detector diffractometer equipped with an Oxford Cryosystems 800 low-temperature device operating at $T = 100(2)$ K.

Data were measured using ω and ϕ scans using MoK α radiation. The total number of runs and images was based on the strategy calculation from the program **APEX2** (Bruker) The maximum resolution that was achieved was $\theta = 25.131^\circ$ (0.84 Å).

The diffraction pattern was indexed. The total number of runs and images was based on the strategy calculation from the program **APEX2** (Bruker) and the unit cell was refined using **SAINT** (Bruker, V8.38A, after 2013) on 3787 reflections, 6% of the observed reflections.

Data reduction, scaling and absorption corrections were performed using **SAINT** (Bruker, V8.38A, after 2013). The final completeness is 99.90 % out to 25.131° in θ . A multi-scan absorption correction was performed using **SADABS-2016/2** (Bruker,2016/2) was used for absorption correction. $wR_2(\text{int})$ was 0.1541 before and 0.0943 after correction. The Ratio of minimum to maximum transmission is 0.6122. The $\lambda/2$ correction factor is Not present.. The absorption coefficient μ of this material is 0.092 mm⁻¹ at this wavelength ($\lambda = 0.711\text{Å}$) and the minimum and maximum transmissions are 0.456 and 0.745.

The structure was solved and the space group *Pbca* (# 61) determined by the **ShelXT** (Sheldrick, 2015) structure solution program using Intrinsic Phasing and refined by Least Squares using version 2018/3 of **ShelXL** (Sheldrick, 2015). All non-hydrogen atoms were refined anisotropically. Hydrogen atom positions were calculated geometrically and refined using the riding model. Hydrogen atom positions were calculated geometrically and refined using the riding model.

There is a single molecule in the asymmetric unit, which is represented by the reported sum formula. In other words: Z is 8 and Z' is 1.

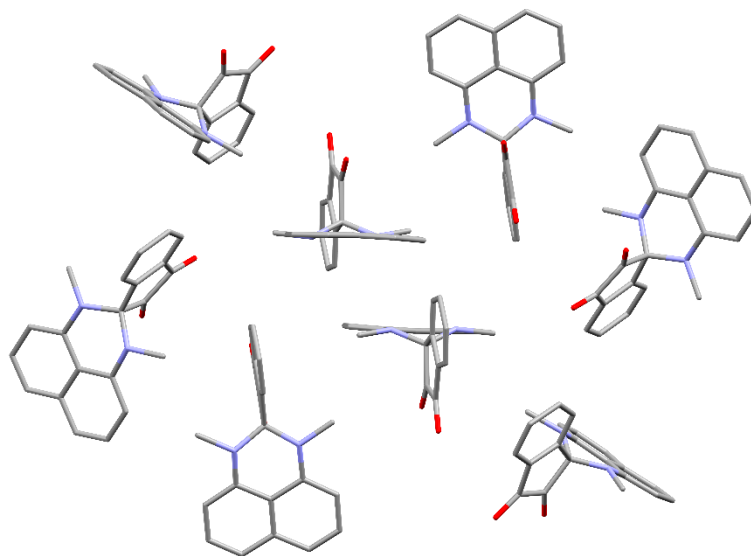
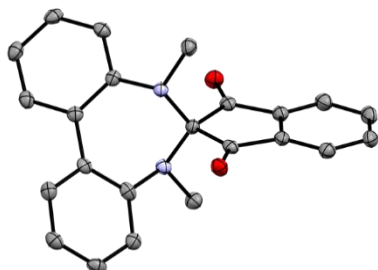


Figure S5: Packing model of 9.

4.5 Single-crystal structure and packing of 5

Crystal Data and Experimental



Experimental. Single orange needle-shaped crystals of **5** were recrystallised from a mixture of CHCl_3 and methanol by solvent layering. A suitable crystal ($0.30 \times 0.05 \times 0.04$) mm^3 was selected and mounted on a MITIGEN holder in perfluoroether oil on an Bruker SMART APEX2 area detector diffractometer. The crystal was kept at $T = 100(2)$ K during data collection. Using **Olex2** (Dolomanov et al., 2009), the structure was solved with the ShelXT 2014/5 (Sheldrick, 2014) structure solution program, using the direct solution method. The model was refined with version 2016/6 of **XL** (Sheldrick, 2008) using Least Squares minimisation.

Compound	5
CCDC	1573404
Formula	$\text{C}_{23}\text{H}_{18}\text{N}_2\text{O}_2$
$D_{\text{calc.}} / \text{g cm}^{-3}$	1.364
μ / mm^{-1}	0.088
Formula Weight	354.39
Colour	orange
Shape	needle
Size/ mm^3	$0.30 \times 0.05 \times 0.04$
T / K	100(2)
Crystal System	orthorhombic
Flack Parameter	0.0(6)
Hooft Parameter	-0.1(6)
Space Group	$\text{Pna}2_1$
$a / \text{\AA}$	28.7181(8)
$b / \text{\AA}$	16.0940(4)
$c / \text{\AA}$	7.4702(2)
$\alpha / ^\circ$	90
$\beta / ^\circ$	90
$\gamma / ^\circ$	90
$V / \text{\AA}^3$	3452.65(16)
Z	8
Z'	2
Wavelength/ \AA	0.710730
Radiation type	$\text{MoK}\alpha$
$\theta_{\text{min}} / ^\circ$	1.418
$\theta_{\text{max}} / ^\circ$	27.502
Measured Refl.	36153
Independent Refl.	7658
Reflections Used	6375
R_{int}	0.0549
Parameters	491
Restraints	1
Largest Peak	0.218
Deepest Hole	-0.228
Goof	1.037
wR_2 (all data)	0.1004
wR_2	0.0946
R_1 (all data)	0.0623
R_1	0.0470

An orange needle-shaped crystal with dimensions 0.30×0.05×0.04 mm³ was mounted on a MITIGEN holder in perfluoroether oil. X-ray diffraction data were collected using a Bruker APEX-II CCD diffractometer equipped with an Oxford Cryosystems 800 low-temperature device, operating at $T = 100(2)$ K.

Data were measured using ω and ϕ scans scans of 0.50 ° per frame for 250.00 s using MoK α radiation (sealed tube, 0.6 kV, 50 mA). The total number of runs and images was based on the strategy calculation from the program APEX2. The maximum resolution achieved was $\theta = 27.502^\circ$.

Cell parameters were retrieved using the **SAINT** (Bruker, V8.38A, after 2013) software and refined using **SAINT** (Bruker, V8.38A, after 2013) on 5756 reflections, 16 % of the observed reflections. Data reduction was performed using the **SAINT** (Bruker, V8.38A, after 2013) software which corrects for Lorentz polarisation. The final completeness is 100.00 % out to 27.502° in θ .

A multi-scan absorption correction was performed using SADABS-2016/2 (Bruker, 2016/2) was used for absorption correction. $wR_2(\text{int})$ was 0.1195 before and 0.0547 after correction. The Ratio of minimum to maximum transmission is 0.9384. The $\lambda/2$ correction factor is Not present. The absorption coefficient μ of this material is 0.088 mm⁻¹ at this wavelength ($\lambda = 0.71073\text{\AA}$) and the minimum and maximum transmissions are 0.6997 and 0.7456.

The structure was solved in the space group Pna2₁ (# 33) by direct using the ShelXT 2014/5 (Sheldrick, 2014) structure solution program and refined by Least Squares using version 2016/6 of **XL** (Sheldrick, 2008). All non-hydrogen atoms were refined anisotropically. Hydrogen atom positions were calculated geometrically and refined using the riding model.

The value of Z' is 2. This means that there are two independent molecules in the asymmetric unit.

The Flack parameter was refined to 0.0(6). Determination of absolute structure using Bayesian statistics on Bijvoet differences using the Olex2 results in -0.1(6). Note: The Flack parameter is used to determine chirality of the crystal studied, the value should be near 0, a value of 1 means that the stereochemistry is wrong and the model should be inverted. A value of 0.5 means that the crystal consists of a racemic mixture of the two enantiomers.

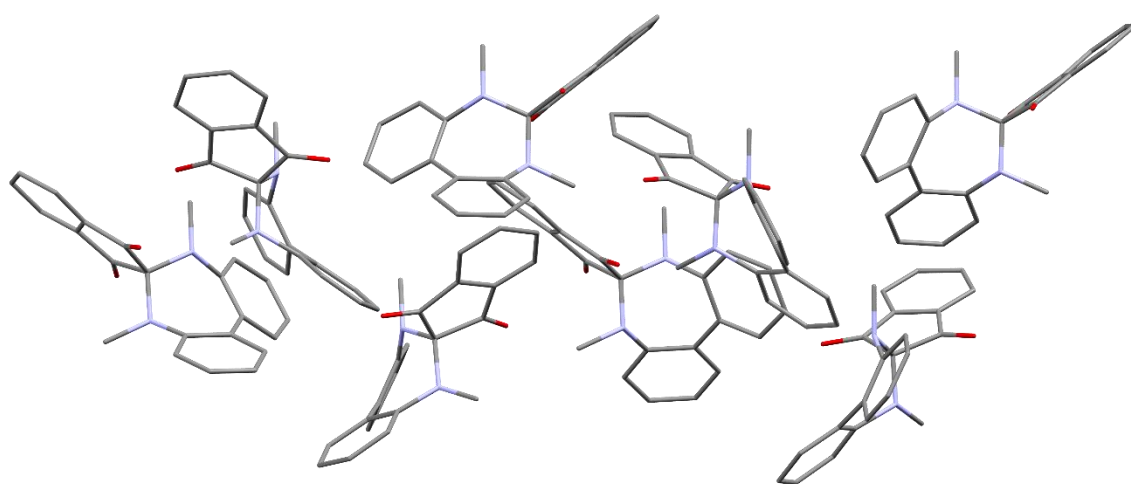
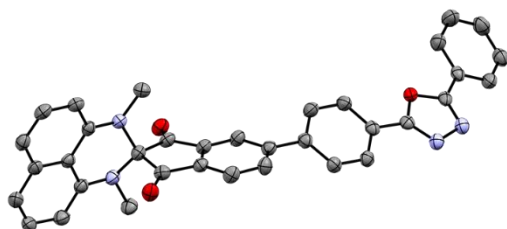


Figure S6: Packing model of 5.

4.6 Single-crystal structure and packing of **14**

Crystal Data and Experimental



Experimental. Single needle-shaped crystals of **14** were recrystallised from a mixture of CHCl₃ and methanol by solvent layering. A suitable crystal 0.11×0.07×0.04 mm³ was selected and mounted on a MITIGEN holder in perfluoroether oil on an Bruker SMART APEX2 area detector diffractometer. The crystal was kept at a steady $T = 100$ K during data collection. The structure was solved with the **ShelXT** (Sheldrick, 2015) structure solution program using the Intrinsic Phasing solution method and by using **Olex2** (Dolomanov et al., 2009) as the graphical interface. The model was refined with version 2018/3 of **XL** (Sheldrick, 2008) using Least Squares minimisation.

Compound	14
CCDC	1851704
Formula	C ₇₀ H ₄₈ N ₈ O ₆
$D_{calc.}/\text{g cm}^{-3}$	1.394
μ/mm^{-1}	0.091
Formula Weight	1097.16
Colour	None None None
Shape	needle
Size/mm ³	0.11×0.07×0.04
T/K	100
Crystal System	monoclinic
Space Group	$P2_1/c$
$a/\text{Å}$	14.7127(13)
$b/\text{Å}$	13.2097(16)
$c/\text{Å}$	27.114(3)
$\alpha/^\circ$	90
$\beta/^\circ$	97.327(9)
$\gamma/^\circ$	90
$V/\text{Å}^3$	5226.6(9)
Z	4
Z'	1
Wavelength/Å	0.710730
Radiation type	MoK α
$\theta_{min}/^\circ$	1.395
$\theta_{max}/^\circ$	25.442
Measured Refl.	80580
Independent Refl.	9634
Reflections with $I > 6571$	
2(I)	
R_{int}	0.0587
Parameters	761
Restraints	0
Largest Peak	0.581
Deepest Hole	-0.193
GooF	1.061
wR_2 (all data)	0.1489
wR_2	0.1316
R_1 (all data)	0.0920
R_1	0.0563

A needle-shaped crystal with dimensions 0.11×0.07×0.04 mm³ was mounted on a MITIGEN holder in perfluoroether oil. Data were collected using a Bruker SMART APEX2 area detector diffractometer equipped with an Oxford Cryosystems 800 low-temperature device operating at $T = 100$ K.

Data were measured using ω and ϕ scans using MoK α radiation. The total number of runs and images was based on the strategy calculation from the program **APEX2** (Bruker) The maximum resolution that was achieved was $\Theta = 25.442^\circ$ (0.83 Å).

The diffraction pattern was indexed. The total number of runs and images was based on the strategy calculation from the program **APEX2** (Bruker) and the unit cell was refined using **SAINT** (Bruker, V8.38A, after 2013) on 9322 reflections, 12% of the observed reflections.

Data reduction, scaling and absorption corrections were performed using **SAINT** (Bruker, V8.38A, after 2013). The final completeness is 99.90 % out to 25.442° in Θ . A multi-scan absorption correction was performed using **SADABS-2016/2** (Bruker,2016/2) was used for absorption correction. $wR_2(\text{int})$ was 0.0875 before and 0.0536 after correction. The Ratio of minimum to maximum transmission is 0.9592. The $\lambda/2$ correction factor is Not present. The absorption coefficient μ of this material is 0.091 mm⁻¹ at this wavelength ($\lambda = 0.711\text{Å}$) and the minimum and maximum transmissions are 0.715 and 0.745.

The structure was solved and the space group $P2_1/c$ (# 14) determined by the **ShelXT** (Sheldrick, 2015) structure solution program using Intrinsic Phasing and refined by Least Squares using version 2018/3 of **XL** (Sheldrick, 2008). All non-hydrogen atoms were refined anisotropically. Hydrogen atom positions were calculated geometrically and refined using the riding model. Hydrogen atom positions were calculated geometrically and refined using the riding model.

There is a single molecule in the asymmetric unit, which is represented by the reported sum formula. In other words: Z is 4 and Z' is 1.

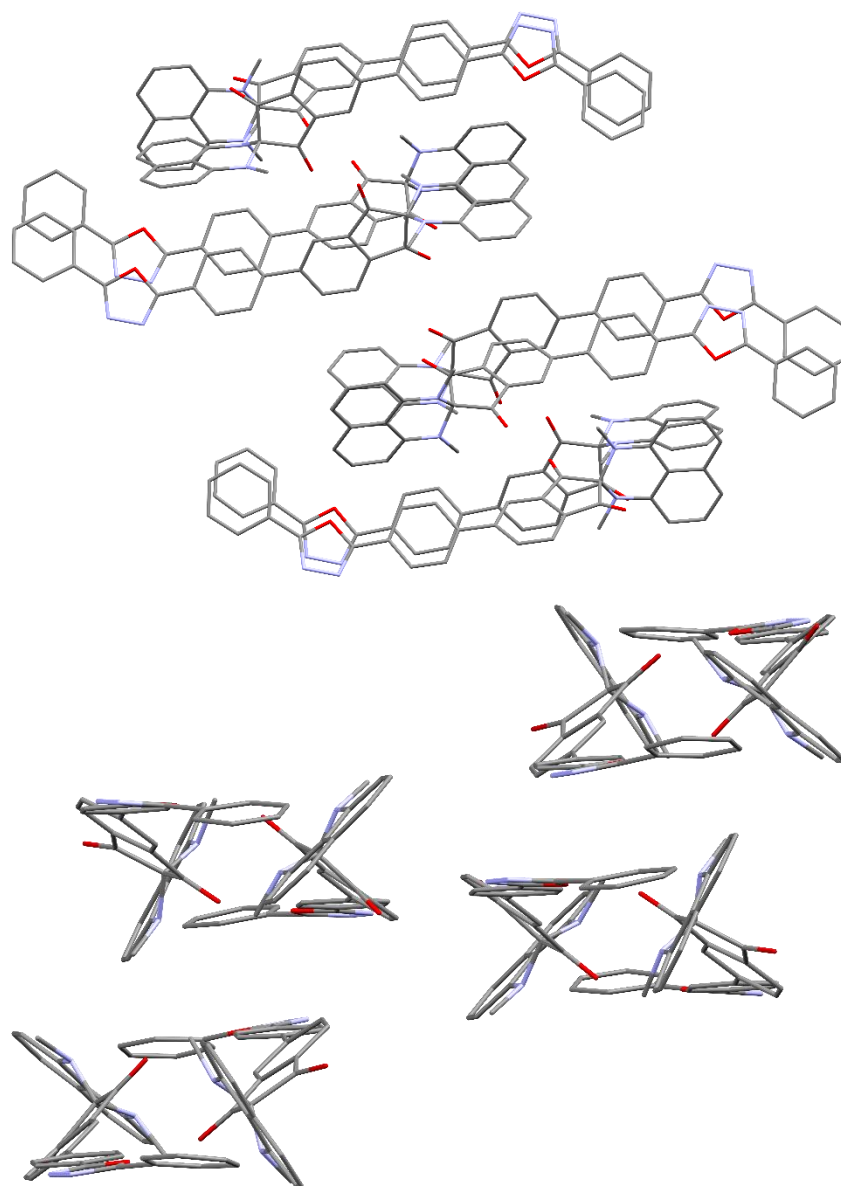
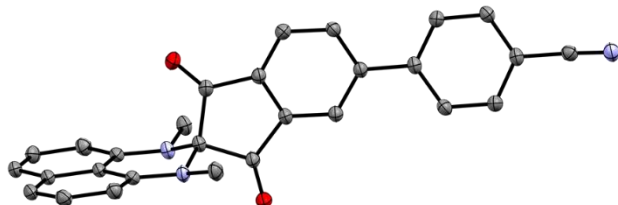


Figure S7: Two views of the packing models of **14**.

4.7 Single-crystal structure and packing of 15

Crystal Data and Experimental



Experimental. Single red plate-shaped crystals of **15** were recrystallised from a mixture of CHCl_3 and methanol by solvent layering. A suitable crystal $0.17 \times 0.13 \times 0.09 \text{ mm}^3$ was selected and mounted on a MITIGEN holder in perfluoroether oil on a Bruker SMART APEX2 area detector diffractometer. The crystal was kept at a steady $T = 100(2) \text{ K}$ during data collection. The structure was solved with the **ShelXT** (Sheldrick, 2015) structure solution program using the Intrinsic Phasing solution method and by using **Olex2** (Dolomanov et al., 2009) as the graphical interface. The model was refined with version 2018/3 of **XL** (Sheldrick, 2008) using Least Squares minimisation.

Compound	15
CCDC	1856006
Formula	$\text{C}_{28}\text{H}_{19}\text{N}_3\text{O}_2$
$D_{\text{calc.}} / \text{g cm}^{-3}$	1.419
μ / mm^{-1}	0.091
Formula Weight	429.46
Colour	red
Shape	plate
Size/ mm^3	$0.17 \times 0.13 \times 0.09$
T / K	100(2)
Crystal System	triclinic
Space Group	$P-1$
$a / \text{\AA}$	8.360(5)
$b / \text{\AA}$	9.772(4)
$c / \text{\AA}$	13.225(6)
$\alpha / ^\circ$	79.646(11)
$\beta / ^\circ$	71.931(19)
$\gamma / ^\circ$	81.249(16)
$V / \text{\AA}^3$	1004.9(8)
Z	2
Z'	1
Wavelength/ \AA	0.710730
Radiation type	$\text{MoK}\alpha$
$\theta_{\text{min}} / ^\circ$	1.636
$\theta_{\text{max}} / ^\circ$	27.537
Measured Refl.	25689
Independent Refl.	4614
Reflections with $I > 3\sigma(I)$	>3897
R_{int}	0.0266
Parameters	300
Restraints	0
Largest Peak	0.464
Deepest Hole	-0.212
GooF	1.071
wR_2 (all data)	0.1468
wR_2	0.1406
R_1 (all data)	0.0594
R_1	0.0511

A red plate-shaped crystal with dimensions 0.17×0.13×0.09 mm³ was mounted on a MITIGEN holder in perfluoroether oil. Data were collected using a Bruker SMART APEX2 area detector diffractometer equipped with an Oxford Cryosystems 800 low-temperature device operating at $T = 100(2)$ K.

Data were measured using ω and ϕ scans using MoK α radiation. The total number of runs and images was based on the strategy calculation from the program **APEX2** (Bruker) The maximum resolution that was achieved was $\Theta = 27.537^\circ$ (0.77 Å).

The diffraction pattern was indexed. The total number of runs and images was based on the strategy calculation from the program **APEX2** (Bruker) and the unit cell was refined using **SAINT** (Bruker, V8.38A, after 2013) on 8694 reflections, 34% of the observed reflections.

Data reduction, scaling and absorption corrections were performed using **SAINT** (Bruker, V8.38A, after 2013). The final completeness is 99.90 % out to 27.537° in Θ . A multi-scan absorption correction was performed using **SADABS-2016/2** (Bruker,2016/2) was used for absorption correction. $wR_2(\text{int})$ was 0.0784 before and 0.0428 after correction. The Ratio of minimum to maximum transmission is 0.9443. The $\lambda/2$ correction factor is Not present. The absorption coefficient μ of this material is 0.091 mm⁻¹ at this wavelength ($\lambda = 0.711\text{Å}$) and the minimum and maximum transmissions are 0.704 and 0.746.

The structure was solved and the space group $P-1$ (# 2) determined by the **ShelXT** (Sheldrick, 2015) structure solution program using Intrinsic Phasing and refined by Least Squares using version 2018/3 of **XL** (Sheldrick, 2008). All non-hydrogen atoms were refined anisotropically. Hydrogen atom positions were calculated geometrically and refined using the riding model. Hydrogen atom positions were calculated geometrically and refined using the riding model.

There is a single molecule in the asymmetric unit, which is represented by the reported sum formula. In other words: Z is 2 and Z' is 1.

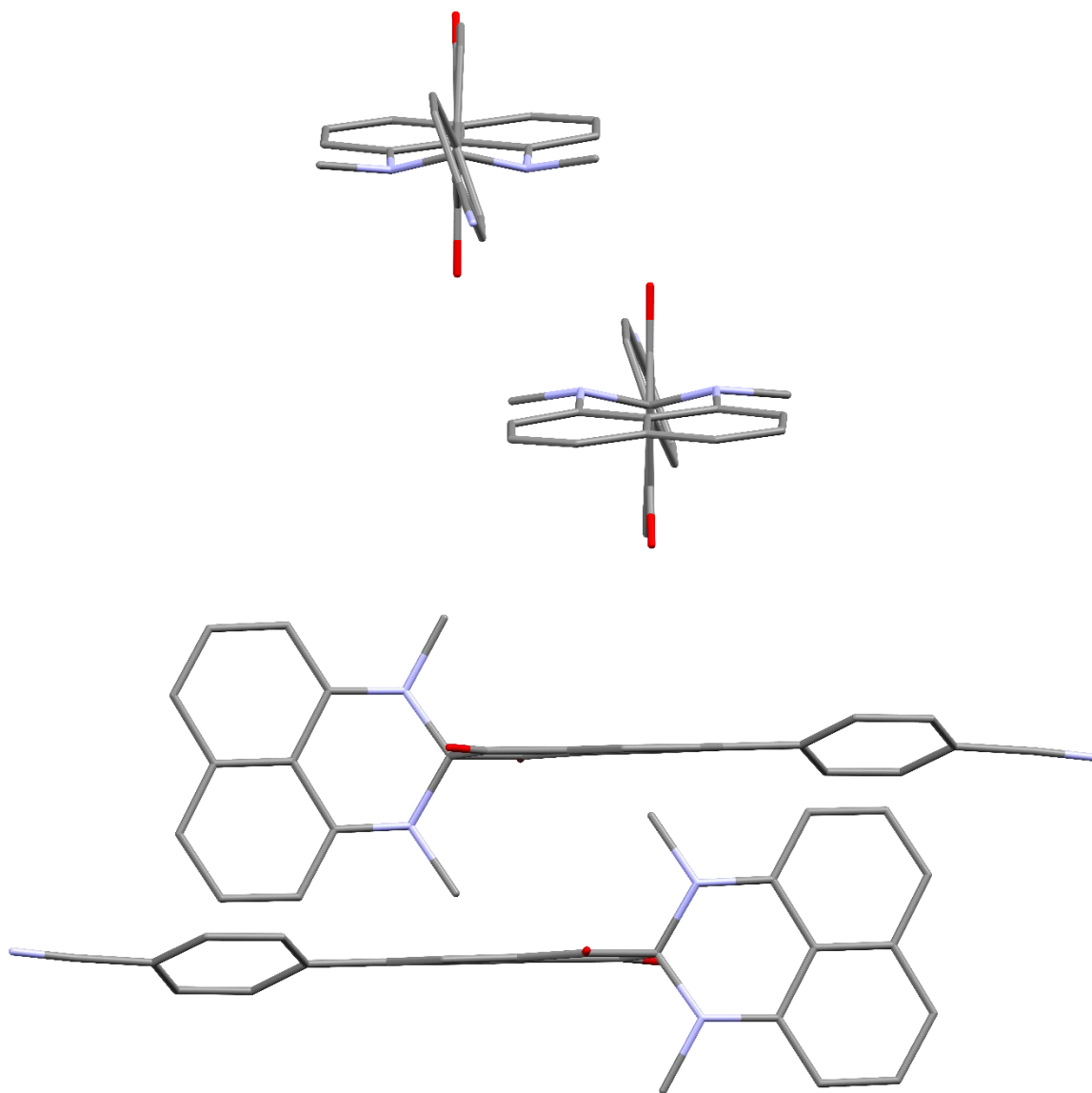
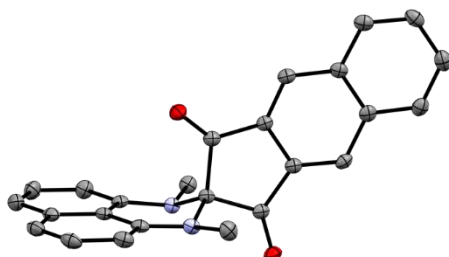


Figure S8: Two views of the packing models of **15**.

4.8 Single-crystal structure and packing of 16

Crystal Data and Experimental



Experimental. Single red block-shaped crystals of **16** were recrystallised from a mixture of CH_2Cl_2 and MeOH by solvent layering. A suitable crystal $0.10 \times 0.07 \times 0.06 \text{ mm}^3$ was selected and mounted on a MITIGEN holder in perfluoroether oil on a Bruker SMART APEX2 area detector diffractometer. The crystal was kept at a steady $T = 100(2) \text{ K}$ during data collection. The structure was solved with the **ShelXT** (Sheldrick, 2015) structure solution program using the Intrinsic Phasing solution method and by using **Olex2** (Dolomanov et al., 2009) as the graphical interface. The model was refined with version 2018/3 of **ShelXL** (Sheldrick, 2015) using Least Squares minimisation.

Compound	16
CCDC	1898124
Formula	$\text{C}_{25}\text{H}_{18}\text{N}_2\text{O}_2$
$D_{\text{calc.}} / \text{g cm}^{-3}$	1.390
μ / mm^{-1}	0.089
Formula Weight	378.41
Colour	red
Shape	block
Size/ mm^3	$0.10 \times 0.07 \times 0.06$
T / K	100(2)
Crystal System	orthorhombic
Space Group	<i>Pbcn</i>
$a / \text{\AA}$	18.714(3)
$b / \text{\AA}$	15.974(3)
$c / \text{\AA}$	12.0964(18)
$\alpha / ^\circ$	90
$\beta / ^\circ$	90
$\gamma / ^\circ$	90
$V / \text{\AA}^3$	3616.1(10)
Z	8
Z'	1
Wavelength/ \AA	0.710730
Radiation type	$\text{MoK}\alpha$
$\theta_{\text{min}} / ^\circ$	1.676
$\theta_{\text{max}} / ^\circ$	27.486
Measured Refl.	28900
Independent Refl.	4129
Reflections with $I > 3\sigma(I)$	>3172
R_{int}	0.0483
Parameters	264
Restraints	0
Largest Peak	0.275
Deepest Hole	-0.234
Goof	1.030
wR_2 (all data)	0.1091
wR_2	0.0984
R_1 (all data)	0.0605
R_1	0.0423

A red block-shaped crystal with dimensions 0.10×0.07×0.06 mm³ was mounted on a MITIGEN holder in perfluoroether oil. Data were collected using a Bruker SMART APEX2 area detector diffractometer equipped with an Oxford Cryosystems 800 low-temperature device operating at $T = 100(2)$ K.

Data were measured using ω and ϕ scans using MoK $_{\alpha}$ radiation. The total number of runs and images was based on the strategy calculation from the program **APEX2** (Bruker) The maximum resolution that was achieved was $\Theta = 27.486^{\circ}$ (0.77 Å).

The diffraction pattern was indexed. The total number of runs and images was based on the strategy calculation from the program **APEX2** (Bruker) and the unit cell was refined using **SAINT** (Bruker, V8.38A, after 2013) on 4577 reflections, 16% of the observed reflections.

Data reduction, scaling and absorption corrections were performed using **SAINT** (Bruker, V8.38A, after 2013). The final completeness is 99.80 % out to 27.486° in Θ . A multi-scan absorption correction was performed using **SADABS-2016/2** (Bruker,2016/2) was used for absorption correction. $wR_2(\text{int})$ was 0.0791 before and 0.0518 after correction. The Ratio of minimum to maximum transmission is 0.9447. The $\lambda/2$ correction factor is Not present. The absorption coefficient μ of this material is 0.089 mm⁻¹ at this wavelength ($\lambda = 0.711\text{Å}$) and the minimum and maximum transmissions are 0.704 and 0.746.

The structure was solved and the space group *Pbcn* (# 60) determined by the **ShelXT** (Sheldrick, 2015) structure solution program using Intrinsic Phasing and refined by Least Squares using version 2018/3 of **ShelXL** (Sheldrick, 2015). All non-hydrogen atoms were refined anisotropically. Hydrogen atom positions were calculated geometrically and refined using the riding model. Hydrogen atom positions were calculated geometrically and refined using the riding model.

There is a single molecule in the asymmetric unit, which is represented by the reported sum formula. In other words: Z is 8 and Z' is 1.

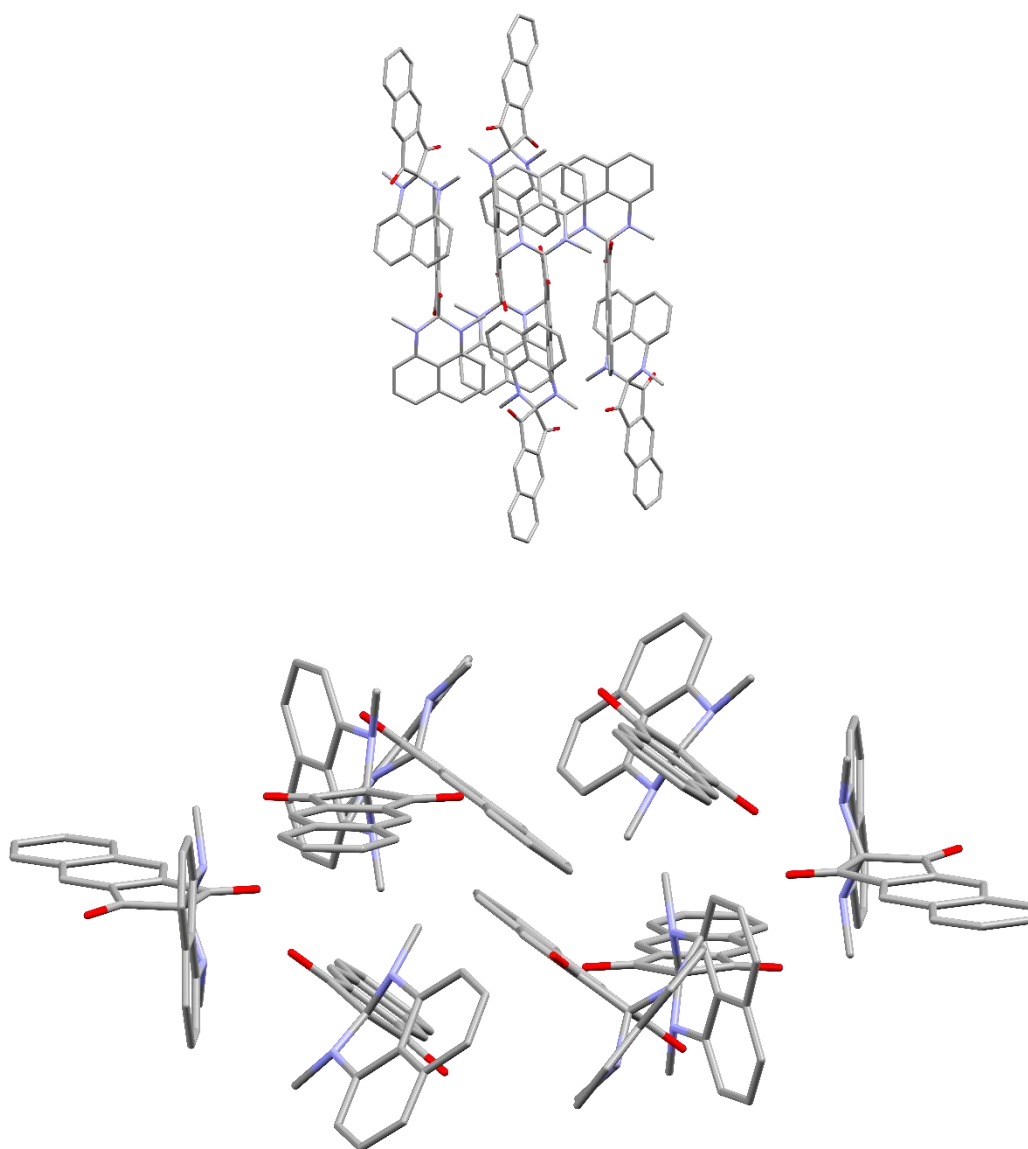
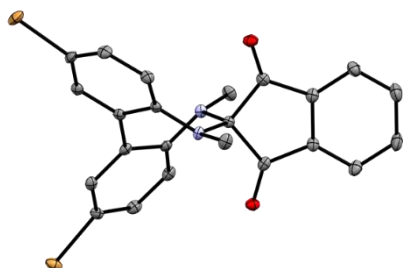


Figure S9: Two views of the packing models of 16.

4.9 Single-crystal structure and packing of 27

Crystal Data and Experimental



Experimental. Single yellow block-shaped crystals of **27** were recrystallised from a mixture of CH_2Cl_2 and methanol by solvent layering. A suitable crystal $0.27 \times 0.11 \times 0.10 \text{ mm}^3$ was selected and mounted on a MITIGEN holder in perfluoroether oil on a Bruker SMART APEX2 area detector diffractometer. The crystal was kept at a steady $T = 100 \text{ K}$ during data collection. The structure was solved with the **ShelXT** (Sheldrick, 2015) structure solution program using the Intrinsic Phasing solution method and by using **Olex2** (Dolomanov et al., 2009) as the graphical interface. The model was refined with version 2018/3 of **XL** (Sheldrick, 2008) using Least Squares minimisation.

Compound	27
CCDC	1855187
Formula	$\text{C}_{23}\text{H}_{16}\text{Br}_2\text{N}_2\text{O}_2$
$D_{\text{calc.}}/\text{g cm}^{-3}$	1.737
m/mm^{-1}	4.163
Formula Weight	512.20
Colour	yellow
Shape	block
Size/ mm^3	$0.27 \times 0.11 \times 0.10$
T/K	100
Crystal System	monoclinic
Space Group	$P2_1/n$
$a/\text{\AA}$	14.667(4)
$b/\text{\AA}$	9.231(3)
$c/\text{\AA}$	15.139(4)
$a/^\circ$	90
$b/^\circ$	107.187(8)
$g/^\circ$	90
$V/\text{\AA}^3$	1958.2(9)
Z	4
Z'	1
Wavelength/ \AA	0.710730
Radiation type	MoK_α
$Q_{\text{min}}/^\circ$	1.699
$Q_{\text{max}}/^\circ$	27.485
Measured Refl.	21928
Independent Refl.	4475
Reflections with $I > 4\sigma(I)$	>4043
R_{int}	0.0236
Parameters	264
Restraints	0
Largest Peak	0.462
Deepest Hole	-0.355
Goof	1.052
wR_2 (all data)	0.0509
wR_2	0.0496
R_1 (all data)	0.0254
R_1	0.0212

A yellow block-shaped crystal with dimensions $0.27 \times 0.11 \times 0.10 \text{ mm}^3$ was mounted on a MITIGEN holder in perfluoroether oil. Data were collected using a Bruker SMART APEX2 area detector diffractometer equipped with an Oxford Cryosystems 800 low-temperature device operating at $T = 100 \text{ K}$.

Data were measured using ω and ϕ scans using MoK_α radiation. The total number of runs and images was based on the strategy calculation from the program **APEX2** (Bruker) The maximum resolution that was achieved was $Q = 27.485^\circ$ (0.77 \AA).

The diffraction pattern was indexed. The total number of runs and images was based on the strategy calculation from the program **APEX2** (Bruker) and the unit cell was refined using **SAINT** (Bruker, V8.38A, after 2013) on 9961 reflections, 45% of the observed reflections.

Data reduction, scaling and absorption corrections were performed using **SAINT** (Bruker, V8.38A, after 2013). The final completeness is 100.00 % out to 27.485° in Q . A multi-scan absorption correction was performed using **SADABS-2016/2** (Bruker,2016/2) was used for absorption correction. $wR_2(\text{int})$ was 0.0881 before and 0.0342 after correction. The Ratio of minimum to maximum transmission is 0.7169. The $l/2$ correction factor is Not present. The absorption coefficient m of this material is 4.163 mm^{-1} at this wavelength ($\lambda = 0.711 \text{ \AA}$) and the minimum and maximum transmissions are 0.534 and 0.746.

The structure was solved and the space group $P2_1/n$ (# 14) determined by the **ShelXT** (Sheldrick, 2015) structure solution program using Intrinsic Phasing and refined by Least Squares using version 2018/3 of **XL** (Sheldrick, 2008). All non-hydrogen atoms were refined anisotropically. Hydrogen atom positions were calculated geometrically and refined using the riding model. Hydrogen atom positions were calculated geometrically and refined using the riding model.

There is a single molecule in the asymmetric unit, which is represented by the reported sum formula. In other words: Z is 4 and Z' is 1.

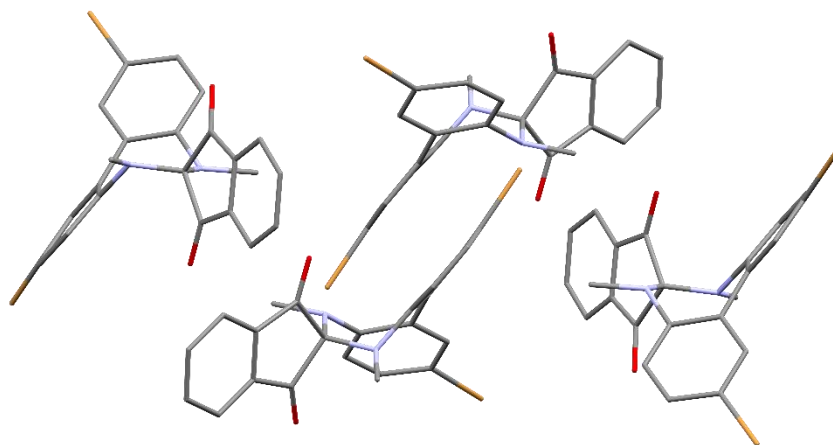


Figure S10: Packing model of **27**.

5. Photophysical Properties

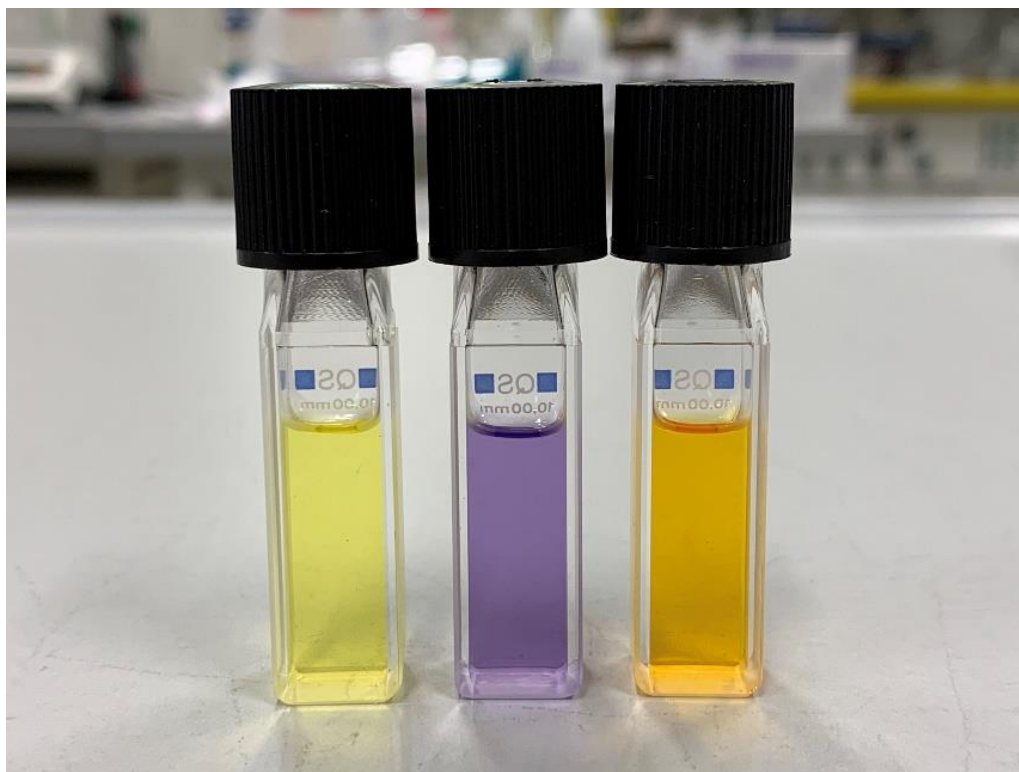


Figure S11: Comparison of the different colours of the spiro compounds in CH_2Cl_2 . Left (**5**), middle (**9**) and right (**4**).

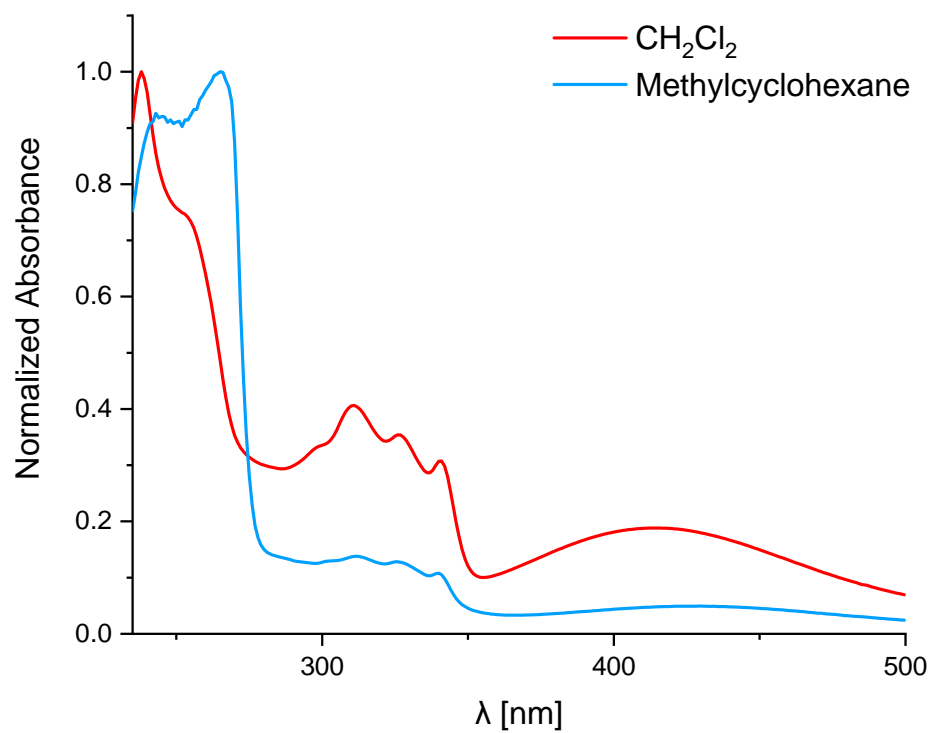


Figure S12: Solvent dependence of the absorption maximum of **4**.

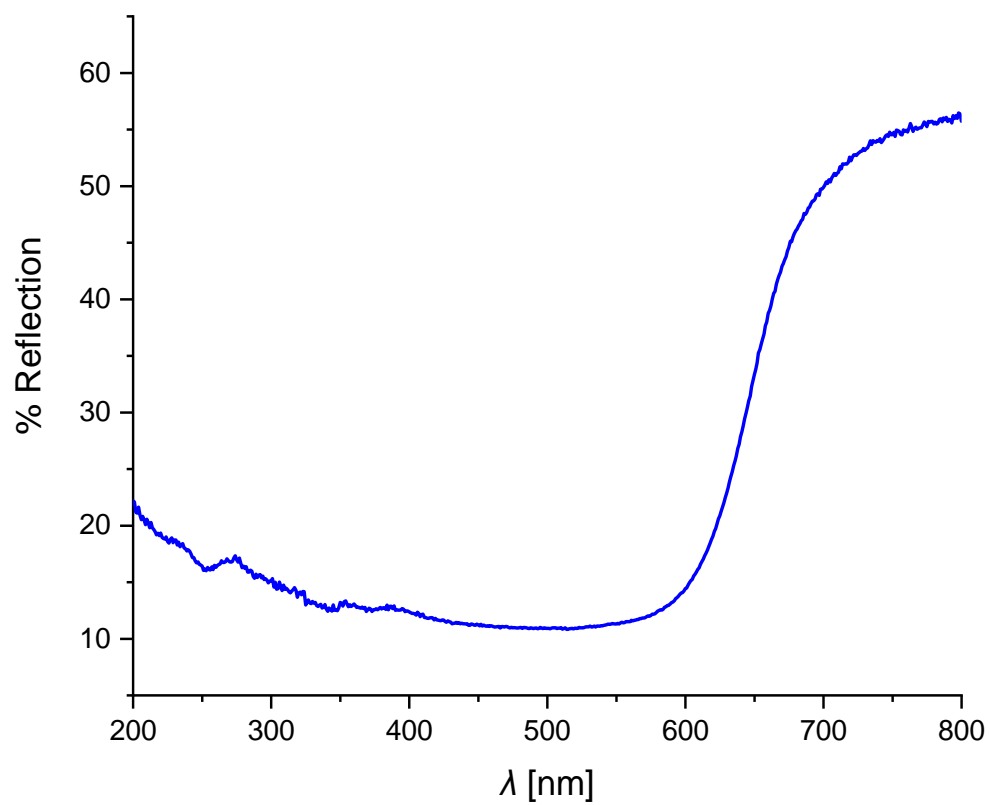


Figure S13: Room-temperature diffuse reflectance spectra of **16**.

6. Thermal Measurements

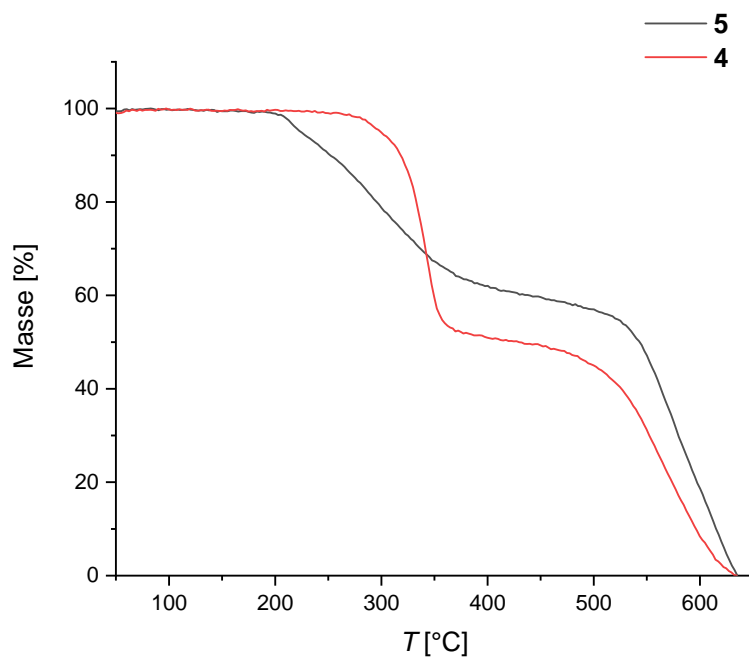


Figure S14: TGA measurement of **5** and **4** under inert N₂ atmosphere at a heating rate of 10 K·min⁻¹.

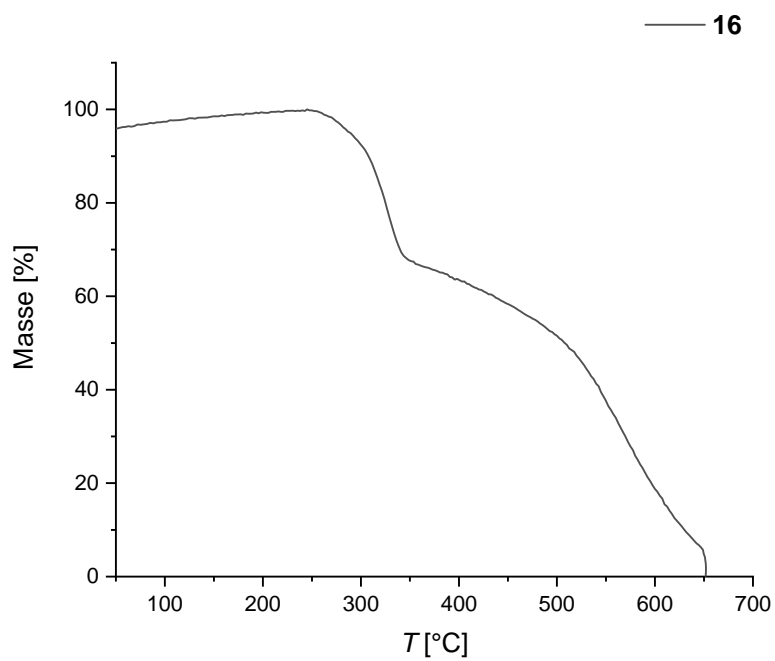


Figure S15: TGA measurement of **16** under inert N₂ atmosphere at a heating rate of 10 K·min⁻¹.

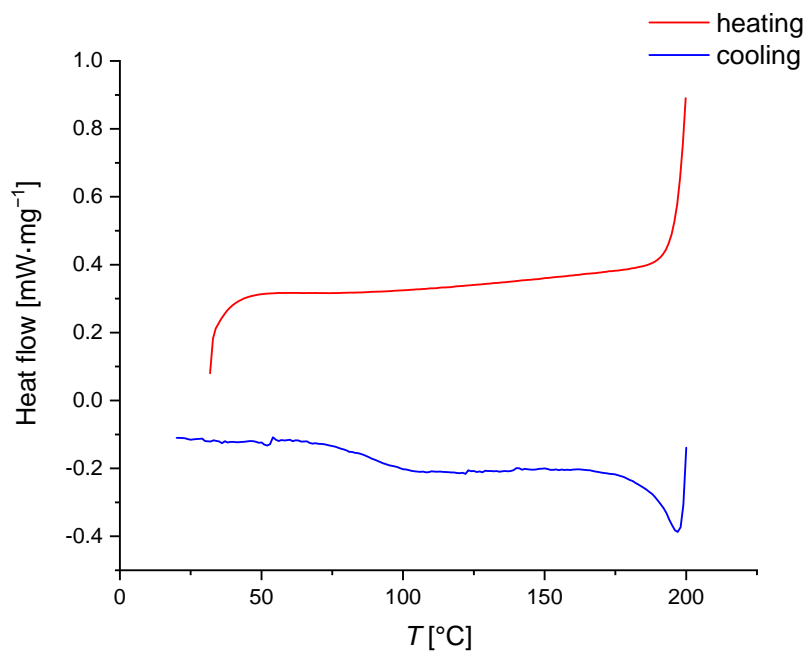


Figure S16: DSC of **5** at a heating rate of 10 K·min⁻¹.

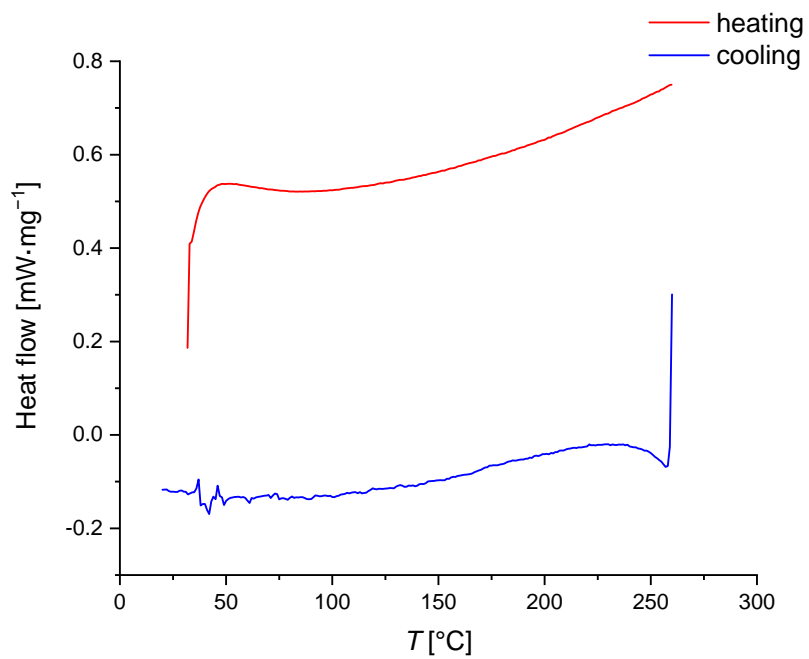


Figure S17: DSC of **4** at a heating rate of 10 K·min⁻¹.

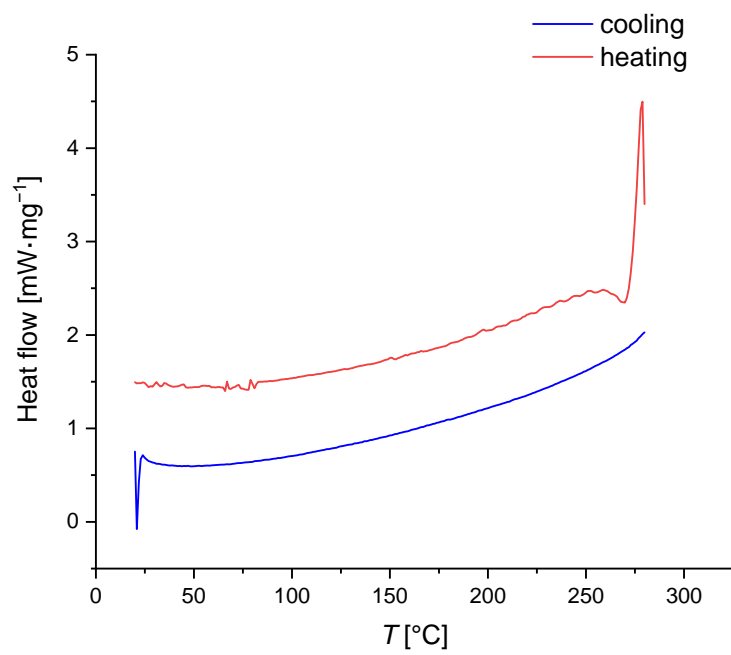


Figure S18: DSC of **16** at a heating rate of $10\text{ K}\cdot\text{min}^{-1}$.

7. Cyclic Voltammograms

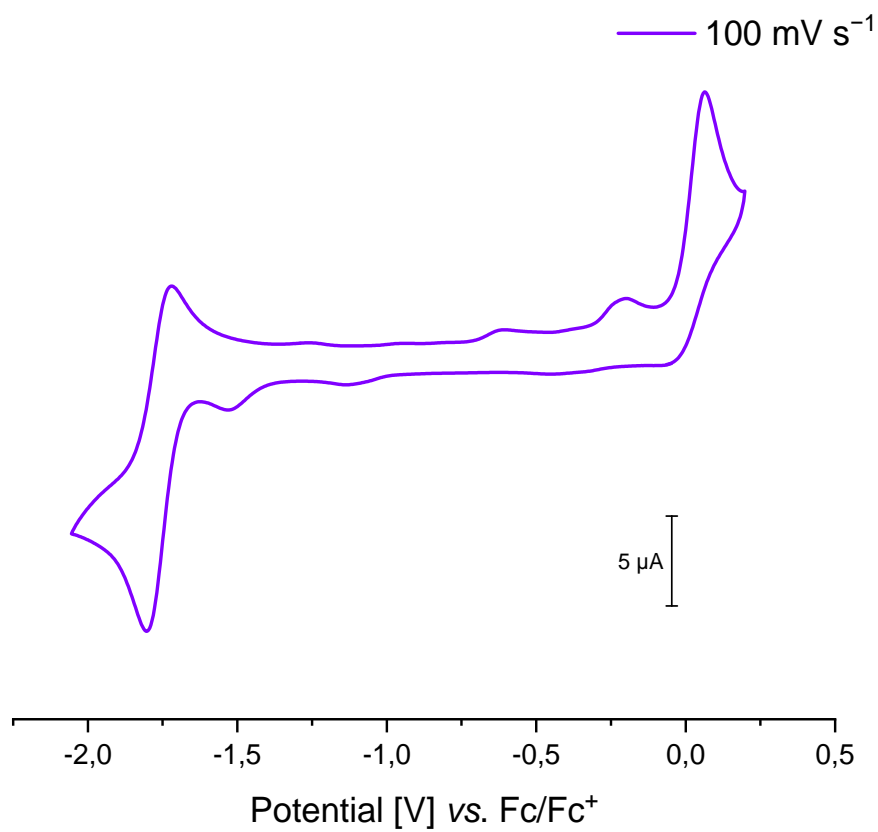


Figure S19: Cyclic voltammograms of **3** in acetonitrile at 100 mV/s scan rate using a glassy carbon electrode.

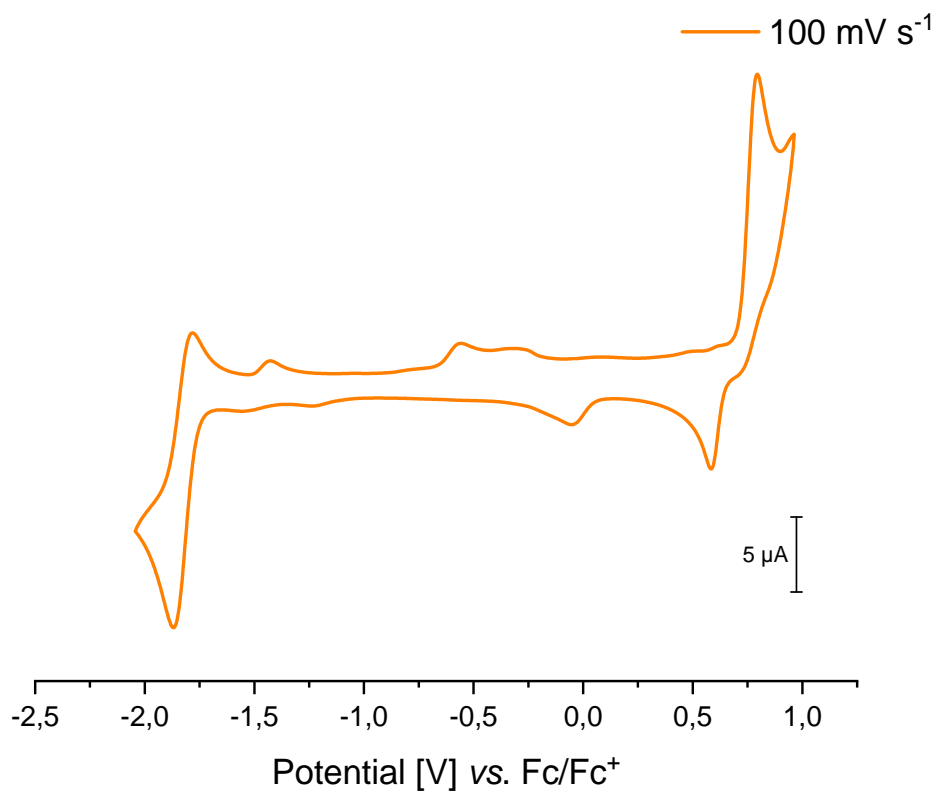


Figure S20: Cyclic voltammograms of **5** in acetonitrile at 100 mV/s scan rate using a glassy carbon electrode.

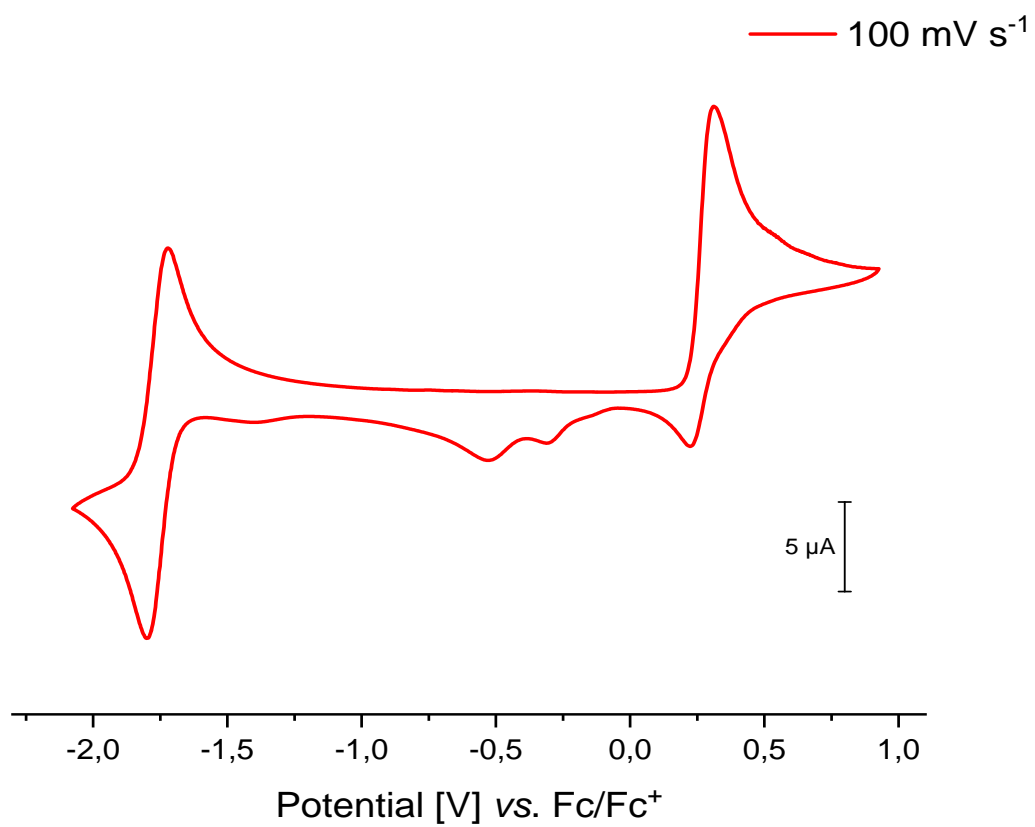


Figure S21: Cyclic voltammograms of **4** in acetonitrile at 100 mV/s scan rate using a glassy carbon electrode.

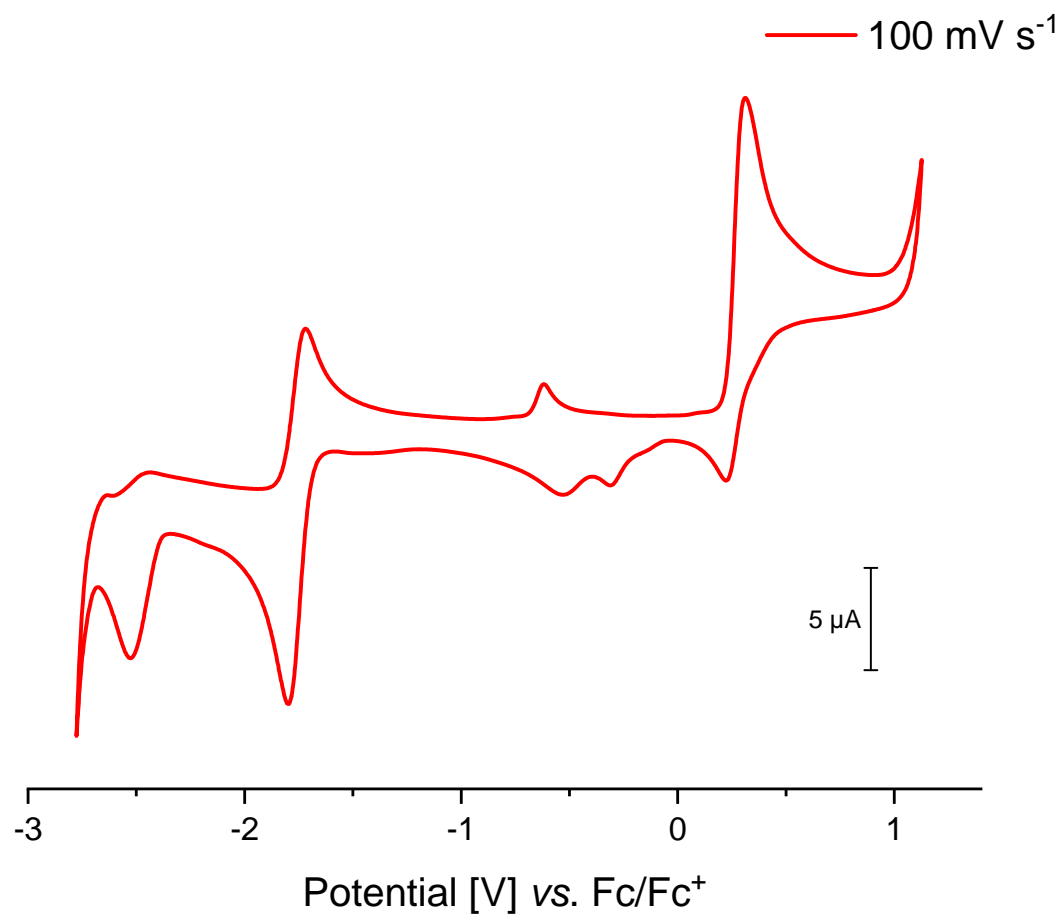


Figure S22: Cyclic voltammograms of **4** in acetonitrile at 100 mV/s scan rate using a glassy carbon electrode.

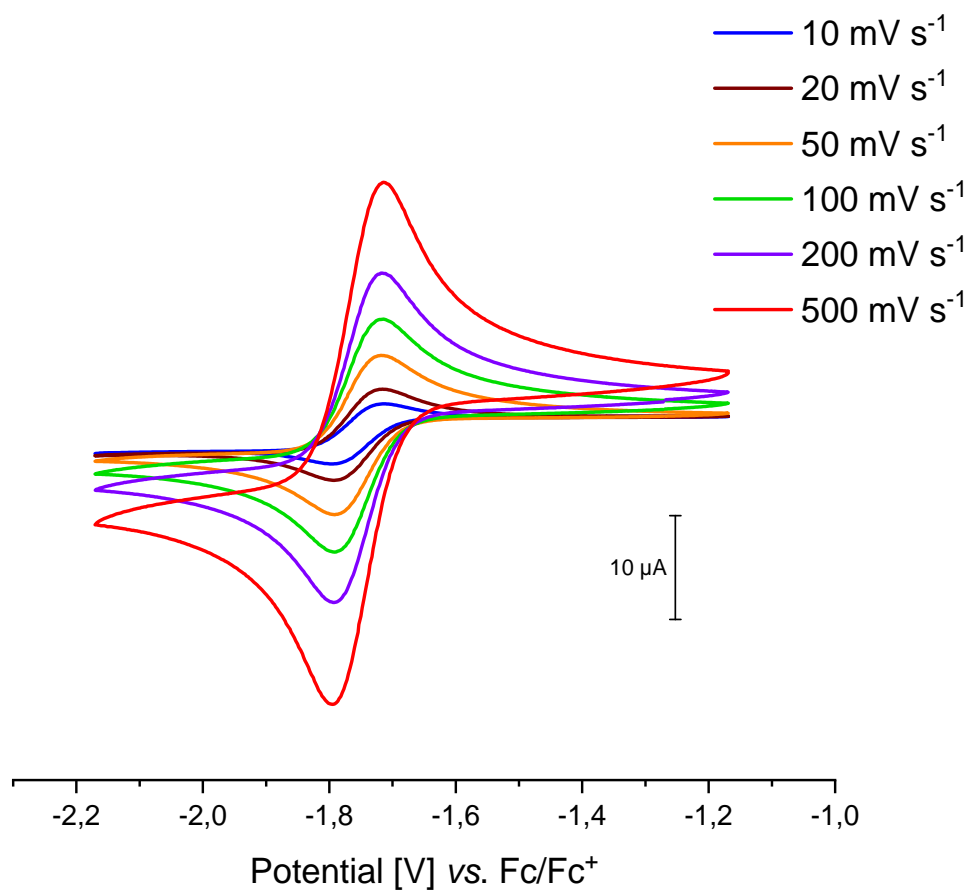


Figure S23: Cyclic voltammograms of **4** in acetonitrile at various scanrates.

8. Infrared Spectra

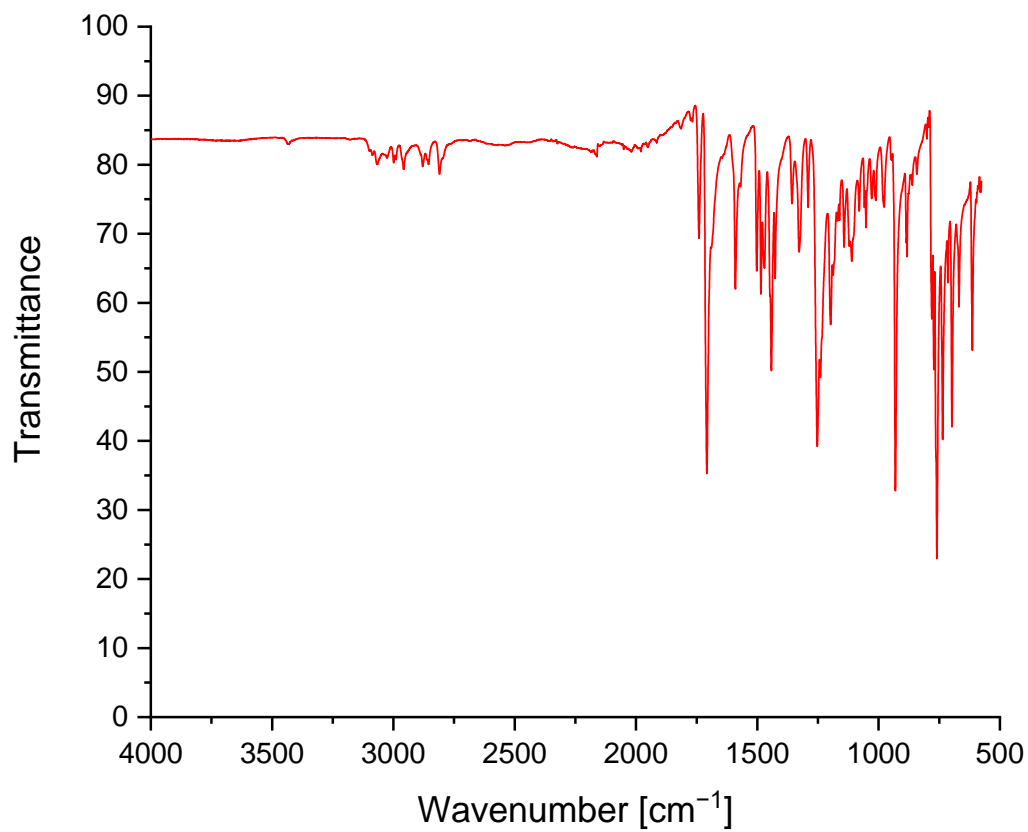


Figure S24: Infrared Spectrum of 5.

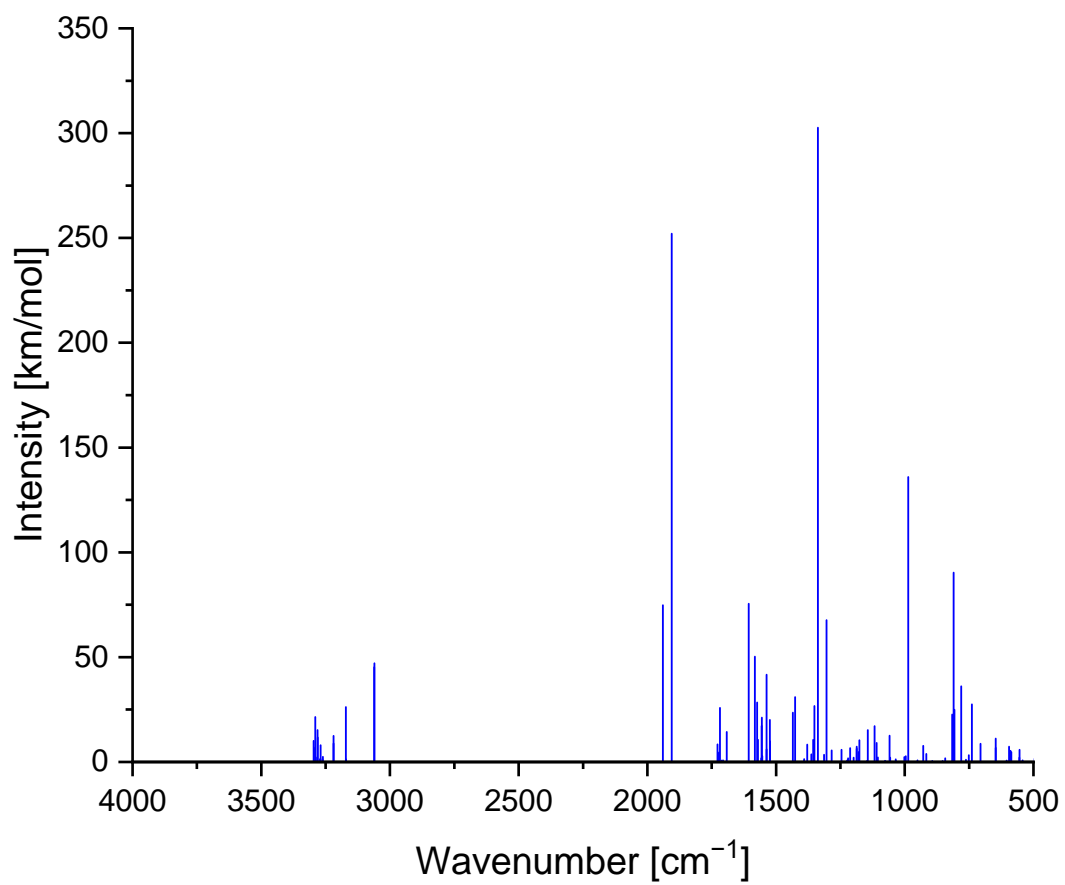


Figure S25: Calculated Infrared Spectrum of **5** (PBEh-3c/def2-mSVP).

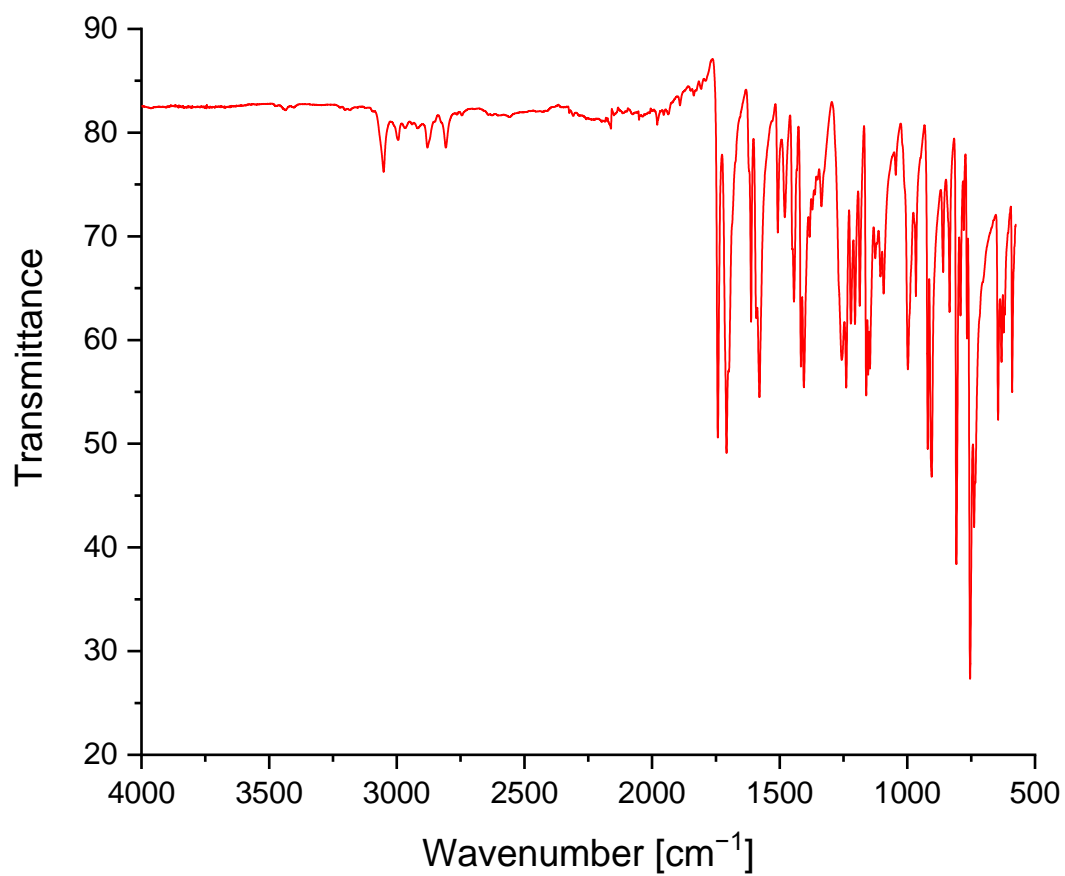


Figure S26: Infrared Spectrum of 16.

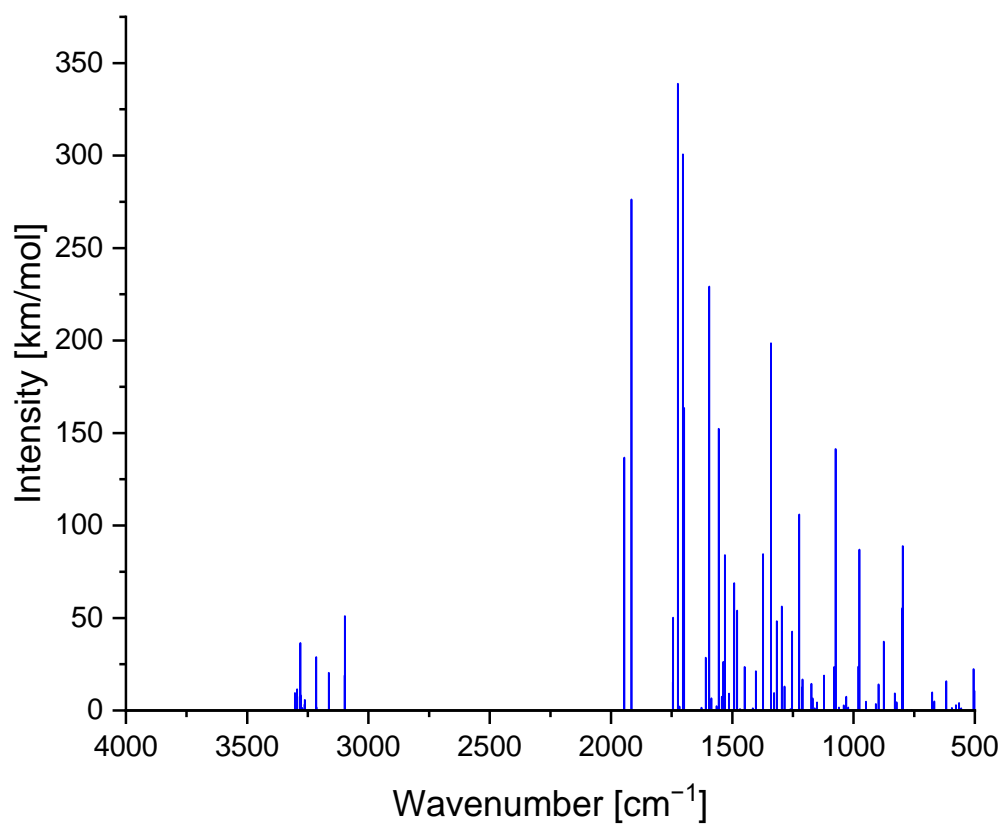


Figure S27: Calculated Infrared Spectrum of **16** (PBEh-3c/def2-mSVP).

9. DFT Calculations

DFT calculations were performed with the TURBOMOLE v7.3 program package.^[11] The resolution-of-identity^[12] (RI, RIJDX for SP) approximation for the Coulomb integrals was used in all DFT calculations employing matching auxiliary basis set def2-XVP/J.^[13] Further, the D3 dispersion correction scheme^[14] with the Becke-Johnson damping function was applied.^[15] Using the TURBOMOLE v7.3 program package, the geometries of all molecules were optimized without symmetry restrictions with the PBEh-3c^[16]-D3/def2-mSVP composite scheme followed by harmonic vibrational frequency analysis to confirm minima as stationary points. Vertical excitation energies were calculated using TDDFT applying the B3LYP^[16] functional with the def2-TZVP basis set.^[17]

9.1 Frontier Orbitals

Table S1: Frontier molecular orbitals of **9** (above) and **17** (below) (B3LYP-D3/def2-TZVP).

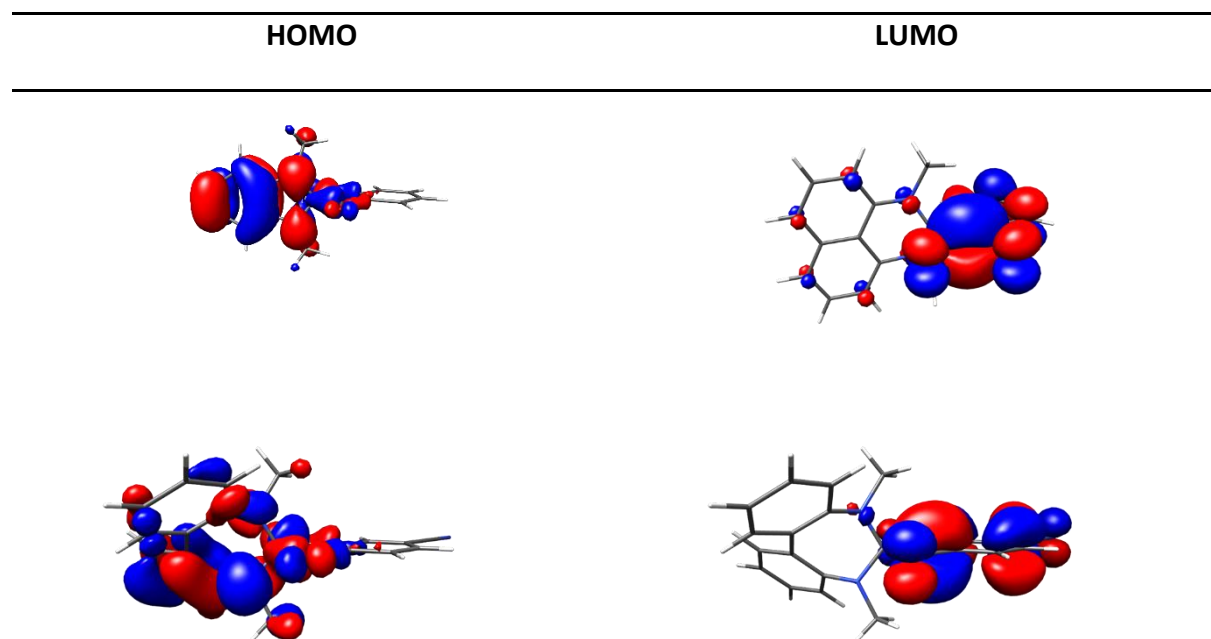
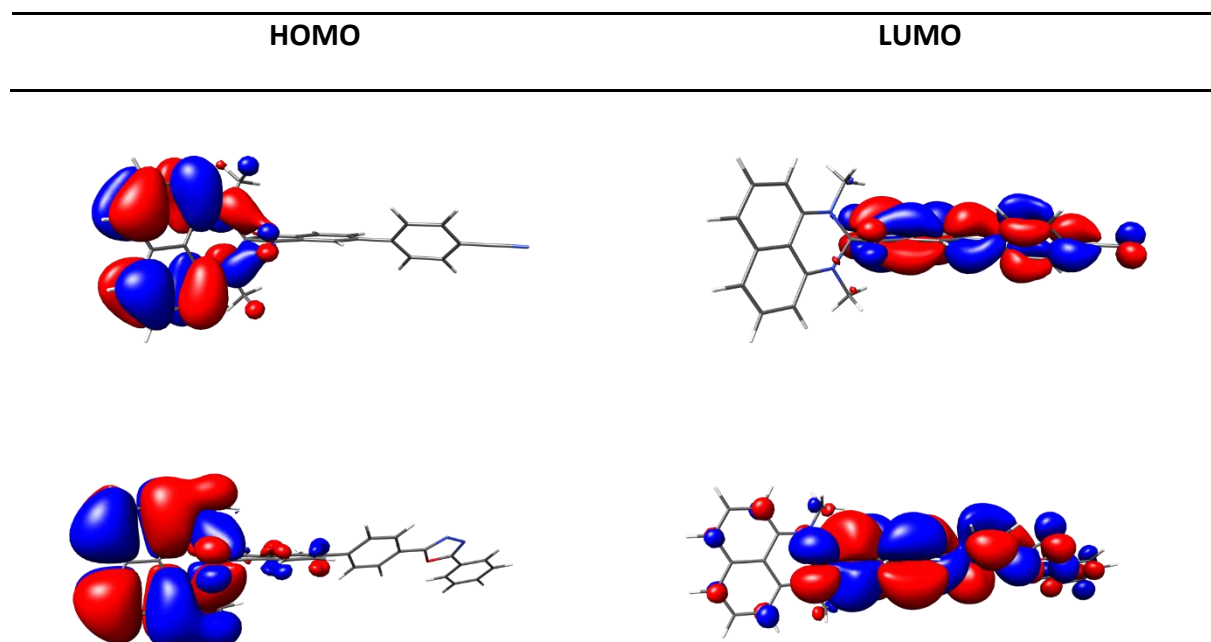


Table S2: Frontier molecular orbitals of **15** (above) and **14** (below) (B3LYP-D3/def2-TZVP).



9.2 TDDFT Calculations

9.2.1 Charge transfer transitions

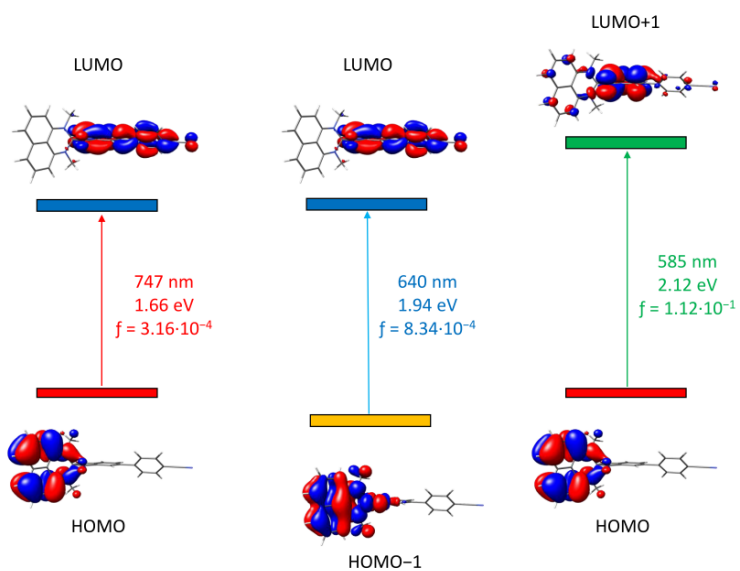


Figure S28: Calculated intramolecular charge transfer transition of **15** (B3LYP-D3/def2-TZVP).

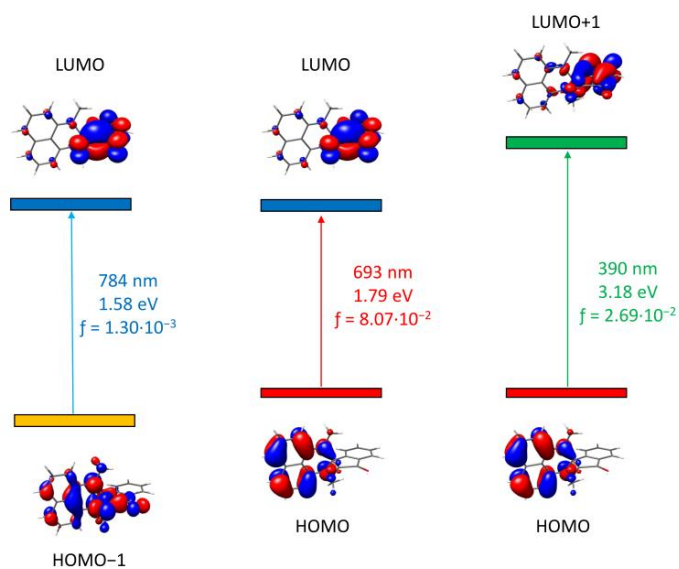


Figure S29: Calculated intramolecular charge transfer transition of **9** (B3LYP-D3/def2-TZVP).

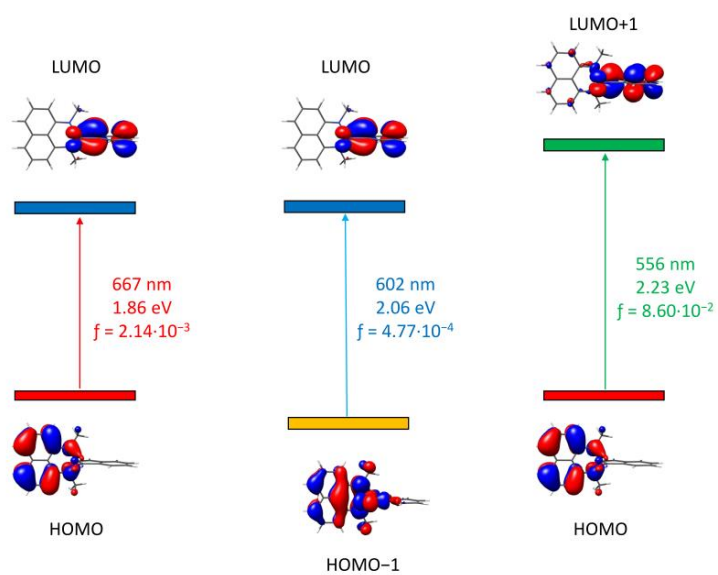


Figure S30: Calculated intramolecular charge transfer transition of **4** (B3LYP-D3/def2-TZVP).

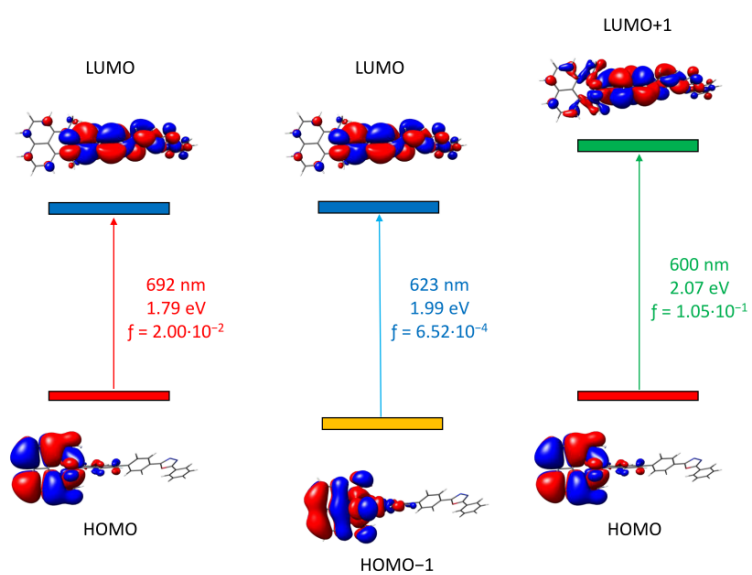


Figure S31: Calculated intramolecular charge transfer transition of **14** (B3LYP-D3/def2-TZVP).

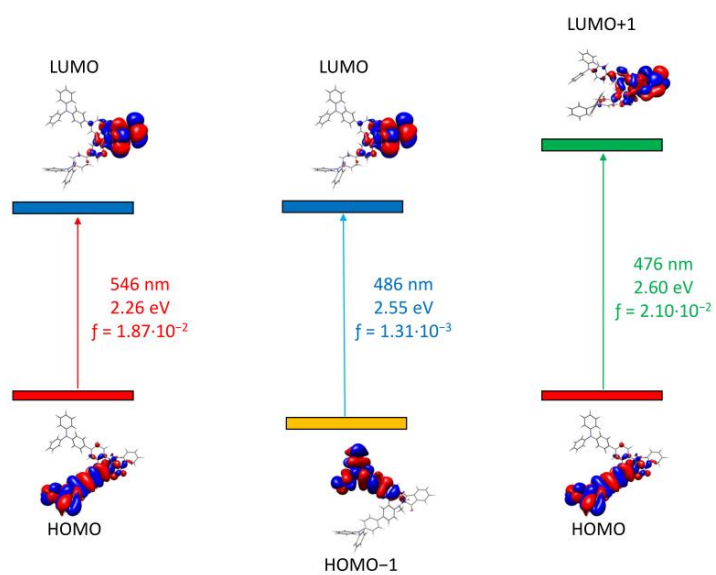


Figure S32: Calculated intramolecular charge transfer transition of **29** (B3LYP-D3/def2-TZVP).

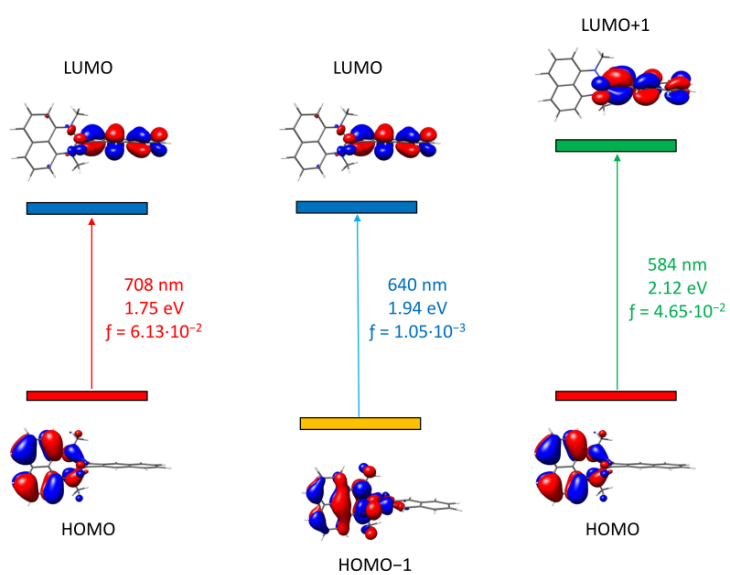


Figure S33: Calculated intramolecular charge transfer transition of **16** (B3LYP-D3/def2-TZVP).

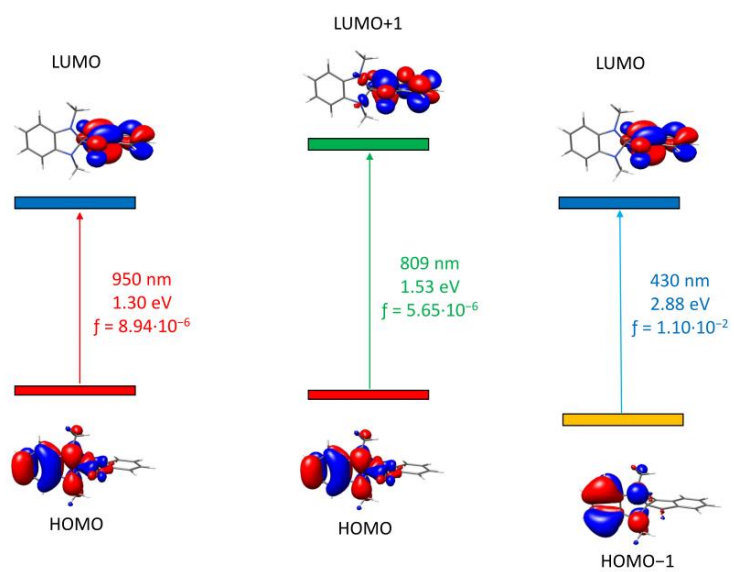


Figure S34: Calculated intramolecular charge transfer transition of **3** (B3LYP-D3/def2-TZVP).

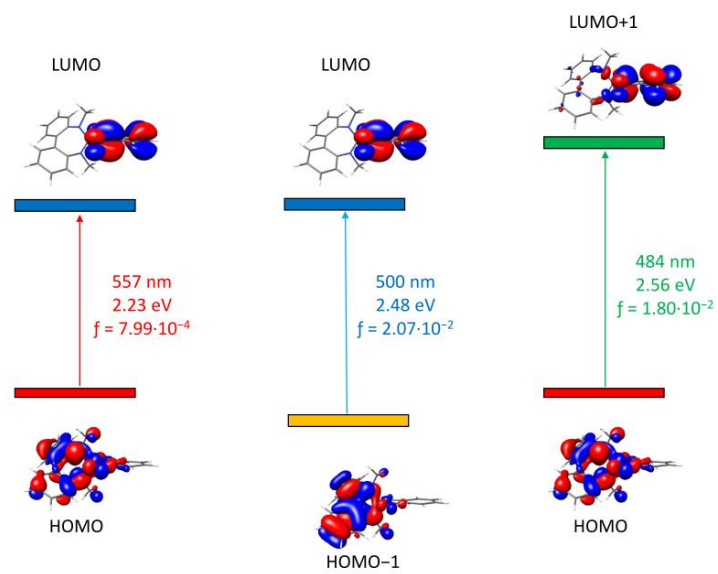


Figure S35: Calculated intramolecular charge transfer transition of **5** (B3LYP-D3/def2-TZVP).

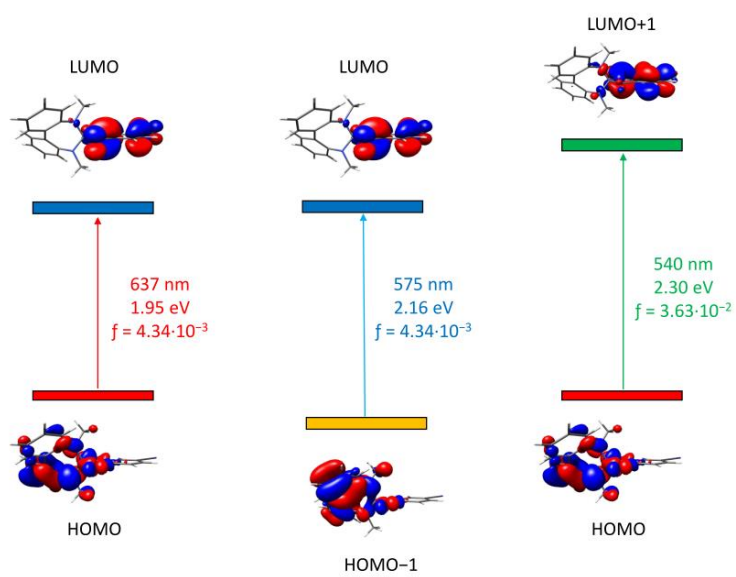


Figure S36: Calculated intramolecular charge transfer transition of **17** (B3LYP-D3/def2-TZVP).

9.2.2 Calculated Band gaps

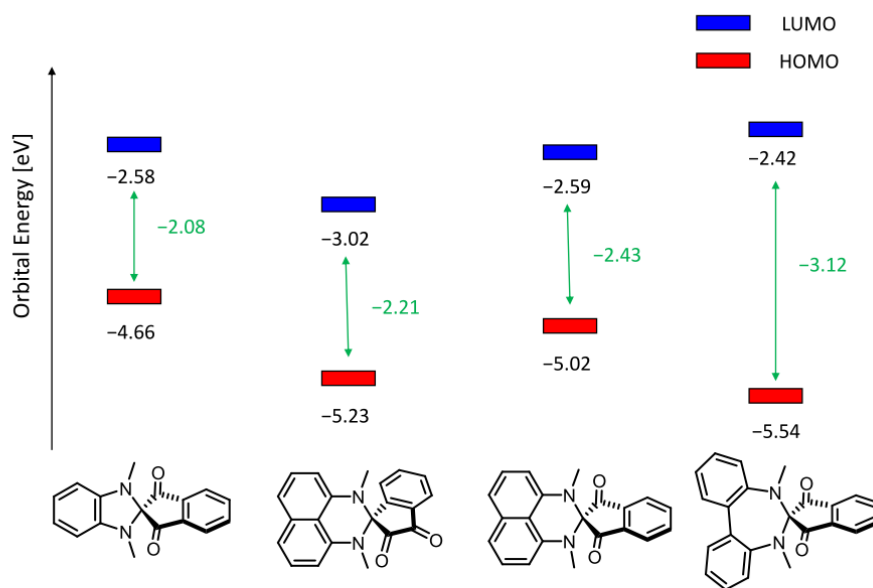


Figure S37: Calculated HOMO energy level (red), LUMO energy level (blue) and band gaps (green) in eV (B3LYP-D3/def2-TZVP).

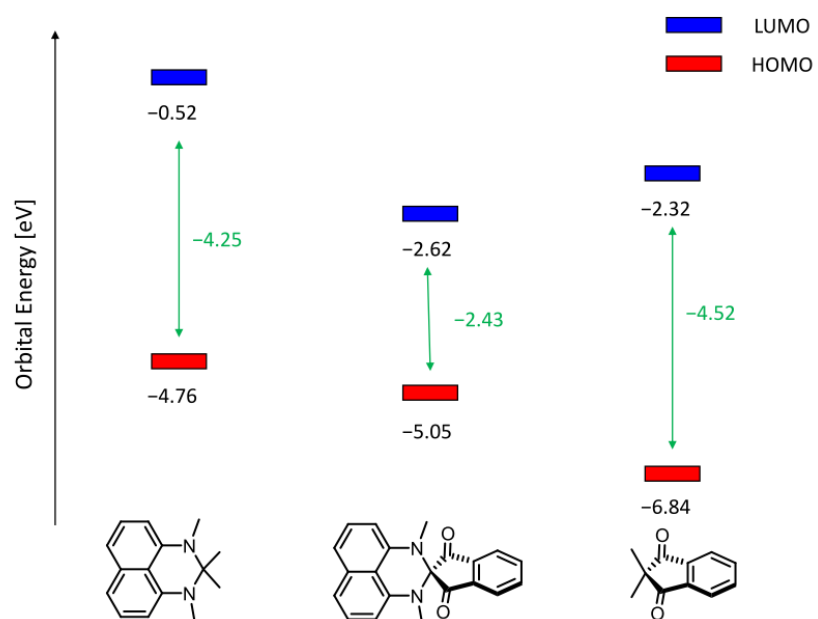


Figure S38: Calculated HOMO energy level (red), LUMO energy level (blue) and band gaps (green) in eV. (B3LYP-D3/def2-TZVP).

9.2.3 Calculated Absorption Spectra

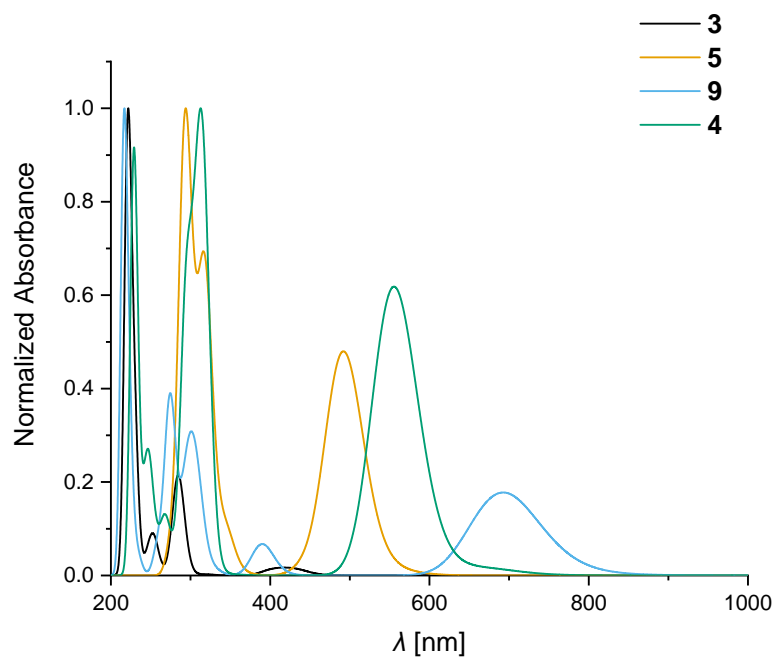


Figure S39: Calculated absorption spectra of **3**, **5**, **9** and **4** (B3LYP-D3/def2-TZVP).

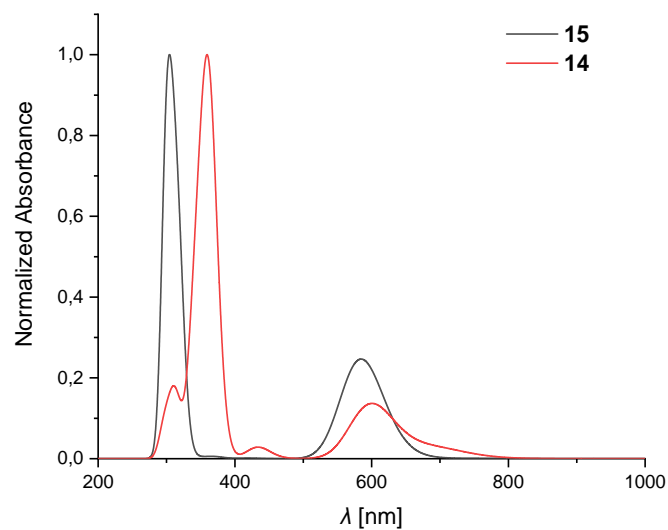


Figure S40: Calculated absorption spectra of **15** and **14** (B3LYP-D3/def2-TZVP).

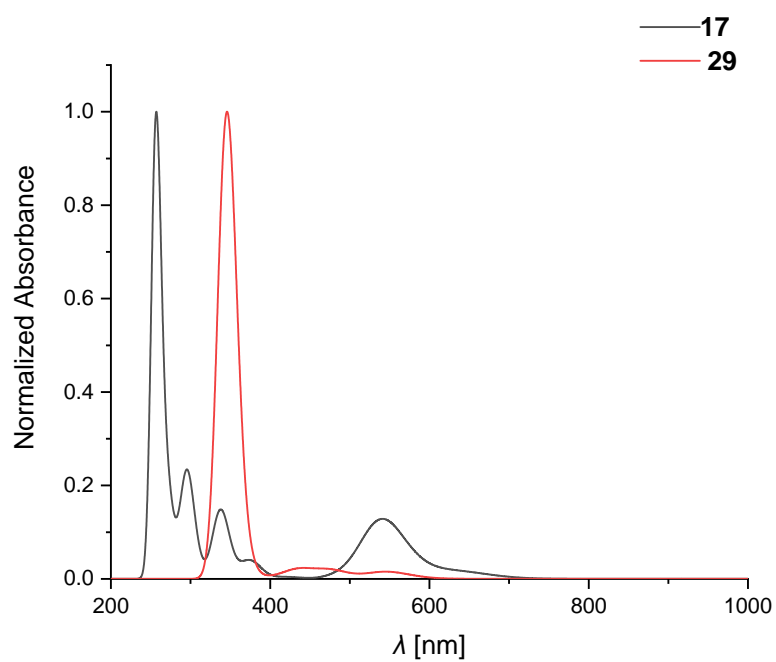


Figure S41: Calculated absorption spectra of **17** and **29** (B3LYP-D3/def2-TZVP).

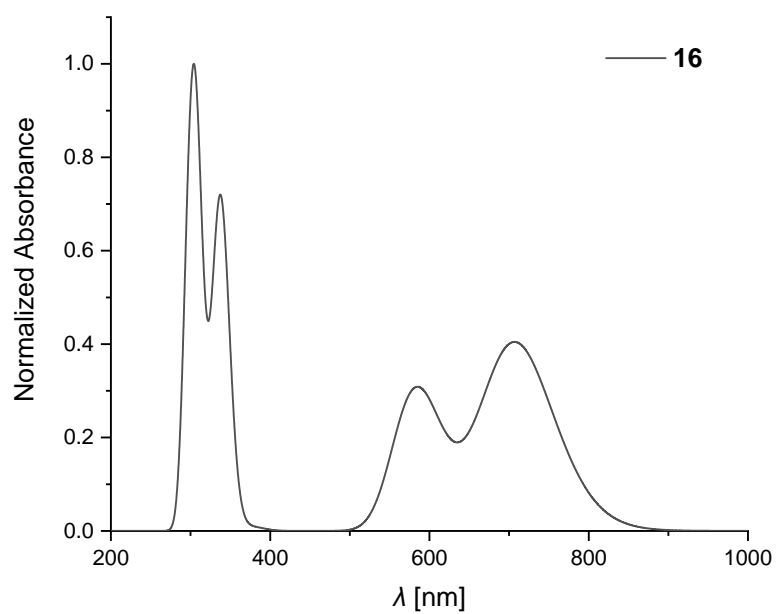


Figure S42: Calculated absorption spectra of **16** (B3LYP-D3/def2-TZVP).

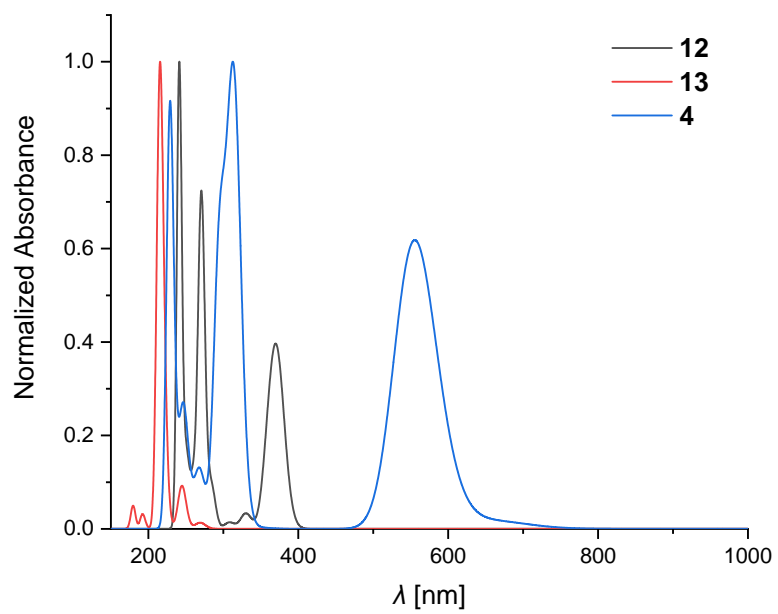


Figure S43: Calculated absorption spectra of **12**, **13**, **4** (B3LYP-D3/def2-TZVP).

9.3 Excited State Geometry Optimization

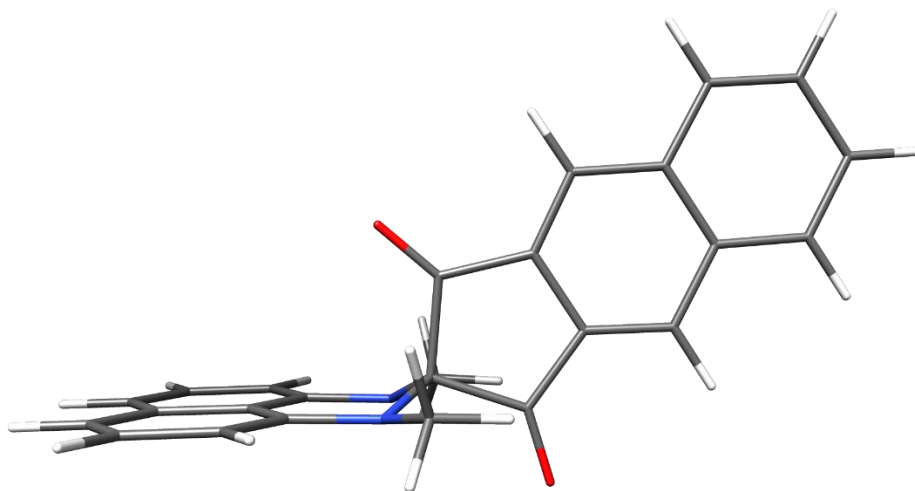


Figure S44: Structure of the optimized geometry of **16** (PBEh-3c/def2-mSVP).

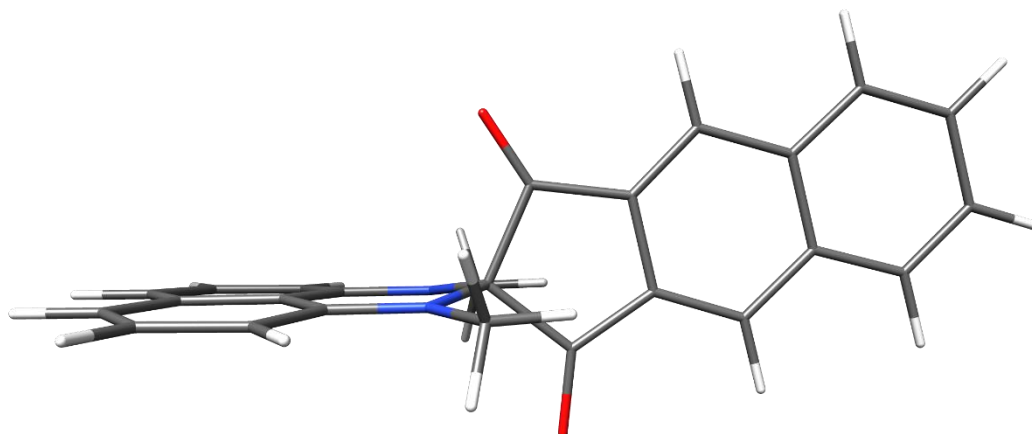


Figure S45: Structure of the optimized geometry of the first excited state of **16** (PBEh-3c/def2-mSVP).

9.4 Total Energies

Table S3: Single point energies (B3LYP-D3/def2-TZVP).

Compound	[hartrees]
3	-916.05195
5	-1147.06295
9	-1069.66679
4	-1069.67449
15	-1392.92687
14	-1792.61008
17	-1239.29457
16	-1223.29239
29	-2643.83478
13	-575.57974
12	-691.82225

9.5 Cartesian Coordinates of the Calculated Structures

The Cartesian coordinates are listed in angstrom.

Table S4: Coordinates of the calculated structure of **3** (PBEh-3c/def2-mSVP).

	x	y	z	C	1.1088775	1.8732856	-0.7757197
O	-1.7490091	-0.6011753	-2.0277236	C	1.6400566	3.1390023	-0.8294543
N	-0.1703818	1.4387174	-0.4642590	H	1.0527914	4.0118555	-0.5766070
C	-0.1391449	0.0109757	-0.2880651	C	2.9823969	3.2722895	-1.2132928
O	0.6083495	-0.0946027	2.0495419	H	3.4218473	4.2594174	-1.2597963
N	1.0767585	-0.3717311	-0.9600727	C	3.7461125	2.1646463	-1.5151750
C	-0.1758247	-0.4299401	1.2044759	H	4.7830697	2.2850714	-1.7978748
C	-1.3370982	-1.3235885	1.3828240	C	3.2017127	0.8739097	-1.4468016
C	-1.7585479	-1.9685113	2.5374917	H	3.8129728	0.0089211	-1.6677639
H	-1.2144746	-1.8497765	3.4650496	C	1.8831195	0.7502277	-1.0821582
C	-2.8898639	-2.7618601	2.4601472	C	1.6183631	-1.6919006	-0.8095047
H	-3.2453422	-3.2792474	3.3414110	H	0.8234328	-2.4351093	-0.8764563
C	-3.5864423	-2.9072151	1.2564749	H	2.1553617	-1.8398807	0.1342497
H	-4.4679218	-3.5340636	1.2292638	H	2.3058849	-1.8972384	-1.6292852
C	-3.1650644	-2.2630294	0.1063169	C	-1.1024625	2.2521595	0.2622752
H	-3.6989038	-2.3703777	-0.8285267	H	-1.2270644	3.2063579	-0.2486484
C	-1.3849390	-0.6878477	-0.8901251	H	-0.7957315	2.4521232	1.2949793
C	-2.0292352	-1.4688893	0.1851251	H	-2.0836552	1.7770247	0.2776840

Table S5: Coordinates of the calculated structure of **5** (PBEh-3c/def2-mSVP).

	x	y	z	C	0.8110200	-2.1924672	1.8039647
O	2.4233437	0.7512876	0.7939870	C	-0.2752870	-1.6163040	0.9847016
N	-0.5776116	0.8216825	0.7496731	C	-0.8298608	0.9344957	2.1702610
C	0.2441305	-0.2937482	0.3560179	H	0.0569026	1.1383742	2.7845199
O	-1.3489455	-2.1144302	0.7851431	H	-1.2959744	0.0239171	2.5459800
N	0.3023582	-0.4077451	-1.0811254	H	-1.5408403	1.7413520	2.3360538
C	1.6739178	-0.1727901	0.9527051	C	-0.9269336	-0.3064940	-1.7735889
C	1.9158355	-1.3519733	1.8092092	C	1.2534459	-1.3695465	-1.5966072
C	3.0565948	-1.6703494	2.5320503	H	1.0482152	-2.4155062	-1.3335308
H	3.9143236	-1.0109382	2.5288367	H	2.2599085	-1.1292594	-1.2547451
C	3.0590496	-2.8555893	3.2476623	H	1.2663355	-1.2976086	-2.6822196
H	3.9331187	-3.1362530	3.8203163	C	-1.5017714	-1.3965124	-2.4170824
C	1.9464330	-3.7017906	3.2426718	H	-1.0542023	-2.3772424	-2.3260940
H	1.9789931	-4.6199523	3.8141954	C	-2.6550735	-1.2453493	-3.1702178
C	0.8093296	-3.3802262	2.5212093	H	-3.0909199	-2.1058123	-3.6605013
H	-0.0574402	-4.0276733	2.5149585	C	-2.6873357	1.0870596	-2.6350166

H	-3.1590860	2.0592660	-2.7056985	C	-0.2363965	4.4515793	-1.3378665
C	-3.2557296	-0.0016291	-3.2760625	H	-0.1717955	5.3850394	-1.8806820
H	-4.1624844	0.1215399	-3.8529739	C	0.2314794	4.3618695	-0.0372057
C	-1.5193929	0.9555974	-1.8918023	H	0.6703965	5.2247987	0.4460066
C	-0.8856038	2.1230087	-1.2642349	C	0.1581815	3.1580026	0.6451249
C	-0.7872062	3.3332338	-1.9421020	H	0.5464610	3.0973386	1.6529220
H	-1.1441852	3.3944489	-2.9626827	C	-0.3956977	2.0332993	0.0438698

Table S6: Coordinates of the calculated structure of **9** (PBEh-3c/def2-mSVP).

	x	y	z	C	3.3060303	1.3140453	-2.3583168
C	-2.0918727	-0.2780746	0.3139934	C	2.0460323	1.0037192	-1.8717879
C	-3.4484743	-0.5116682	0.6325360	O	3.4763815	-0.8528444	2.2789452
C	-4.0430139	-1.7377125	0.2630840	C	1.2107163	-0.5870565	1.4047889
C	-3.3040549	-2.6817100	-0.3875845	O	0.5531064	-1.0460481	2.2896346
C	-1.9529494	-2.4621986	-0.6998517	H	-5.0823063	-1.9160625	0.5064898
C	-1.3428092	-1.2695698	-0.3683192	H	-3.7532284	-3.6261713	-0.6655792
C	-1.4791023	0.9475691	0.6773468	H	-1.4116836	-3.2509899	-1.1993295
C	-2.2202611	1.8935163	1.3558425	H	-1.7848103	2.8295008	1.6703488
C	-3.5701043	1.6561374	1.6604186	H	-4.1239298	2.4203569	2.1898379
C	-4.1793997	0.4862635	1.3130037	H	-5.2187027	0.3074584	1.5560350
N	-0.1596681	1.1653641	0.3032297	H	1.5024850	2.4255995	0.4997915
N	-0.0268095	-0.9878503	-0.7104093	H	-0.0420383	3.2355323	0.5166392
C	0.4803059	2.3409975	0.8549018	H	0.4933139	2.3474213	1.9508097
C	0.7538227	-2.0910038	-1.2298230	H	1.7625446	-1.7697632	-1.4695713
C	2.7464028	-0.4862546	1.4010770	H	0.3112986	-2.4478741	-2.1594580
C	0.6795712	0.0038935	0.0777540	H	0.8160718	-2.9362870	-0.5349592
C	3.0968460	0.1394733	0.1187265	H	5.2430060	0.2317933	0.2216664
C	1.9549505	0.4130023	-0.6229326	H	5.4260475	1.2955982	-2.0201575
C	4.3622785	0.4505355	-0.3676588	H	3.4043163	1.7762437	-3.3318680
C	4.4565013	1.0409947	-1.6135549	H	1.1531891	1.2141231	-2.4457394

Table S7: Coordinates of the calculated structure of **4** (PBEh-3c/def2-mSVP).

	x	y	z	C	1.8822195	-1.8525960	-1.2674810
O	0.1012344	-0.1716794	-1.1422435	C	0.1927053	-3.2139524	-2.3436646
N	1.4379478	-2.6074102	-2.4137465	C	2.3709826	0.5436590	-1.4050476
O	4.2659477	-2.4094540	-1.4192666	C	-0.3198703	-3.5504047	-1.0651301
N	1.6265819	-2.5633242	-0.0410150	C	3.5931023	-0.1130416	-1.4814309
C	1.2683442	-0.4302234	-1.2541337	C	0.4054055	-3.2023868	0.1027089

C	-0.5382162	-3.5366885	-3.4682933	H	3.4584396	3.7134825	-1.6624309
H	-0.1944825	-3.2739294	-4.4571772	C	-1.7593208	-4.2199078	-3.3492896
C	4.7808896	0.5908378	-1.6212298	H	-2.3058887	-4.4649118	-4.2506690
H	5.7281672	0.0713082	-1.6788832	C	-0.1106115	-3.5361018	1.3384203
C	3.4072180	-1.5746734	-1.3962290	H	0.4025103	-3.2740806	2.2511820
C	2.2972541	1.9273076	-1.4679495	C	-2.2621025	-4.5663296	-2.1294995
H	1.3420518	2.4315937	-1.4076152	H	-3.2045815	-5.0917273	-2.0460121
C	1.8734365	-2.1520200	-3.7143075	C	-2.0409582	-4.5716912	0.3251264
H	1.2137227	-1.3923881	-4.1495476	H	-2.9823732	-5.0987808	0.4095643
H	1.9200555	-2.9972900	-4.3999540	C	-1.3277585	-4.2289316	1.4364775
H	2.8784625	-1.7415173	-3.6732630	H	-1.7018371	-4.4817085	2.4200739
C	-1.5512373	-4.2339143	-0.9553604	C	2.2366700	-2.0399241	1.1605056
C	4.7096623	1.9720259	-1.6847123	H	3.1802718	-1.5472755	0.9428456
H	5.6159472	2.5526734	-1.7943593	H	2.4706684	-2.8563471	1.8433001
C	3.4803939	2.6330061	-1.6094698	H	1.5955757	-1.3234130	1.6861574

Table S8: Coordinates of the calculated structure of **15** (PBEh-3c/def2-mSVP).

	x	y	z				
				O	-0.5312071	-2.0584058	2.7490470
C	-3.9284140	-0.4846511	-0.1698764	O	-0.8664480	0.5643530	-1.1818844
C	-5.1520143	-0.2026911	-0.8169551	C	4.5087746	0.9160071	-0.2887359
C	-5.6353065	-1.0956048	-1.7980847	C	5.4736070	1.4899983	0.5387561
C	-4.9151805	-2.2099342	-2.1154369	C	6.6100103	2.0688824	0.0075222
C	-3.6903166	-2.4905871	-1.4890947	C	6.8020819	2.0798576	-1.3721604
C	-3.1951093	-1.6482502	-0.5148397	C	5.8462304	1.5093733	-2.2097479
C	-3.4338740	0.3958979	0.8253260	C	4.7118342	0.9358527	-1.6683631
C	-4.1460631	1.5374426	1.1289129	C	7.9758070	2.6752743	-1.9256540
C	-5.3640163	1.8067712	0.4837471	N	8.9228122	3.1554868	-2.3706343
C	-5.8647703	0.9645690	-0.4652176	H	-6.5748859	-0.8822324	-2.2908907
N	-2.2648163	0.0487184	1.4874545	H	-5.2793600	-2.8940877	-2.8707272
N	-2.0153965	-1.9134390	0.1639052	H	-3.1535655	-3.3766547	-1.7922264
C	-1.7107651	1.0268044	2.3958405	H	-3.7888599	2.2456003	1.8610480
C	-1.1923165	-2.9851333	-0.3496905	H	-5.9029200	2.7069991	0.7489091
C	-1.3363906	-0.8112724	0.7951539	H	-6.8033509	1.1798471	-0.9591369
C	-0.2897827	-1.3576465	1.8081424	H	-0.8330728	0.6399611	2.9059932
C	-0.4671384	-0.0124811	-0.2079460	H	-1.4324875	1.9660998	1.9037989
C	1.0360923	-0.8567962	1.3985403	H	-2.4374263	1.2523048	3.1753811
C	0.9389924	-0.0860715	0.2483073	H	-0.2912241	-3.1114677	0.2441159
C	2.2635856	-1.0657778	2.0108883	H	-1.7321214	-3.9294473	-0.2853074
C	3.3801237	-0.4813327	1.4438274	H	-0.8918027	-2.8305284	-1.3921923
C	3.2944939	0.3050477	0.2820537	H	2.3427460	-1.6747677	2.9016257
C	2.0555293	0.5007565	-0.3214624	H	4.3514815	-0.6515595	1.8905020

H	1.9524541	1.1206689	-1.2032969	H	5.9976491	1.5113258	-3.2803076
H	5.3226990	1.5110795	1.6102421	H	3.9867413	0.4756451	-2.3268636
H	7.3466572	2.5201958	0.6576925				

Table S9: Coordinates of the calculated structure of **14** (PBEh-3c/def2-mSVP).

	x	y	z	C	-2.1309494	1.4338467	-0.3046697
C	0.4818473	-0.9029057	2.1048145	C	-0.8652800	1.0960663	-0.7648482
C	1.2848451	-1.8959026	1.5471196	C	-0.6347790	1.6532460	-2.1128109
C	2.1217432	-2.6628226	2.3365119	C	-2.5604083	1.0133080	0.9453769
C	2.1755946	-2.4496586	3.7116702	C	-1.6951849	0.2538472	1.7101191
C	1.3785468	-1.4558955	4.2788783	C	-0.4094954	-0.0916827	1.2574774
C	0.5443670	-0.6968431	3.4839291	C	0.0057644	0.3392202	0.0004662
C	3.0351583	-3.2364489	4.5740897	O	0.3541241	1.5332975	-2.7777820
N	3.1574524	-3.1653331	5.8543957	O	-3.9627562	2.6854352	-1.2026975
N	4.0744440	-4.0998173	6.2160455	H	1.2368578	-2.0942324	0.4841348
C	4.4578073	-4.6879960	5.1348963	H	2.7239916	-3.4332999	1.8747842
O	3.8343897	-4.1844133	4.0541314	H	1.4253345	-1.2809551	5.3451695
C	5.4230710	-5.7612531	4.9884569	H	-0.0462922	0.0871955	3.9401187
C	5.7957191	-6.2410611	3.7345909	H	5.3694539	-5.8181996	2.8349180
C	6.7219815	-7.2660194	3.6344636	H	7.0088011	-7.6339903	2.6586278
C	7.2797723	-7.8181292	4.7776119	H	8.0023285	-8.6190435	4.6952759
C	6.9093879	-7.3407599	6.0278951	H	7.3416540	-7.7690745	6.9220917
C	5.9864842	-6.3171692	6.1370291	H	5.6935407	-5.9409083	7.1078862
C	-3.4144496	3.9694364	-4.3062170	H	-5.9182722	4.6900788	-6.5135111
C	-4.3257489	4.7443988	-5.0575801	H	-5.8936294	2.2358687	-6.7094110
C	-5.2219852	4.0964897	-5.9355726	H	-4.3500753	0.8841989	-5.4030711
C	-5.2038854	2.7366548	-6.0425488	H	-1.8765354	6.4942625	-2.6159454
C	-4.3094894	1.9570476	-5.2917342	H	-3.4358318	7.8149598	-3.9352480
C	-3.4086735	2.5574496	-4.4361913	H	-5.0133651	6.7435824	-5.4926110
C	-2.5043629	4.6032908	-3.4226857	H	-1.8249452	-0.0844415	-3.1480792
C	-2.5366907	5.9766928	-3.2951665	H	-3.5740606	0.0530143	-3.3404165
C	-3.4401479	6.7391484	-4.0528741	H	-2.4992634	0.0194417	-4.7485774
C	-4.3172696	6.1492616	-4.9151629	H	-0.0790666	3.7747539	-1.2821291
N	-1.5860005	3.8155326	-2.7451214	H	-0.1913982	5.2568216	-2.1847252
N	-2.4691789	1.8315440	-3.7203087	H	-1.3882038	4.9056397	-0.9267339
C	-1.9166345	2.4290001	-2.5305369	H	-3.5493319	1.2663402	1.3037228
C	-2.6080123	0.3928022	-3.7307048	H	-2.0230277	-0.1079630	2.6763610
C	-0.7873078	4.4657209	-1.7309083	H	0.9984445	0.1133186	-0.3683297
C	-2.8509179	2.2440056	-1.3081493				

Table S10: Coordinates of the calculated structure of **17** (PBEh-3c/def2-mSVP).

	x	y	z	C			
N	-0.5243816	1.0245467	-0.3790040	C	-3.6142466	-2.3797762	-2.0449788
N	-0.3977334	-1.2161506	0.3940486	C	-2.4547257	-3.1372523	-2.0310884
C	0.1197103	2.1849529	-0.9579512	C	-1.3746720	-2.7385448	-1.2598303
C	0.3729295	-2.2934727	0.9772035	C	-1.4443920	-1.5885213	-0.4818518
C	0.3512870	-0.0366277	0.0565070	C	6.3858971	0.3404081	-0.9961823
C	1.2123016	0.4427590	1.2570958	N	7.4303190	0.3068103	-1.4784348
C	1.4212466	-0.3349677	-1.0304735	H	0.7138597	1.8982333	-1.8255243
C	2.6253346	0.5021508	0.8156509	H	0.7677872	2.7499892	-0.2751389
C	2.7479542	0.0282714	-0.4818472	H	-0.6501391	2.8637891	-1.3185518
C	3.7327910	0.9256343	1.5363060	H	0.8846480	-1.9508198	1.8765558
C	4.9686441	0.8649849	0.9220850	H	1.1213259	-2.7418556	0.3107588
C	5.0914787	0.3857483	-0.3920816	H	-0.3082485	-3.0828837	1.2878208
C	3.9797710	-0.0412329	-1.1100478	H	3.6288643	1.2892068	2.5497185
O	0.8042784	0.7745261	2.3347013	H	5.8573572	1.1851265	1.4487867
O	1.2188635	-0.8352742	-2.1009425	H	4.0729110	-0.4100315	-2.1229288
C	-1.7813072	2.4264227	1.1944188	H	-0.9627483	3.1321589	1.2462767
C	-2.9436932	2.6834848	1.9037232	H	-3.0209722	3.5850067	2.4968854
C	-3.9922236	1.7790716	1.8660692	H	-4.8979807	1.9677040	2.4265475
C	-3.8741306	0.6270166	1.1056011	H	-4.6878845	-0.0869915	1.0810618
C	-2.7215563	0.3635603	0.3736605	H	-4.5870152	-0.6289215	-1.2901946
C	-1.6592451	1.2718550	0.4303337	H	-4.4569037	-2.6785514	-2.6538500
C	-2.6192833	-0.8280051	-0.4797722	H	-2.3806649	-4.0335682	-2.6325593
C	-3.6871422	-1.2311664	-1.2739800	H	-0.4682701	-3.3288032	-1.2746026

Table S11: Coordinates of the calculated structure of **16** (PBEh-3c/def2-mSVP).

	x	y	z	C			
C	-3.2419180	0.0083426	-0.1436453	C	-0.5321415	-2.1340625	-1.5022088
C	-4.5794066	-0.1200814	0.2923219	C	3.9492510	-0.2549983	1.1152290
C	-5.2188999	-1.3753164	0.1952539	C	4.2787363	0.0935681	-0.2297205
C	-4.5397824	-2.4461909	-0.3079742	C	5.6413813	0.1929064	-0.5951386
C	-3.2068986	-2.3311383	-0.7338693	C	6.6284144	-0.0401163	0.3187741
C	-2.5561824	-1.1157356	-0.6699952	C	6.3031527	-0.3843279	1.6474271
C	-2.5847270	1.2619697	-0.0577412	C	4.9980303	-0.4883198	2.0347381
C	-3.2622284	2.3413424	0.4718915	C	2.5960733	-0.3610722	1.5012817
C	-4.5945579	2.2060173	0.8936707	C	1.6228602	-0.1255675	0.5714311
C	-5.2469922	1.0107202	0.8115825	C	1.9489280	0.2186216	-0.7555782
N	-1.2921075	1.3650282	-0.5460749	C	3.2489306	0.3301533	-1.1642134
N	-1.2635434	-0.9419505	-1.1371786	C	0.1564990	-0.1765637	0.7416002
C	-0.5889244	2.6005888	-0.2844363	C	-0.4970529	0.1653236	-0.6223719
				C	0.7250881	0.4175315	-1.5534590

O	-0.4377788	-0.4355712	1.7529609	H	-1.1131324	3.4303003	-0.7577861
O	0.6604225	0.7184456	-2.7115490	H	0.4643326	-1.8921616	-1.8614654
H	-6.2448314	-1.4732545	0.5256249	H	-0.4285375	-2.8431088	-0.6730035
H	-5.0243055	-3.4114071	-0.3779340	H	-1.0376834	-2.6396487	-2.3245300
H	-2.7119858	-3.2147722	-1.1071408	H	5.8909715	0.4578499	-1.6148904
H	-2.7893902	3.3061230	0.5752042	H	7.6669188	0.0382452	0.0266528
H	-5.1005604	3.0733218	1.2974774	H	7.0957846	-0.5666088	2.3605324
H	-6.2728631	0.9137010	1.1423899	H	4.7491533	-0.7513426	3.0551029
H	0.4082905	2.5863401	-0.7157472	H	2.3359530	-0.6267893	2.5188485
H	-0.4912886	2.8194182	0.7849531	H	3.4885480	0.5942472	-2.1872968

Table S12: Coordinates of the calculated structure of **29** (PBEh-3c/def2-mSVP).

	x	y	z	C	0.8349471	0.6072721	9.1147558
N	1.5398975	3.9188138	-2.6117282	C	0.4402322	0.7416601	7.7841629
N	3.6020274	2.6857775	-2.2512746	C	-0.3484081	1.8319624	7.4186081
C	1.1156710	4.8123455	-1.5414527	C	-0.7228929	2.7707620	8.3654198
C	4.9951285	2.5031328	-2.5913607	C	-0.3385729	2.6298292	9.6909378
C	2.9406748	3.7752920	-2.9143796	N	0.8317933	-0.2088333	6.8257609
C	3.6307061	5.1474151	-2.7037744	C	1.2297926	0.2071919	5.5445893
C	2.9546368	3.6486138	-4.4597925	C	0.8124711	-1.5777757	7.1445056
C	3.5856105	5.8687861	-3.9898803	C	-0.2442873	-2.1194358	7.8752125
C	3.1731596	5.0097978	-4.9994448	C	-0.2536068	-3.4672611	8.1937023
C	3.9076778	7.1907610	-4.2567775	C	0.7740542	-4.2994914	7.7741731
C	3.7943690	7.6320685	-5.5650324	C	1.8211154	-3.7639032	7.0382376
C	3.3812606	6.7673006	-6.5810951	C	1.8497783	-2.4134685	6.7324614
C	3.0710574	5.4438969	-6.3112118	C	0.8244328	-0.4940575	4.4103534
O	4.1531315	5.5172273	-1.6875925	C	1.2266286	-0.0850174	3.1524013
O	2.7873695	2.6488564	-5.0981306	C	2.0242948	1.0446587	2.9734020
C	-0.1750829	2.6217408	-3.7392601	C	2.4154030	1.7435058	4.1149291
C	-0.9576894	1.4865149	-3.8530074	C	2.0380960	1.3306924	5.3795298
C	-0.7962900	0.4231306	-2.9662106	C	-7.1327025	-5.0607924	-5.1369578
C	0.1602496	0.5406691	-1.9615014	C	-6.1678343	-4.9599554	-4.1485208
C	0.9491665	1.6780153	-1.8327367	C	-4.9258642	-4.3948754	-4.4347094
C	0.7803050	2.7229255	-2.7404193	C	-4.6746609	-3.9275497	-5.7241025
C	1.9158915	1.8111051	-0.7305940	C	-5.6532366	-4.0142960	-6.7002765
C	1.5565633	1.4156187	0.5518776	C	-6.8856795	-4.5846268	-6.4163628
C	2.4357473	1.4838676	1.6289114	N	-3.9402730	-4.2996095	-3.4366195
C	3.7112193	1.9853526	1.3855804	C	-3.7290653	-5.3761394	-2.5567872
C	4.0797306	2.4122266	0.1226720	C	-3.1657486	-3.1354017	-3.3209679
C	3.1998732	2.3347627	-0.9541450	C	-1.8036428	-3.2119499	-3.0329734
C	0.4374181	1.5399974	10.0581008	C	-1.0474305	-2.0613205	-2.9096985

C	-1.6104817	-0.7984764	-3.0885273	H	-0.6668531	1.9436883	6.3902863
C	-2.9705637	-0.7338900	-3.3873593	H	-1.3335645	3.6119627	8.0643463
C	-3.7412554	-1.8769079	-3.4918851	H	-0.6400951	3.3606898	10.4290060
C	-3.7227293	-6.6862493	-3.0330789	H	-1.0585442	-1.4818836	8.1944320
C	-3.5237048	-7.7440978	-2.1615660	H	-1.0806784	-3.8714578	8.7626941
C	-3.3082726	-7.5149718	-0.8103923	H	0.7591678	-5.3531633	8.0179183
C	-3.3053559	-6.2110598	-0.3364846	H	2.6334813	-4.3988806	6.7095738
C	-3.5240351	-5.1479666	-1.1967782	H	2.6784086	-2.0029160	6.1701114
H	1.5412278	4.5817683	-0.5614217	H	0.1988222	-1.3710136	4.5146420
H	1.3509692	5.8493152	-1.7844248	H	0.9184710	-0.6649313	2.2913870
H	0.0324195	4.7461828	-1.4656021	H	3.0190177	2.6369573	4.0151577
H	5.6696902	3.2663179	-2.1869230	H	2.3631679	1.8915722	6.2461964
H	5.1128927	2.4915502	-3.6750397	H	-8.0912755	-5.5028653	-4.8985491
H	5.3276969	1.5311737	-2.2305502	H	-6.3755453	-5.3216305	-3.1497903
H	4.2349347	7.8516779	-3.4651638	H	-3.7109820	-3.4950655	-5.9601593
H	4.0341248	8.6584784	-5.8091518	H	-5.4426635	-3.6456955	-7.6957410
H	3.3105292	7.1393694	-7.5946887	H	-7.6446817	-4.6575597	-7.1834503
H	2.7621515	4.7655594	-7.0953425	H	-1.3320761	-4.1787229	-2.9139068
H	-0.2935778	3.4418773	-4.4353055	H	0.0135720	-2.1502134	-2.7120908
H	-1.6757170	1.4103484	-4.6595534	H	-3.4479329	0.2314888	-3.5013084
H	0.2908478	-0.2707128	-1.2552927	H	-4.7999381	-1.7929958	-3.7001628
H	0.5438178	1.0676586	0.7179084	H	-3.8750902	-6.8744575	-4.0879484
H	4.4330196	2.0391325	2.1908813	H	-3.5225720	-8.7552982	-2.5470510
H	5.0724015	2.8152536	-0.0244654	H	-3.1444032	-8.3431507	-0.1343090
H	0.7510198	1.4196196	11.0868534	H	-3.1461233	-6.0169999	0.7161845
H	1.4531593	-0.2308685	9.4092175	H	-3.5349122	-4.1353262	-0.8148388

Table S13: Coordinates of the calculated structure of **13** (PBEh-3c/def2-mSVP).

	x	y	z	C	-1.2589935	-0.0000100	-2.3586823
C	0.0000096	0.6934252	0.8442529	C	1.2589920	-0.0000100	-2.3586949
C	0.0000095	-0.6933668	0.8442466	H	-0.0000006	-2.4942220	2.0216035
C	0.0000027	-1.4123920	2.0301825	H	-0.0000138	-1.2266929	4.1617204
C	-0.0000051	-0.6987858	3.2172073	H	-0.0000136	1.2266481	4.1617549
C	-0.0000050	0.6987702	3.2172255	H	-0.0000004	2.4942436	2.0216647
C	0.0000029	1.4124135	2.0302167	H	-1.2751622	0.8848437	-2.9943221
C	0.0000076	1.2006471	-0.5470406	H	-1.2751540	-0.8848888	-2.9942874
C	0.0000037	0.0000095	-1.4916397	H	-2.1699630	-0.0000029	-1.7586431
C	0.0000077	-1.2006131	-0.5470262	H	1.2751456	-0.8848888	-2.9943002
O	0.0000042	2.3567485	-0.8762332	H	1.2751539	0.8848437	-2.9943350
O	0.0000045	-2.3567172	-0.8762054	H	2.1699673	-0.0000028	-1.7586649

Table S14: Coordinates of the calculated structure of **12** (PBEh-3c/def2-mSVP).

	x	y	z	H	0.5441654	3.3685188	-0.5321124
C	0.4768486	2.4411598	-1.0810229	H	1.1559250	3.3748160	-2.8872820
C	0.8397735	2.4426057	-2.4368005	H	1.0968569	1.3112268	-4.2270714
C	0.8131684	1.2998036	-3.1826629	H	0.6272725	-1.1068180	-4.3783531
C	0.4068095	0.0834906	-2.5910428	H	-0.1187364	-3.1885040	-3.2981554
C	0.0345323	0.0704082	-1.2263111	H	-0.7406911	-3.2370606	-0.9456942
C	0.0646581	1.2734370	-0.4668705	H	-1.7593912	0.1619068	2.9330318
C	0.3438422	-1.1160427	-3.3338585	H	-0.5209572	-1.0012614	3.4341035
C	-0.0752597	-2.2670267	-2.7316965	H	-0.1844055	0.6953689	3.5433847
C	-0.4439872	-2.2930164	-1.3777369	H	1.8984844	0.3864480	2.2322359
C	-0.4054382	-1.1386275	-0.6185110	H	1.5597866	-1.3397689	2.1235020
N	-0.3386737	1.2089727	0.8537536	H	1.8812826	-0.4109839	0.6613140
N	-0.7885637	-1.0862625	0.7085662	H	-0.8357820	3.2118149	1.0314010
C	-0.1082769	-0.0750476	1.5248419	H	-0.9061063	2.3277734	2.5245008
C	-0.6895376	-0.0503815	2.9336079	H	0.6673233	2.8004700	1.8650286
C	1.3960775	-0.3771488	1.6357865	H	-1.7902364	-2.0963351	2.2387053
C	-0.3357487	2.4345149	1.6076621	H	-2.0062424	-2.7602319	0.6486341
C	-1.2708604	-2.3019134	1.3084342	H	-0.4879122	-3.0463051	1.5066876

10. NMR Spectra

10.1 NMR Experiments

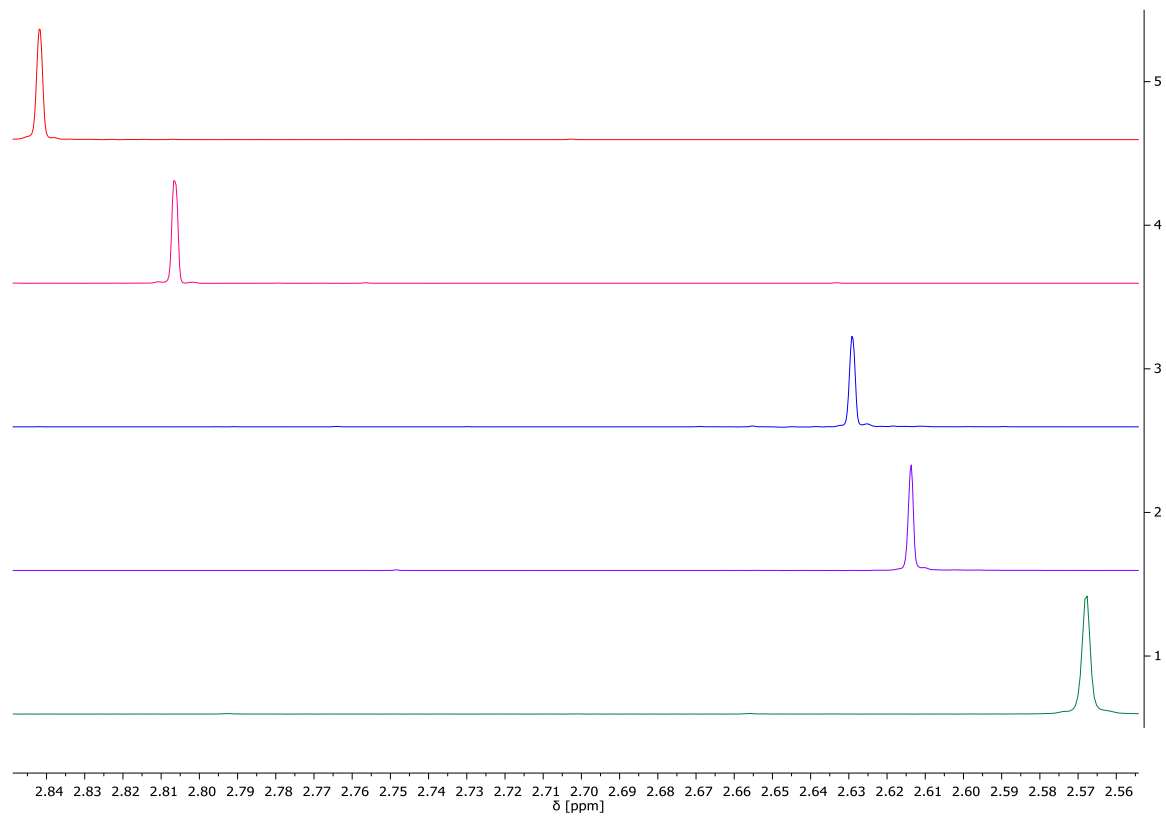


Figure S46: Shift of the methyl groups of the spiro compounds 1 (**5**), 2 (**3**), 3 (**9**), 4 (**4**), 5 (**16**). ¹H NMR-spectra in CDCl₃ (500 MHz).

10.2 Spectra

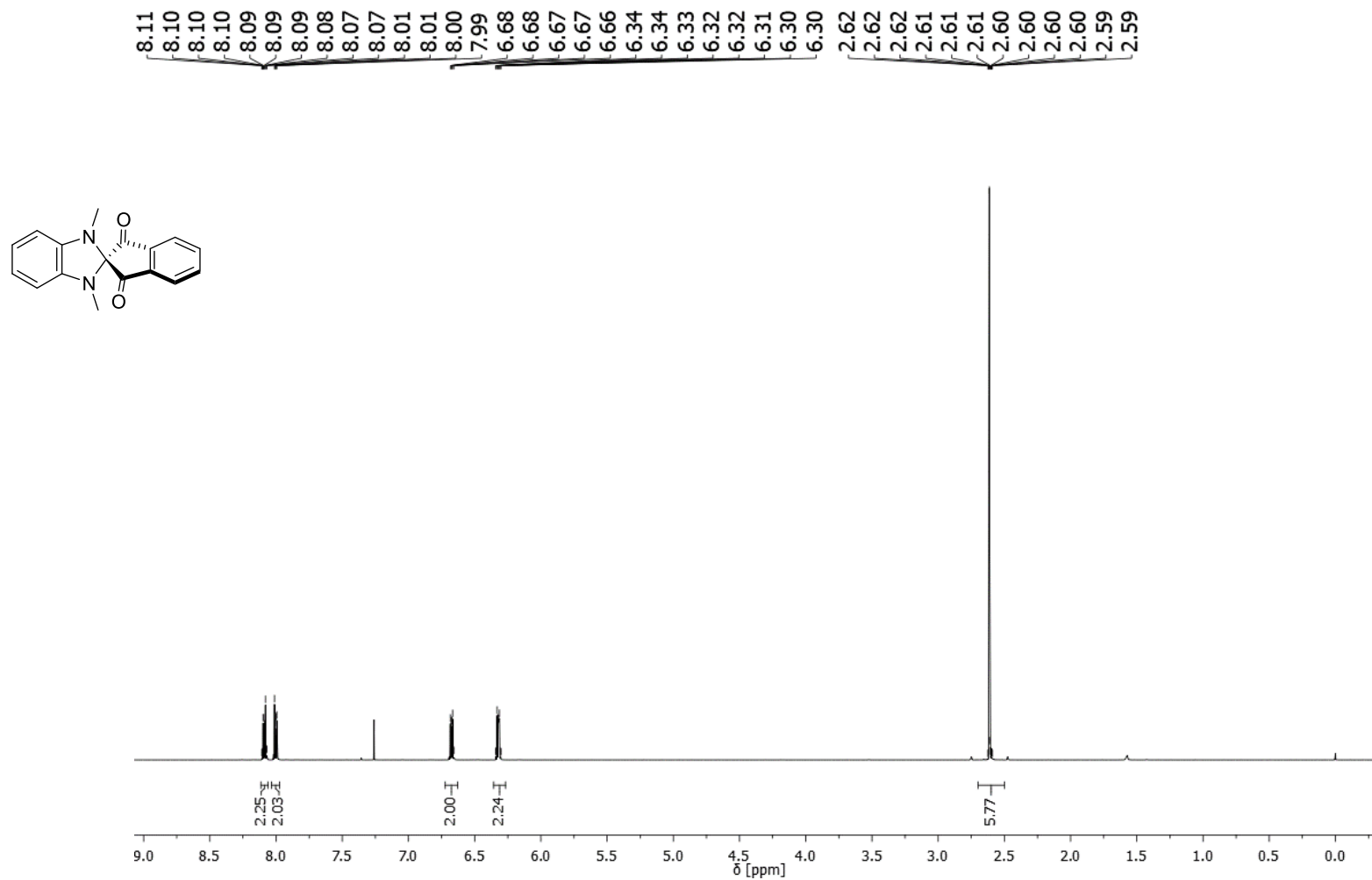


Figure S47: ¹H NMR-spectrum of **3** in CDCl₃ (500 MHz).

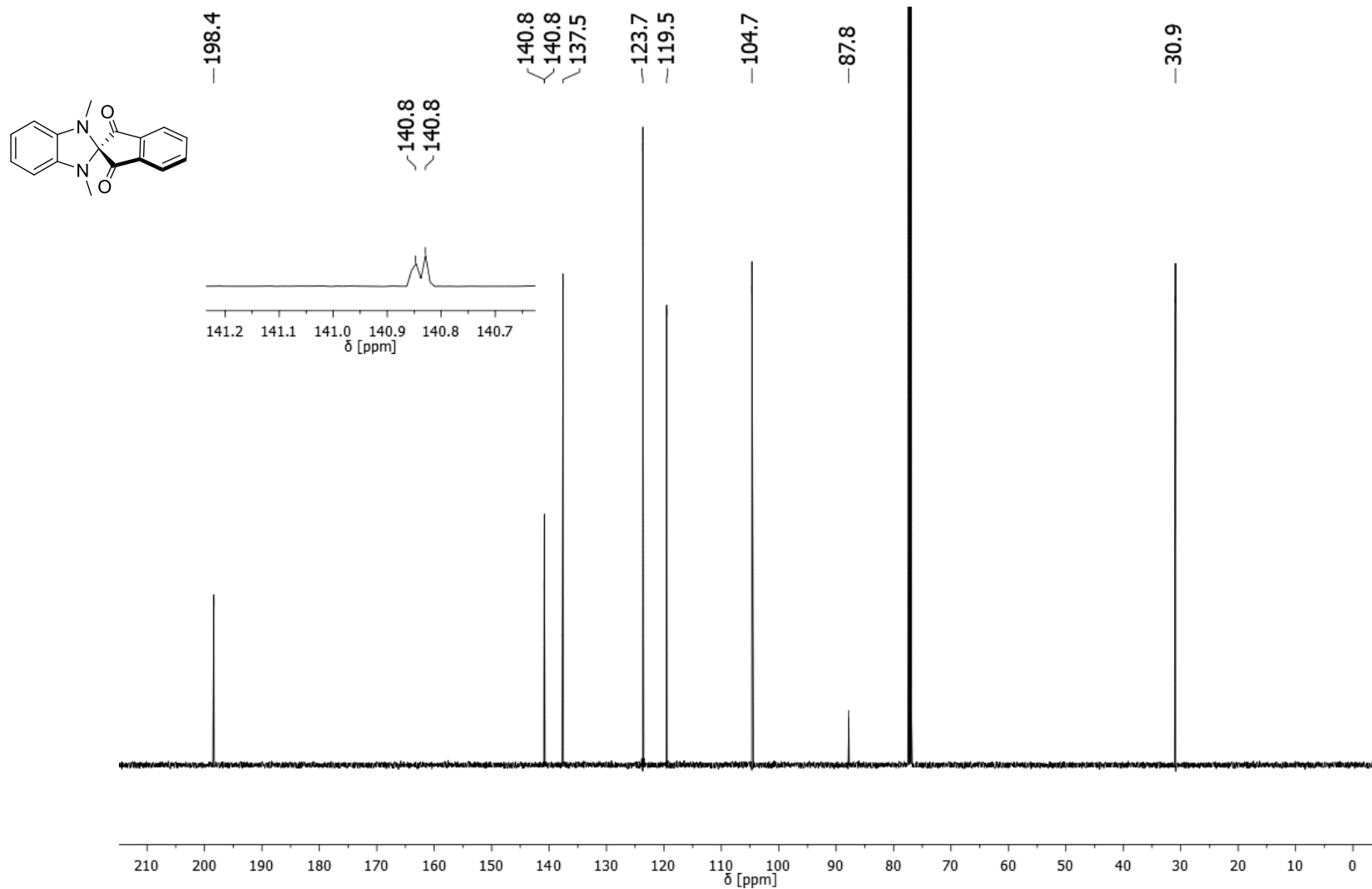


Figure S48: ^{13}C NMR-spectrum of **3** in CDCl_3 (125 MHz).

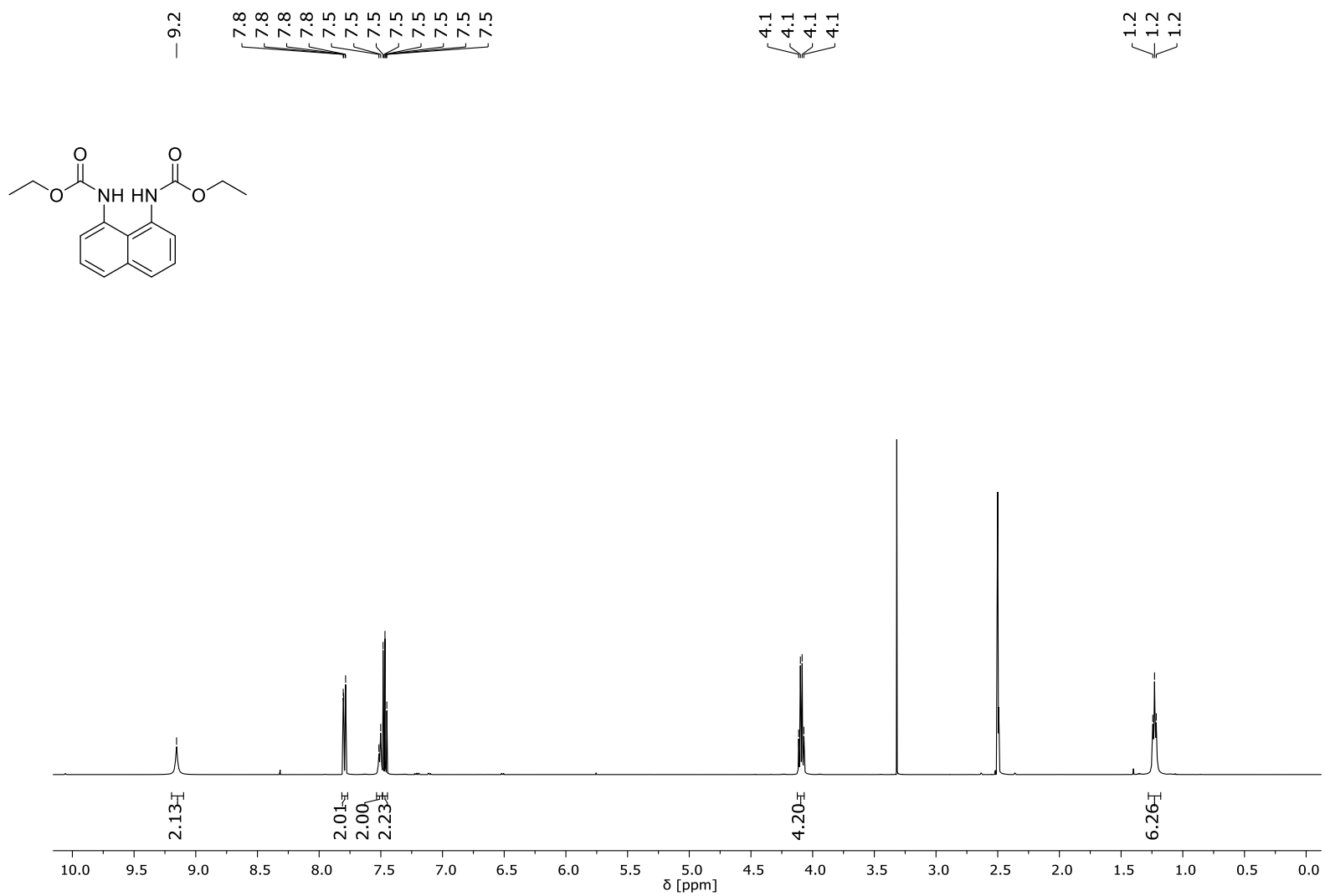


Figure S49: ¹H NMR-spectrum of **30** in DMSO (500 MHz).

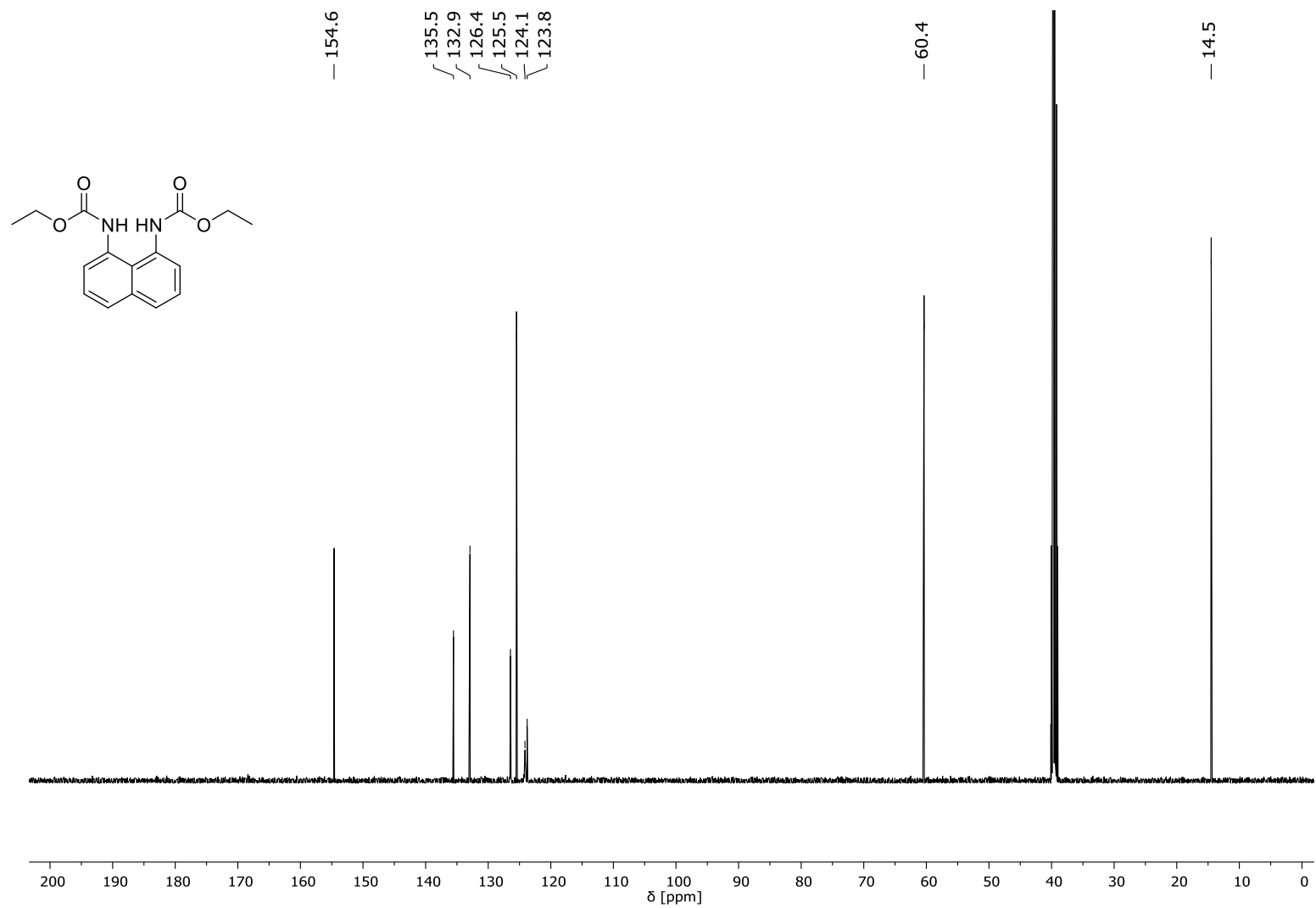


Figure S50: ^{13}C NMR-spectrum of **30** in DMSO (126 MHz).

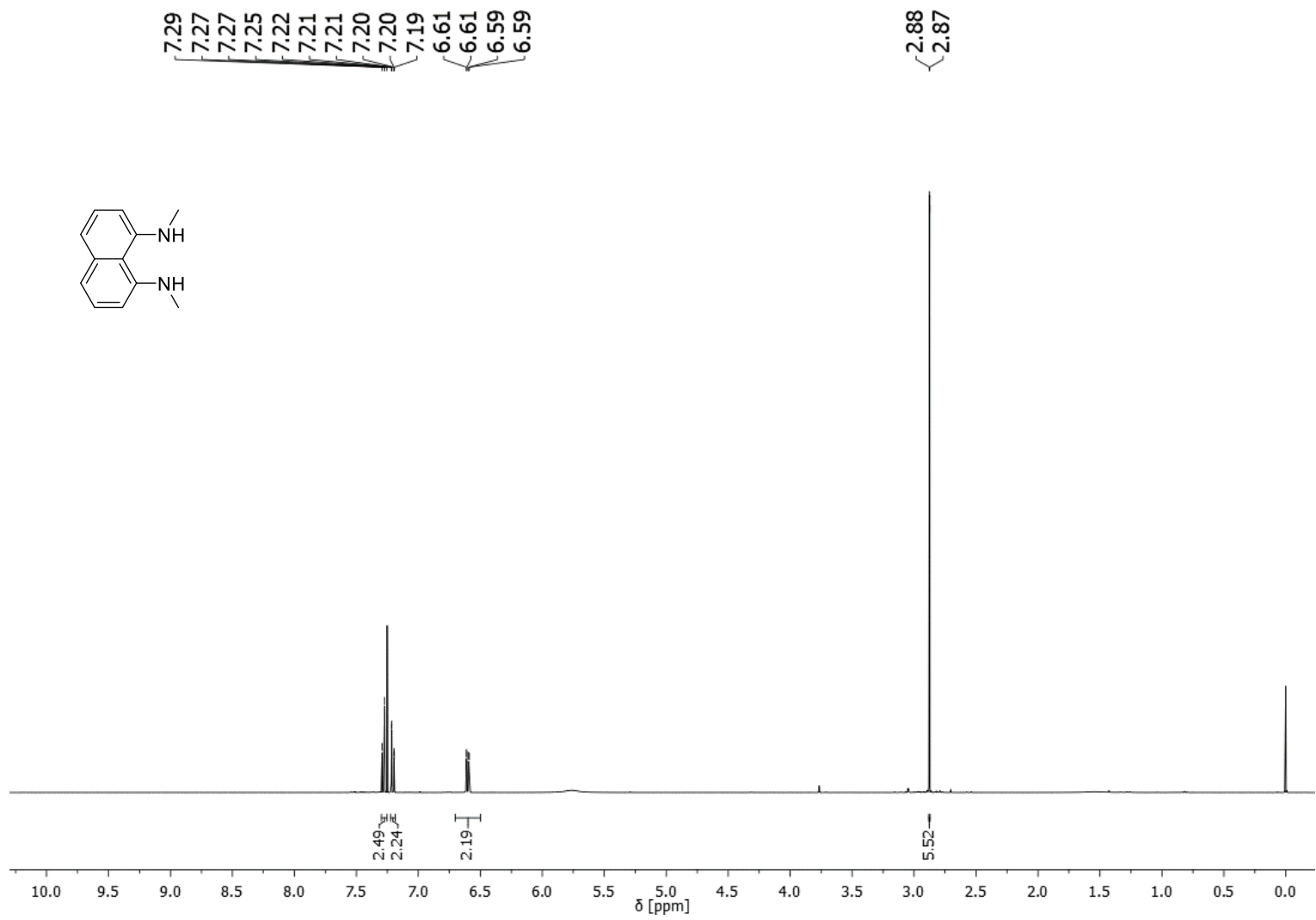


Figure S51: ¹H NMR-spectrum of **7** in CDCl₃ (400 MHz).

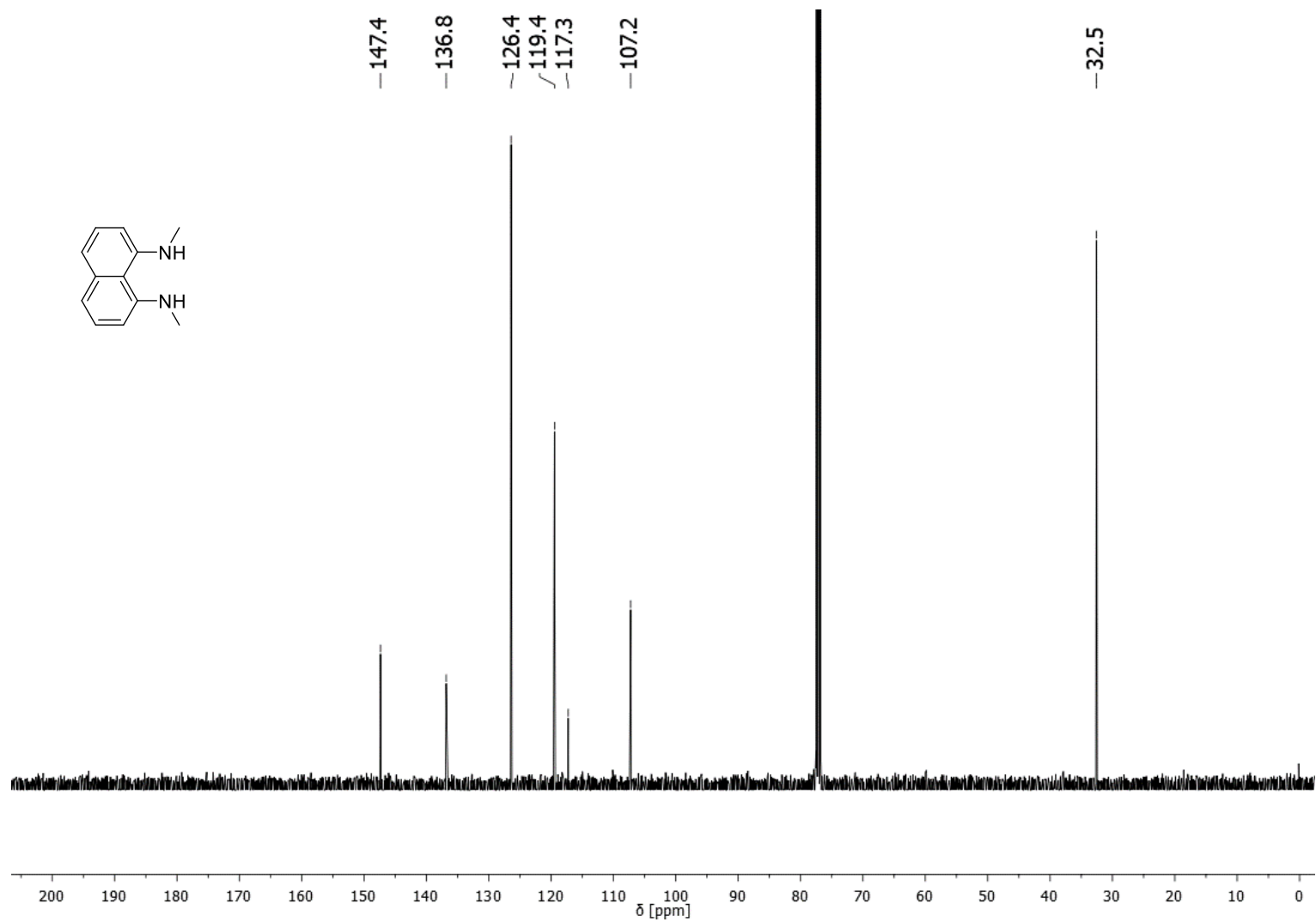


Figure S52: ^{13}C NMR-spectrum of **7** in CDCl_3 (101 MHz).

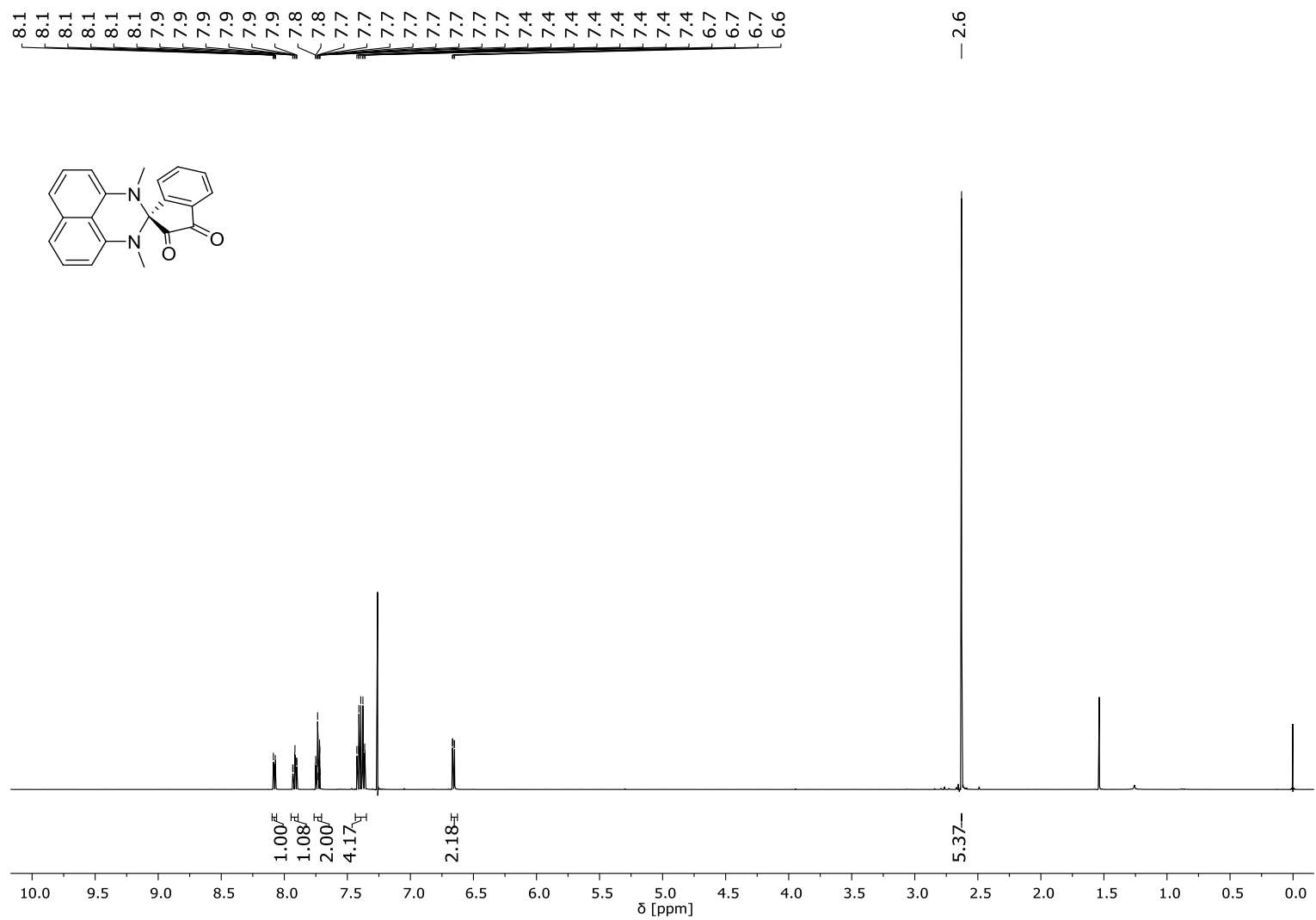


Figure S53: ¹H NMR-spectrum of **9** in CDCl₃ (500 MHz).

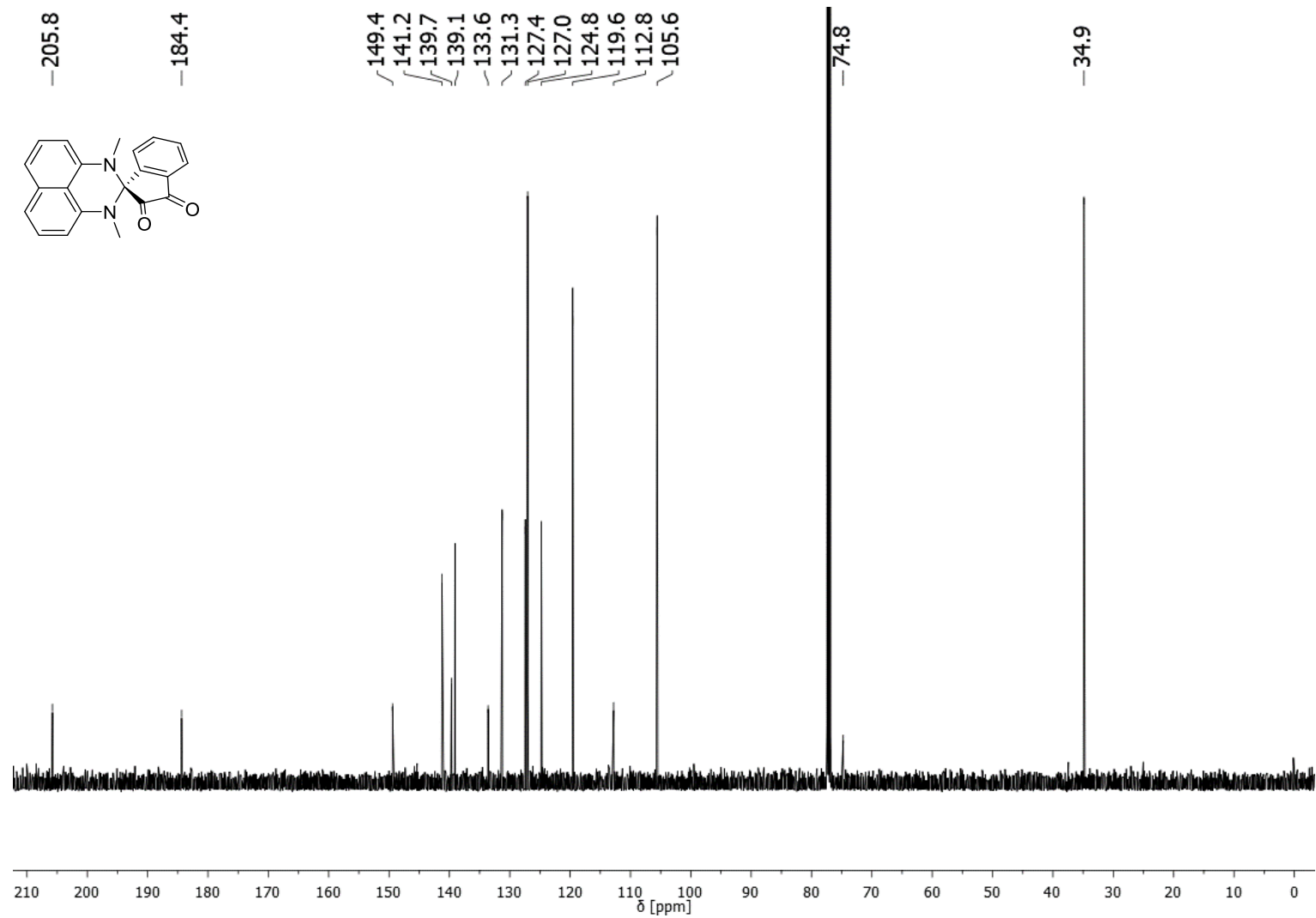


Figure S54: ¹³C NMR-spectrum of **9** in CDCl₃ (126 MHz).

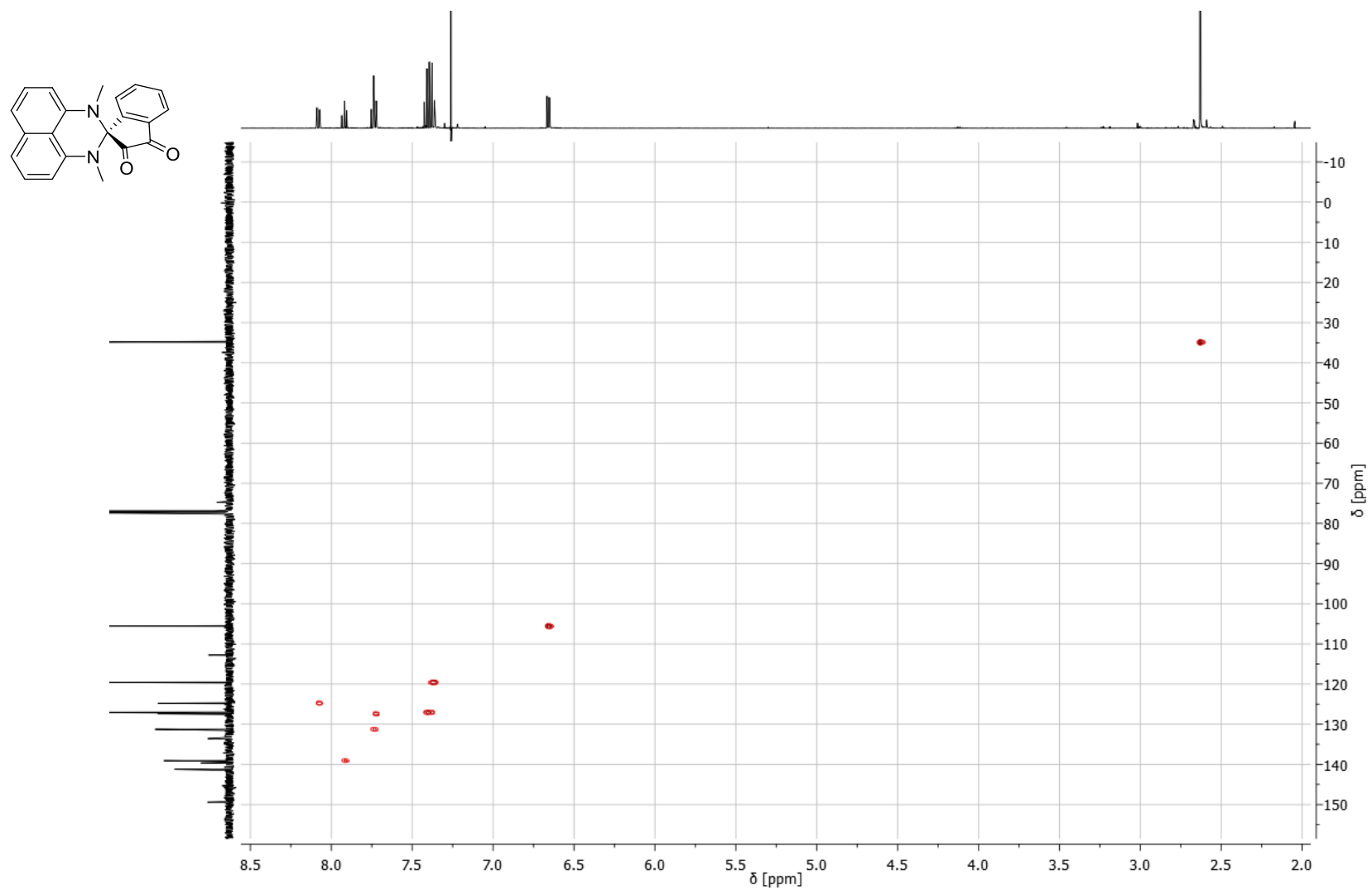


Figure S55: HSQC-spectrum of 9 in CDCl_3 (500/126 MHz).

S100

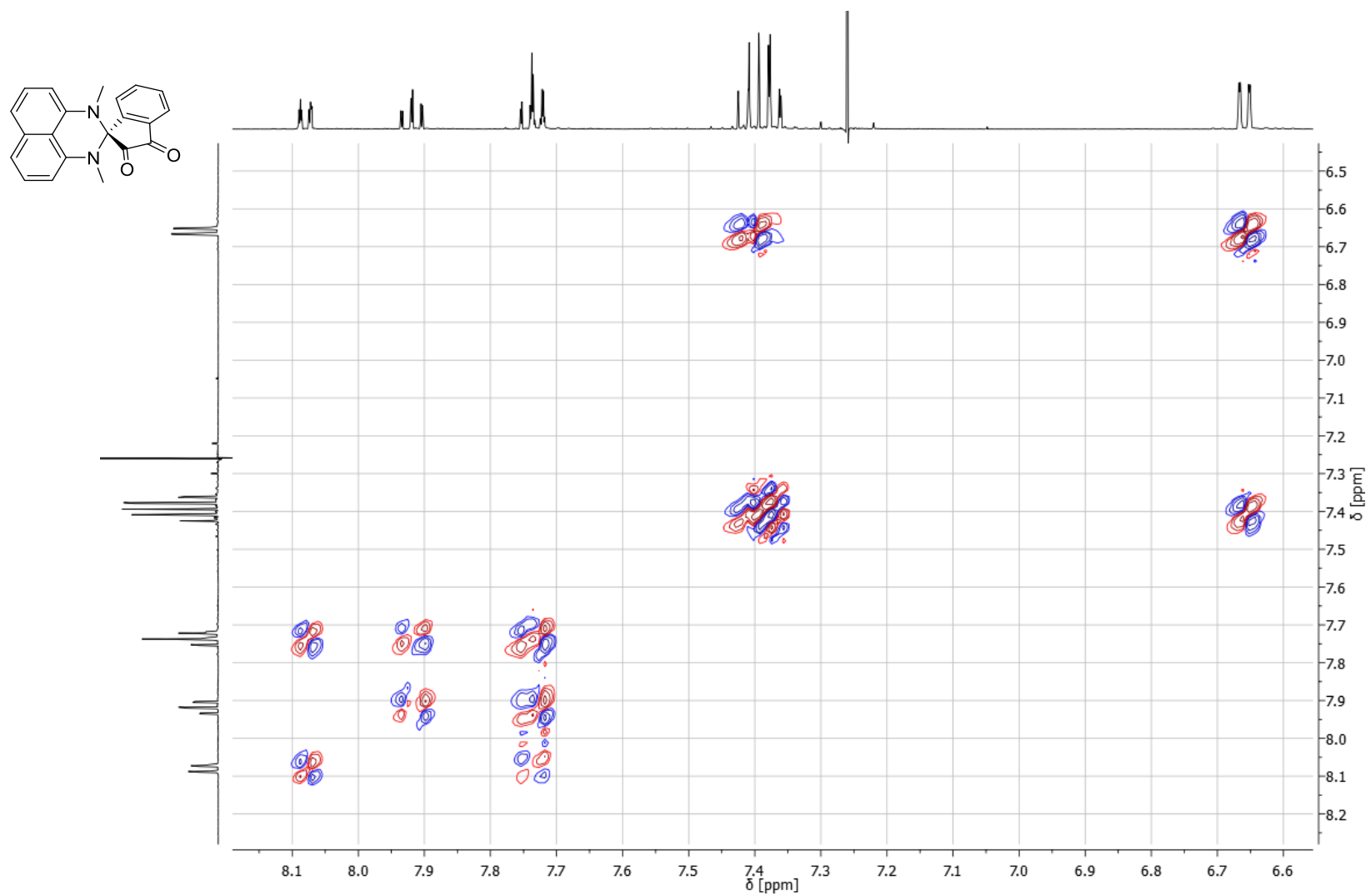


Figure S56: DQF-COSY-spectrum of 9 in CDCl₃ (500 MHz).

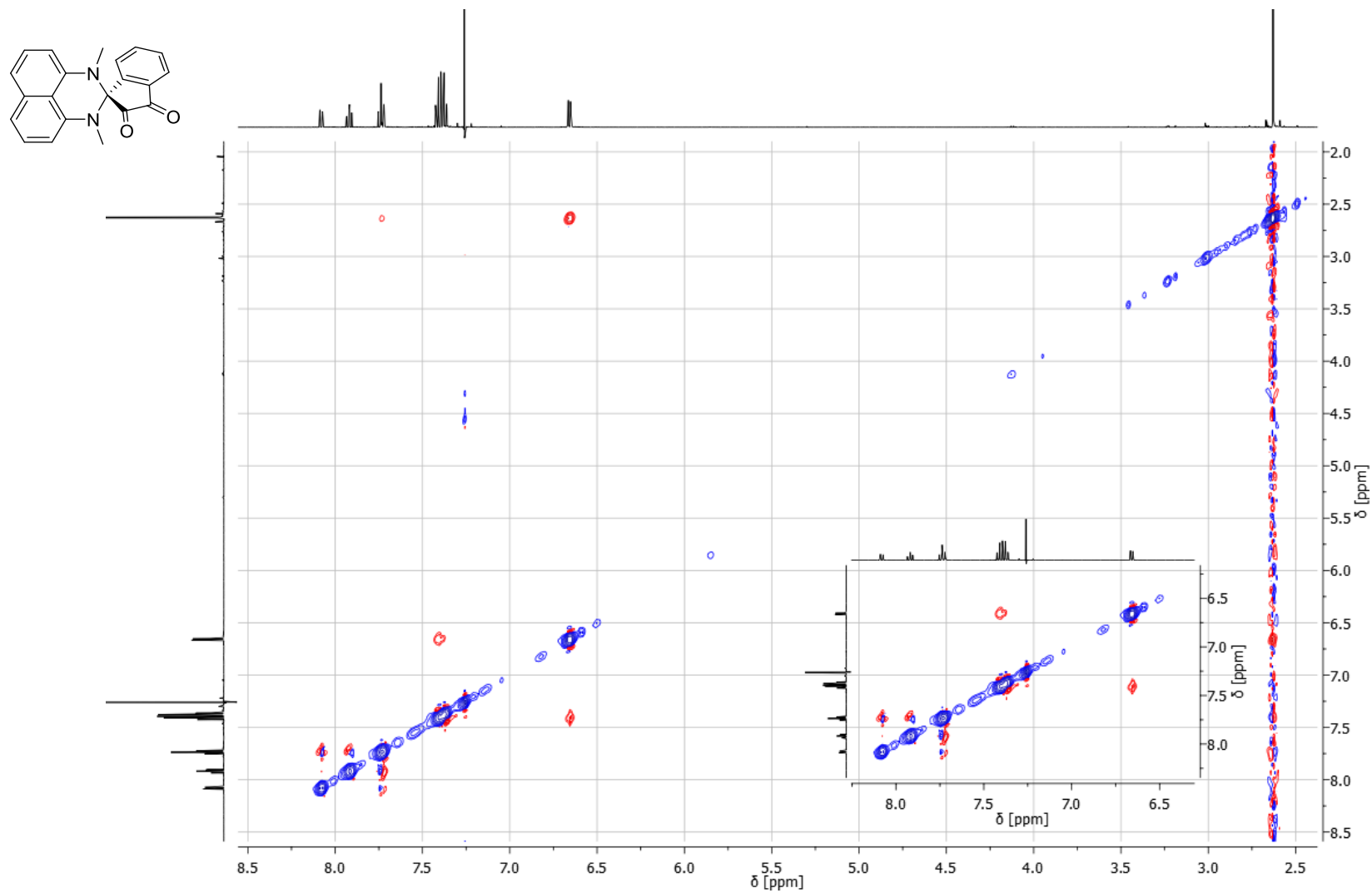


Figure S57: NOESY-spectrum of 9 in CDCl₃ (500 MHz).

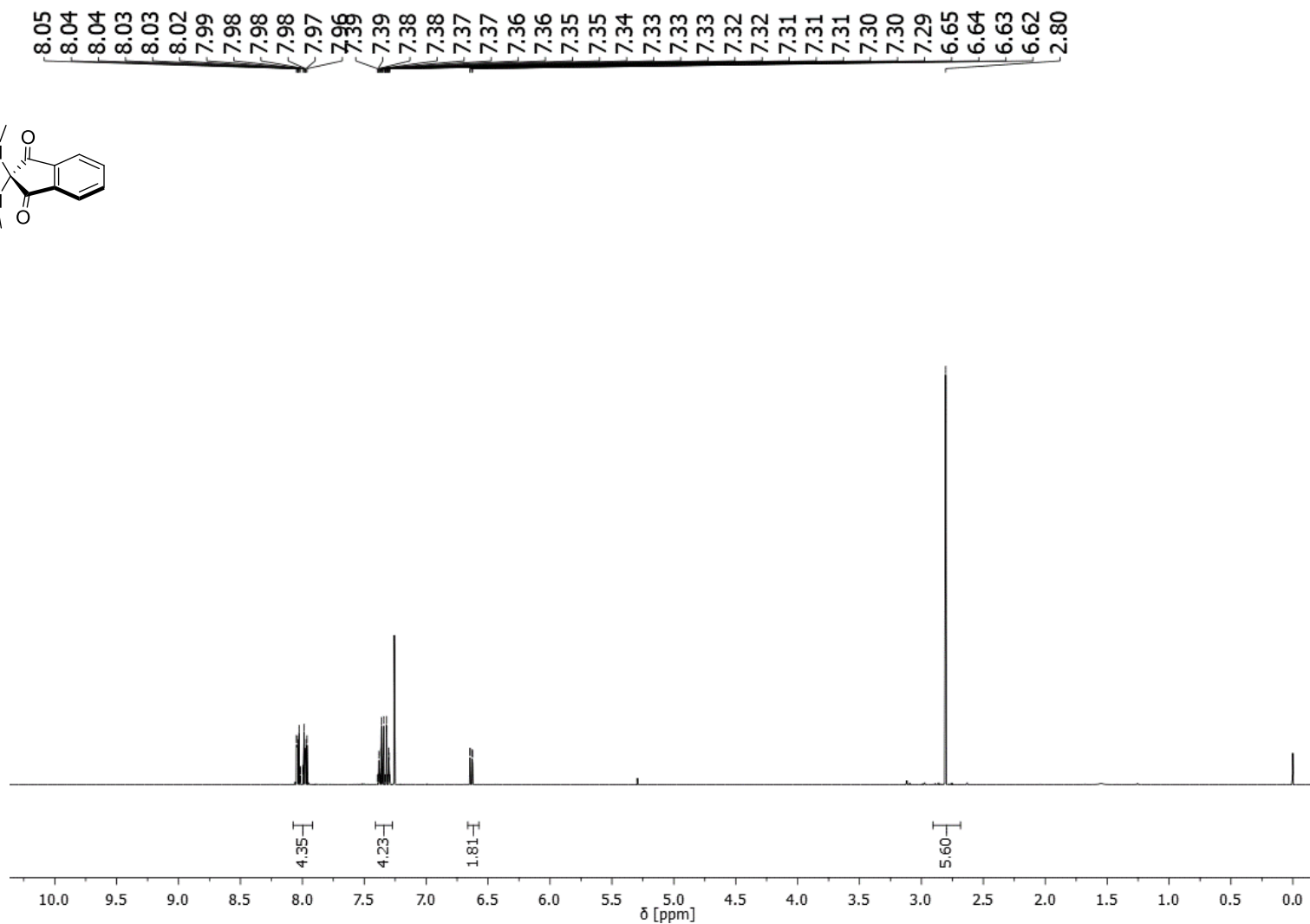
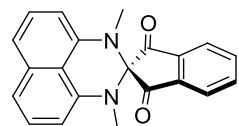


Figure S58: ^1H NMR-spectrum of **4** in CDCl_3 (400 MHz).

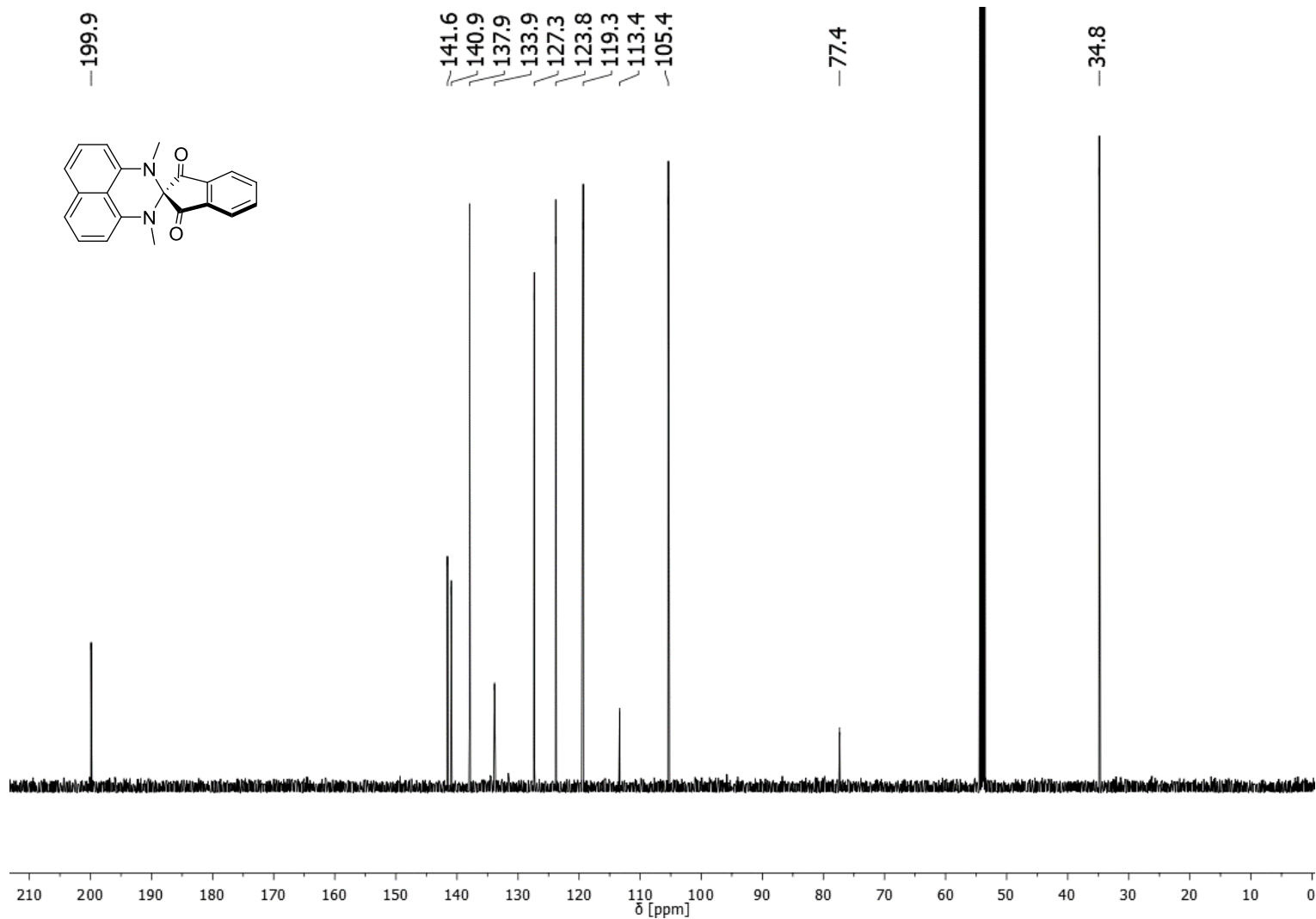


Figure S59: ^{13}C NMR-spectrum of **4** in CH_2Cl_2 (125 MHz).

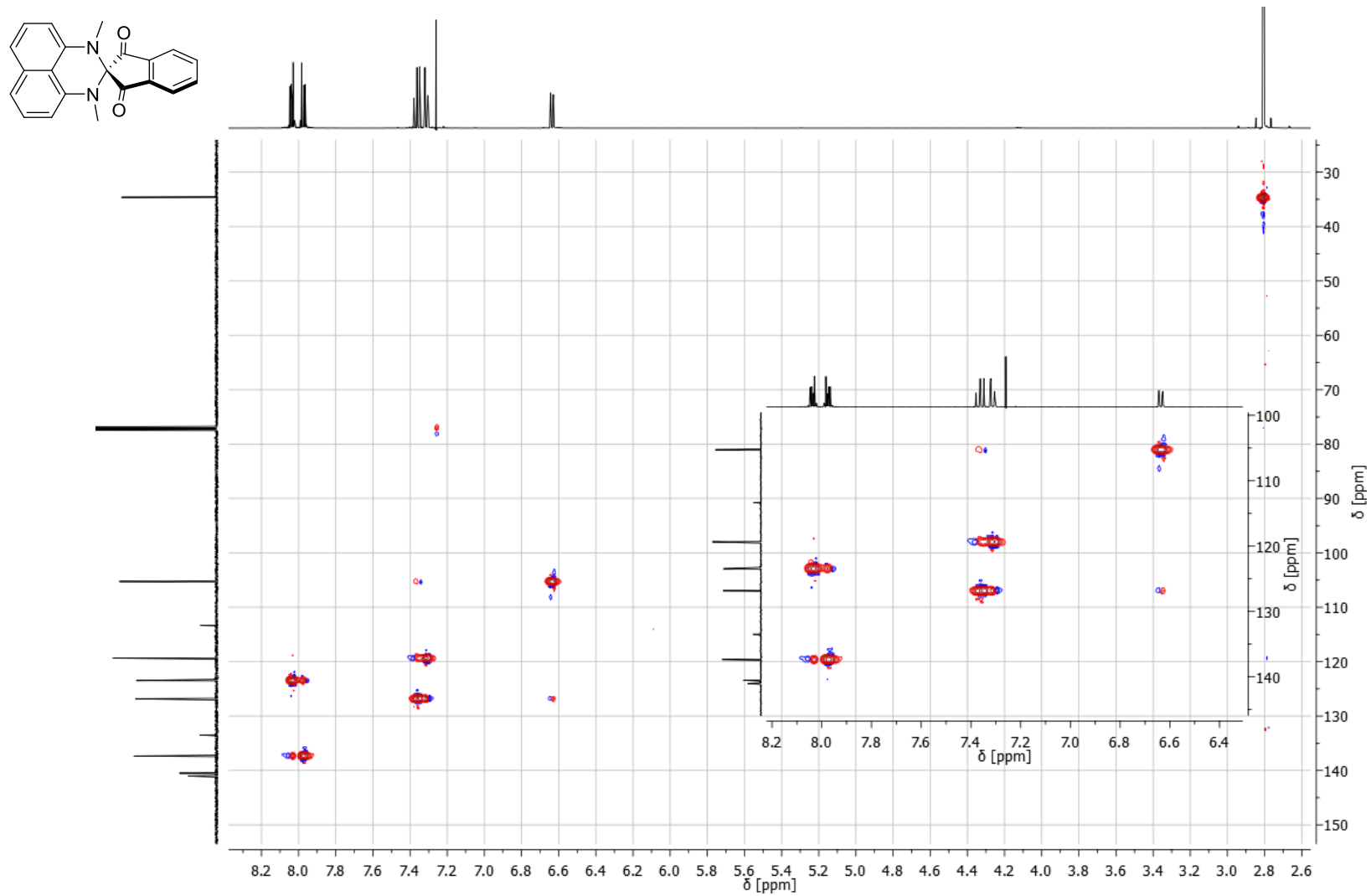


Figure S60: HSQC-spectrum of 4 in CDCl₃ (500/126 MHz).

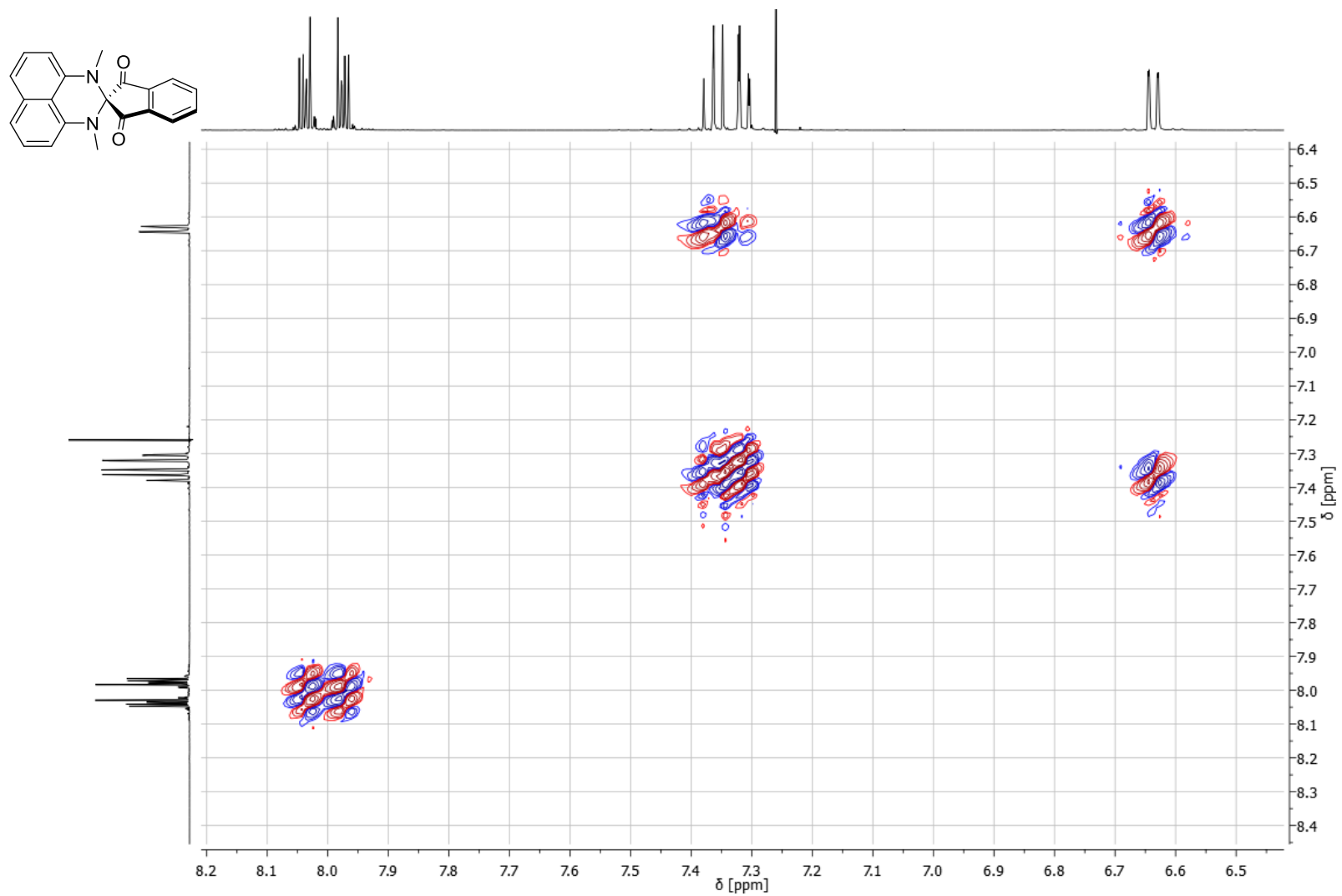


Figure S61: DQF-COSY-spectrum of 4 in CDCl_3 (500 MHz).

S106

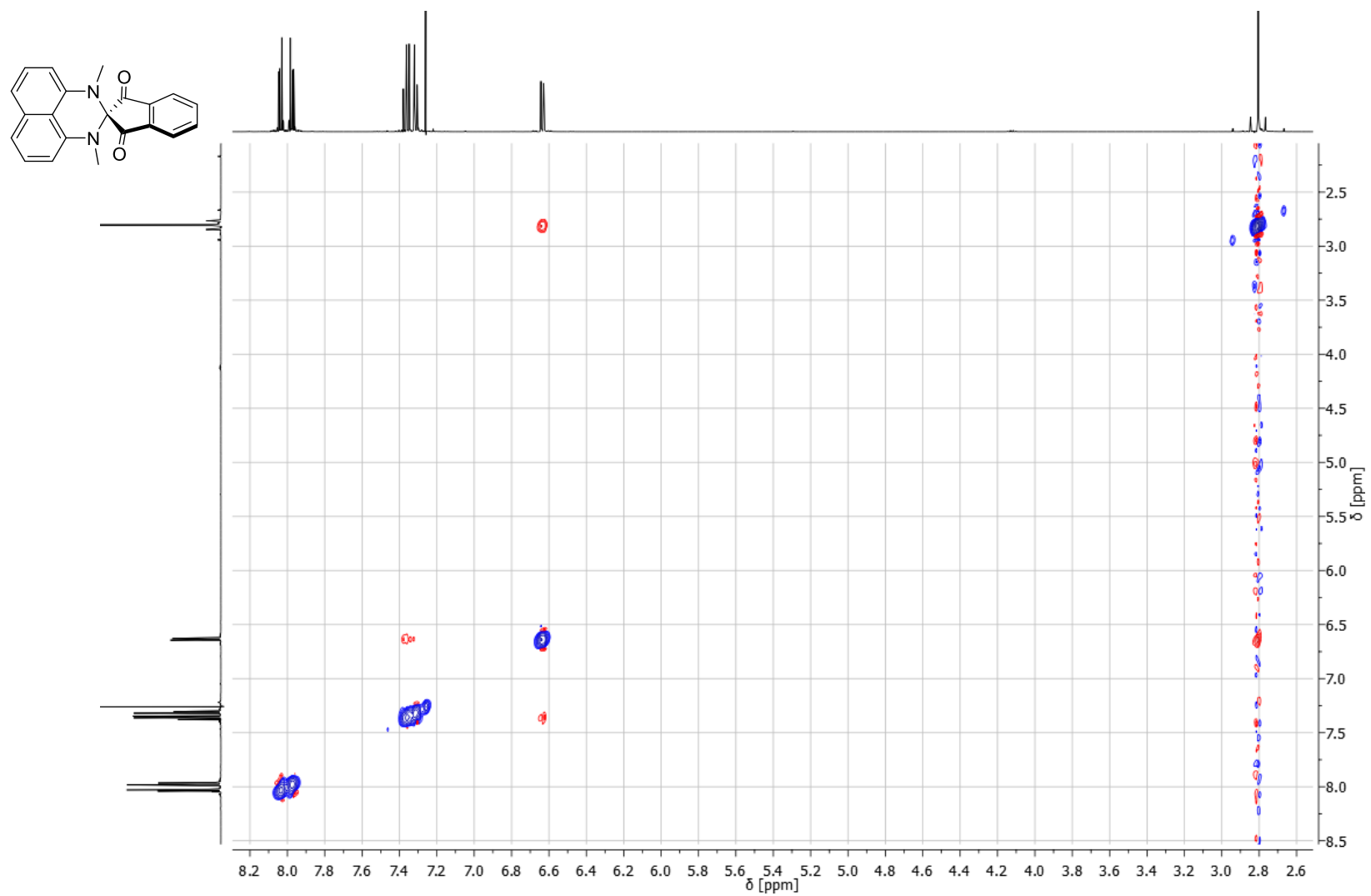


Figure S62: NOESY-spectrum of 4 in CDCl₃ (500 MHz).

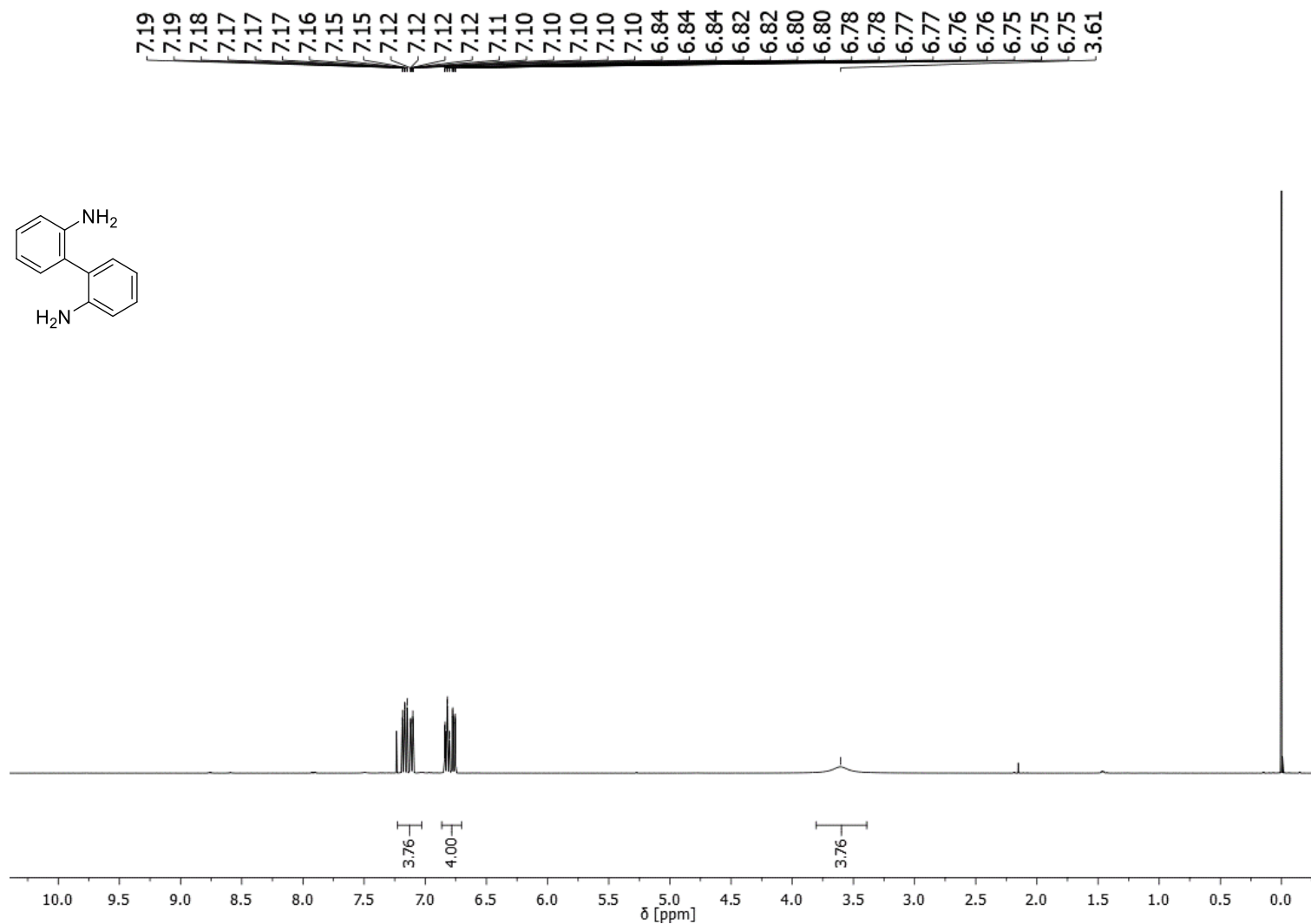


Figure S63: ¹H NMR-spectrum of **31** in CDCl₃ (400 MHz).

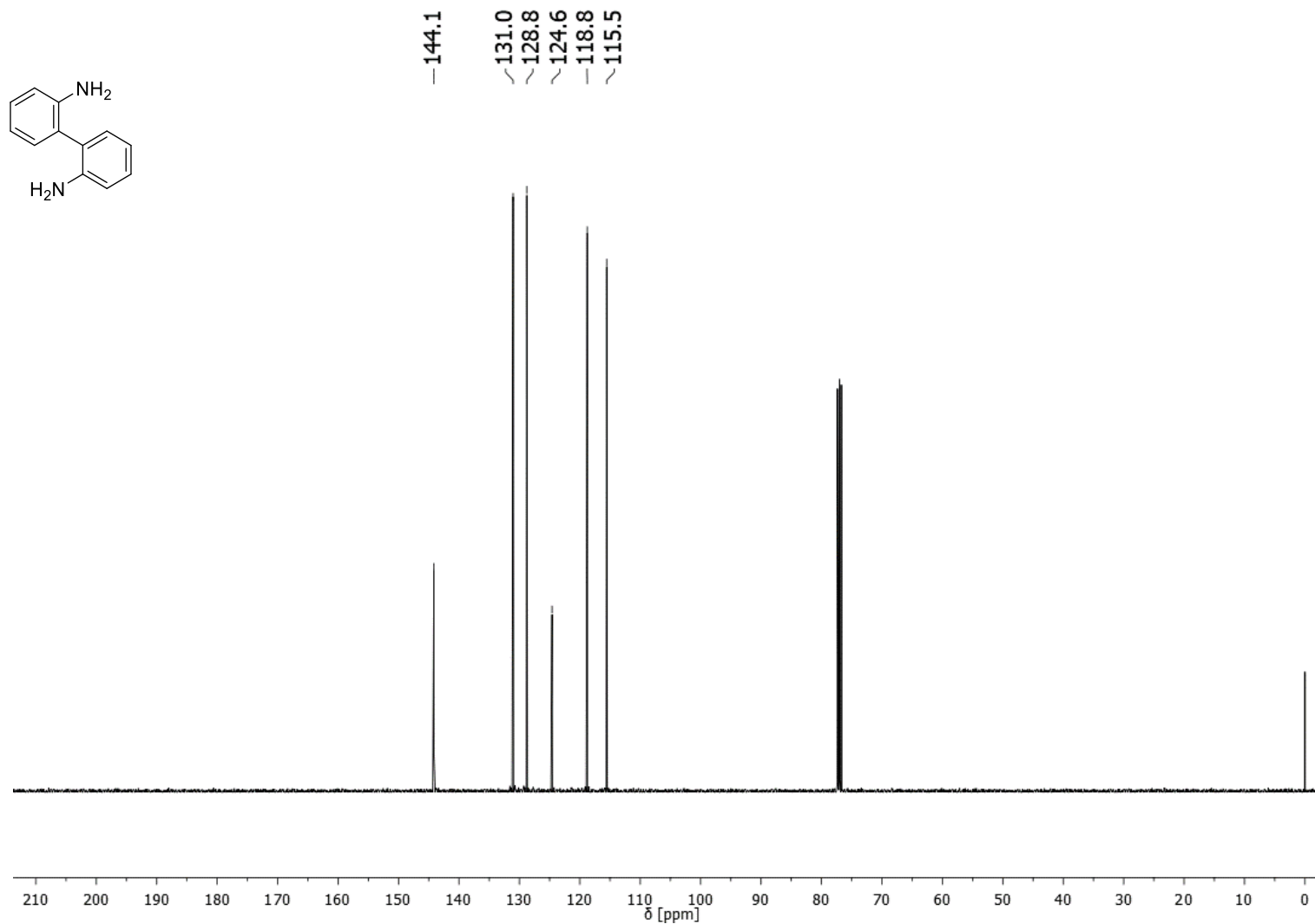


Figure S64: ^{13}C NMR-spectrum of **31** in CDCl_3 (101 MHz).

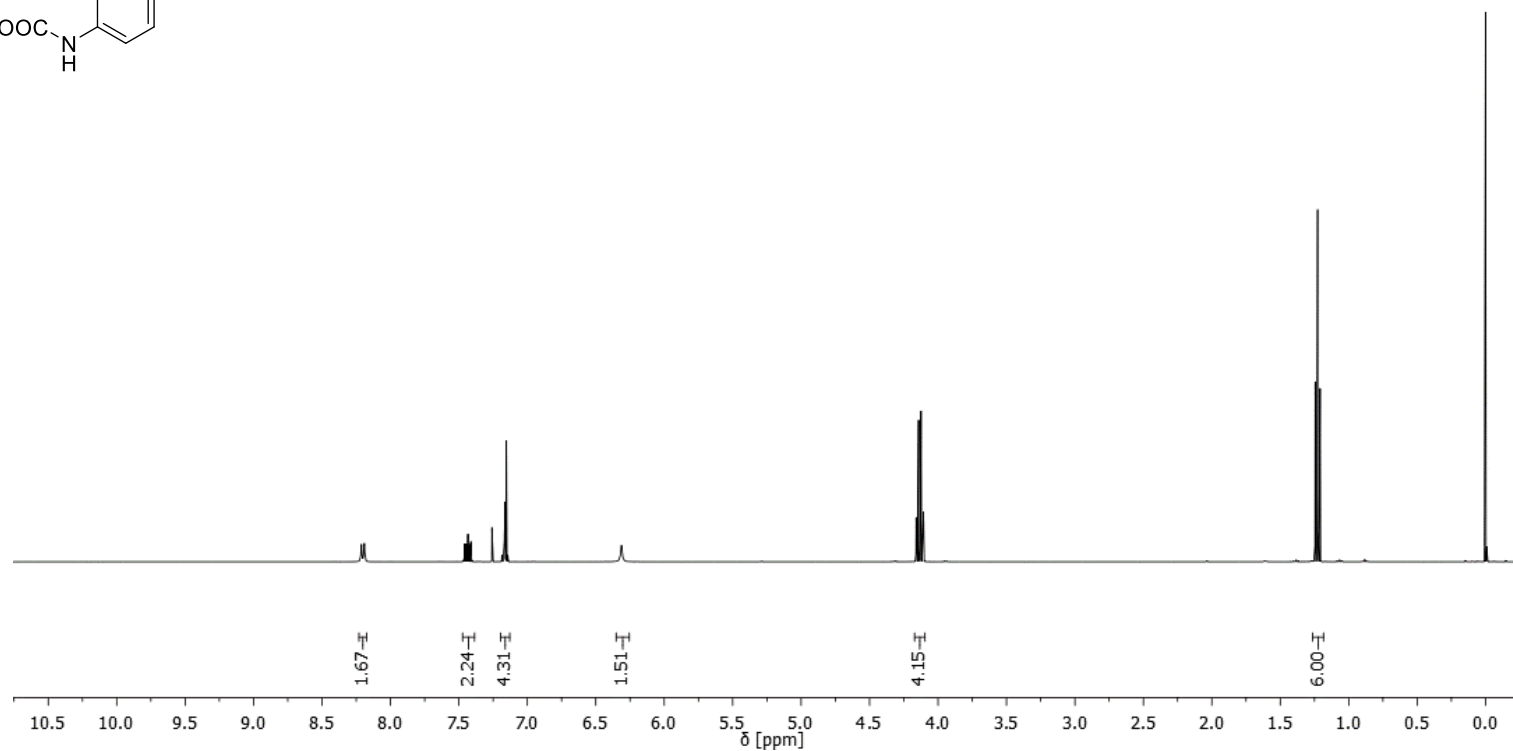
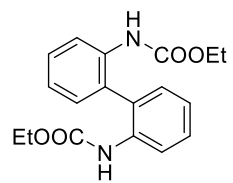


Figure S65: ¹H NMR-spectrum of **32** in CDCl₃ (400 MHz).

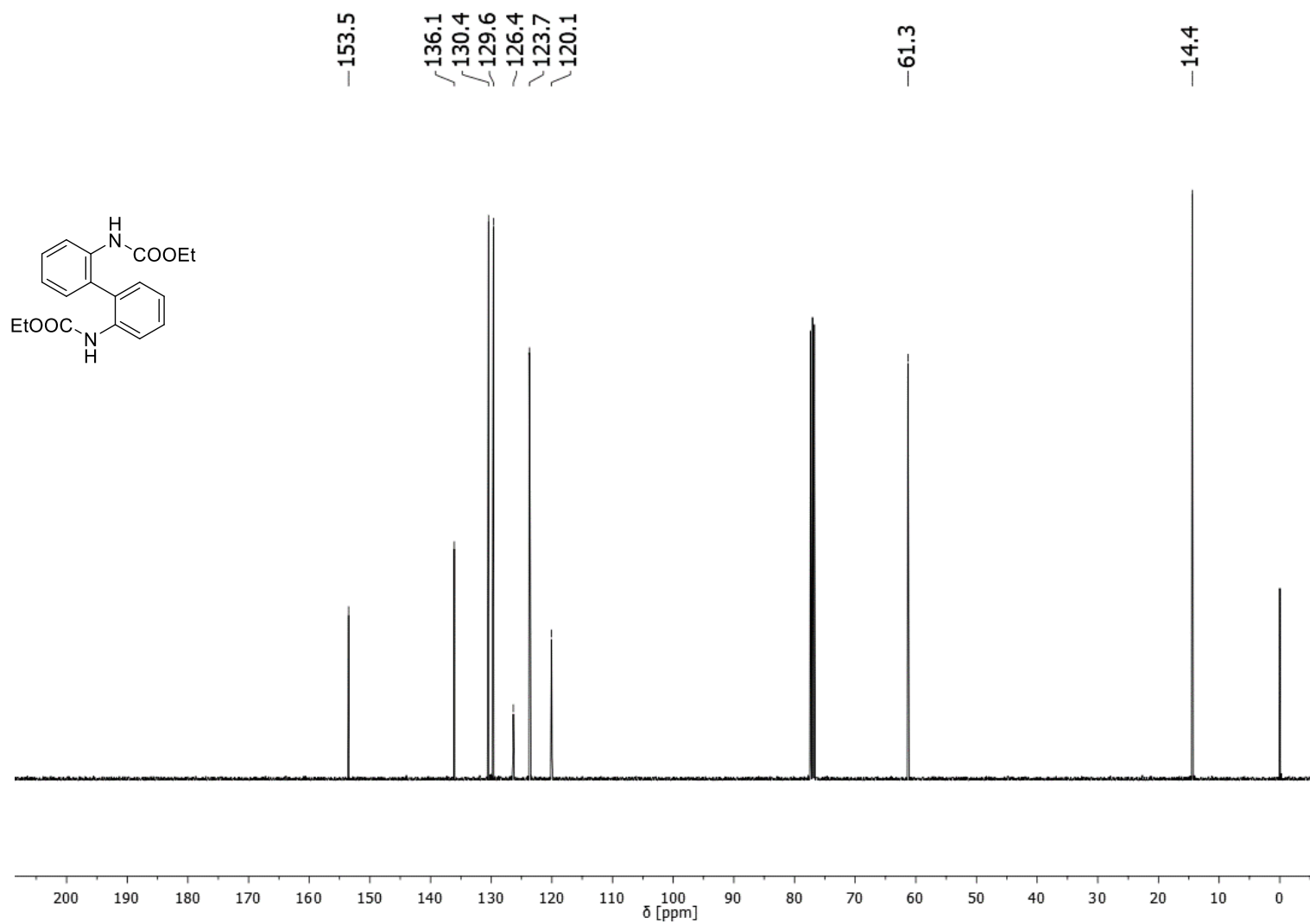


Figure S66: ¹³C NMR-spectrum of **32** in CDCl₃ (101 MHz).

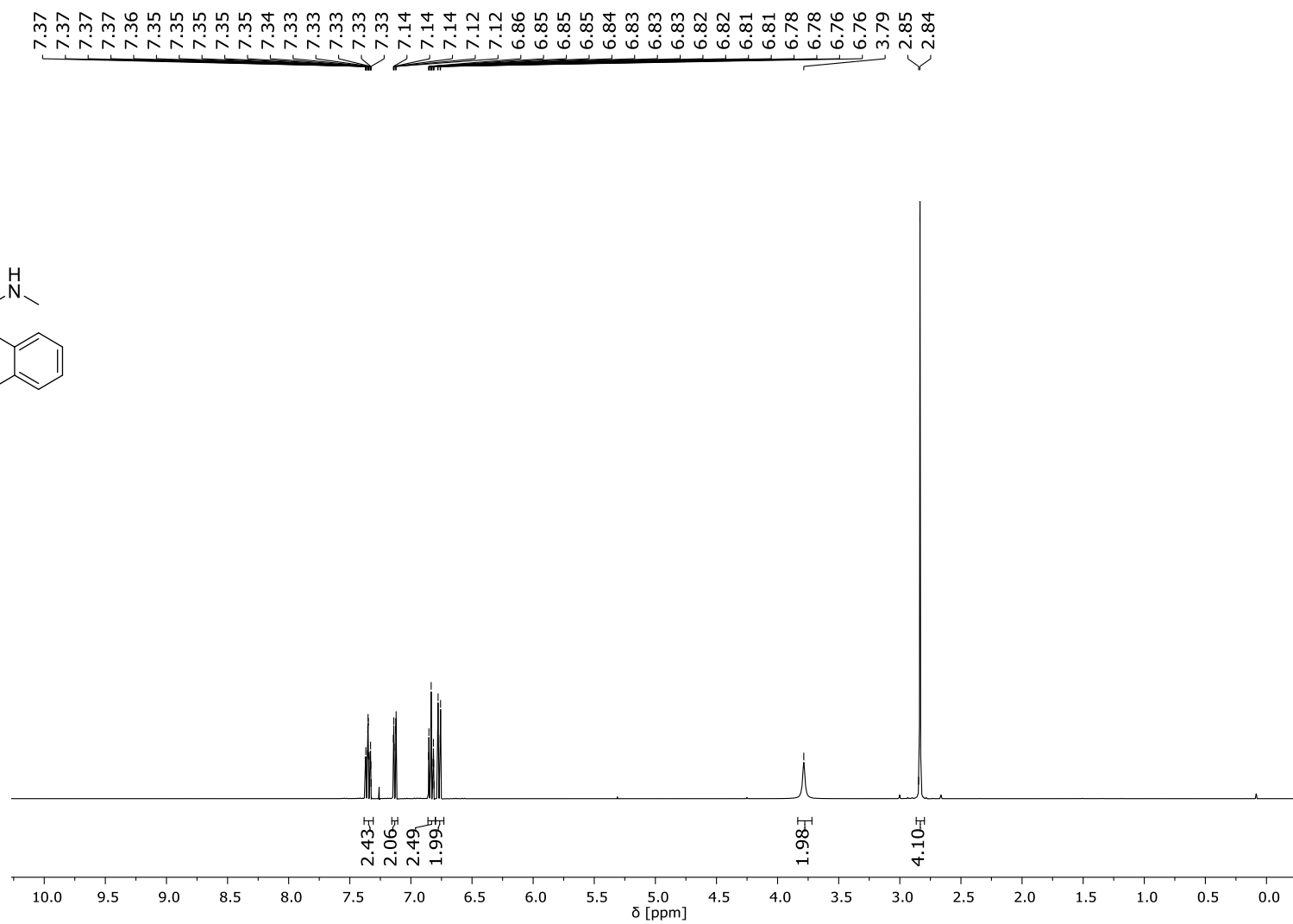
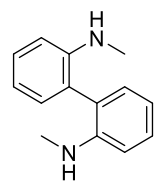


Figure S67: ^1H NMR-spectrum of 8 in CDCl_3 (400 MHz).

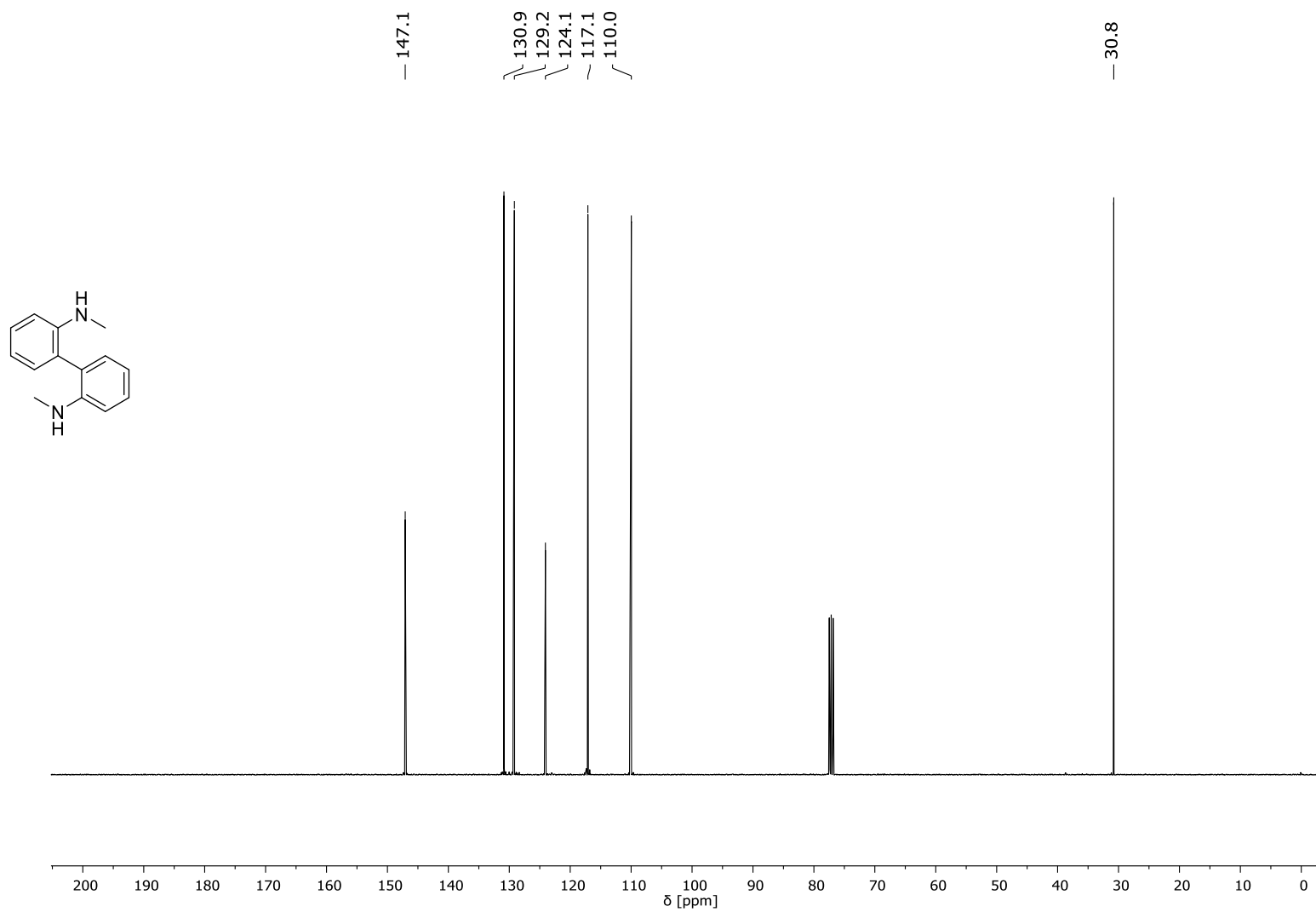


Figure S68: ^{13}C NMR-spectrum of **8** in CDCl_3 (101 MHz).

S113

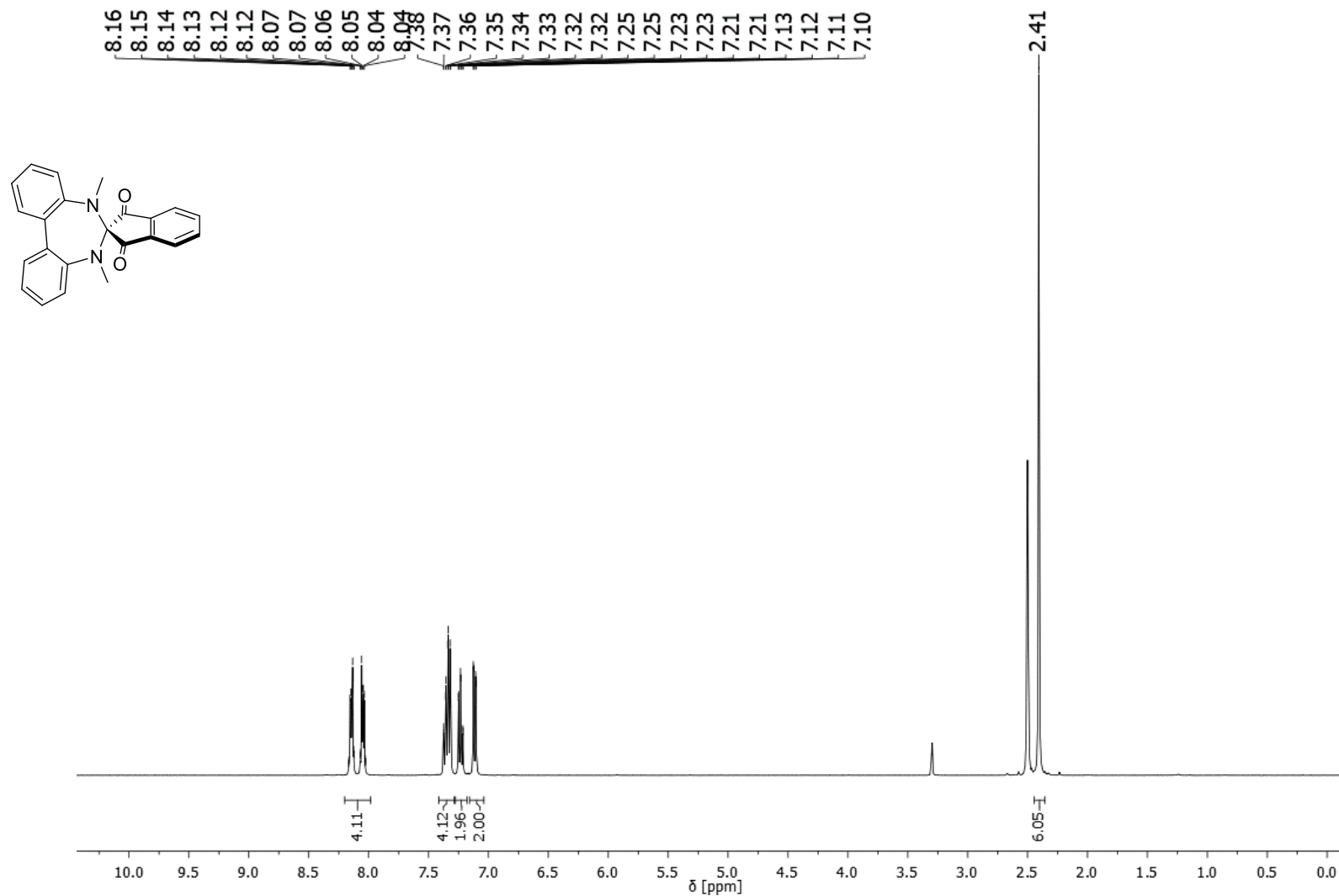


Figure S69: ¹H NMR-spectrum of 5 in DMSO-*d*₆ (400 MHz).

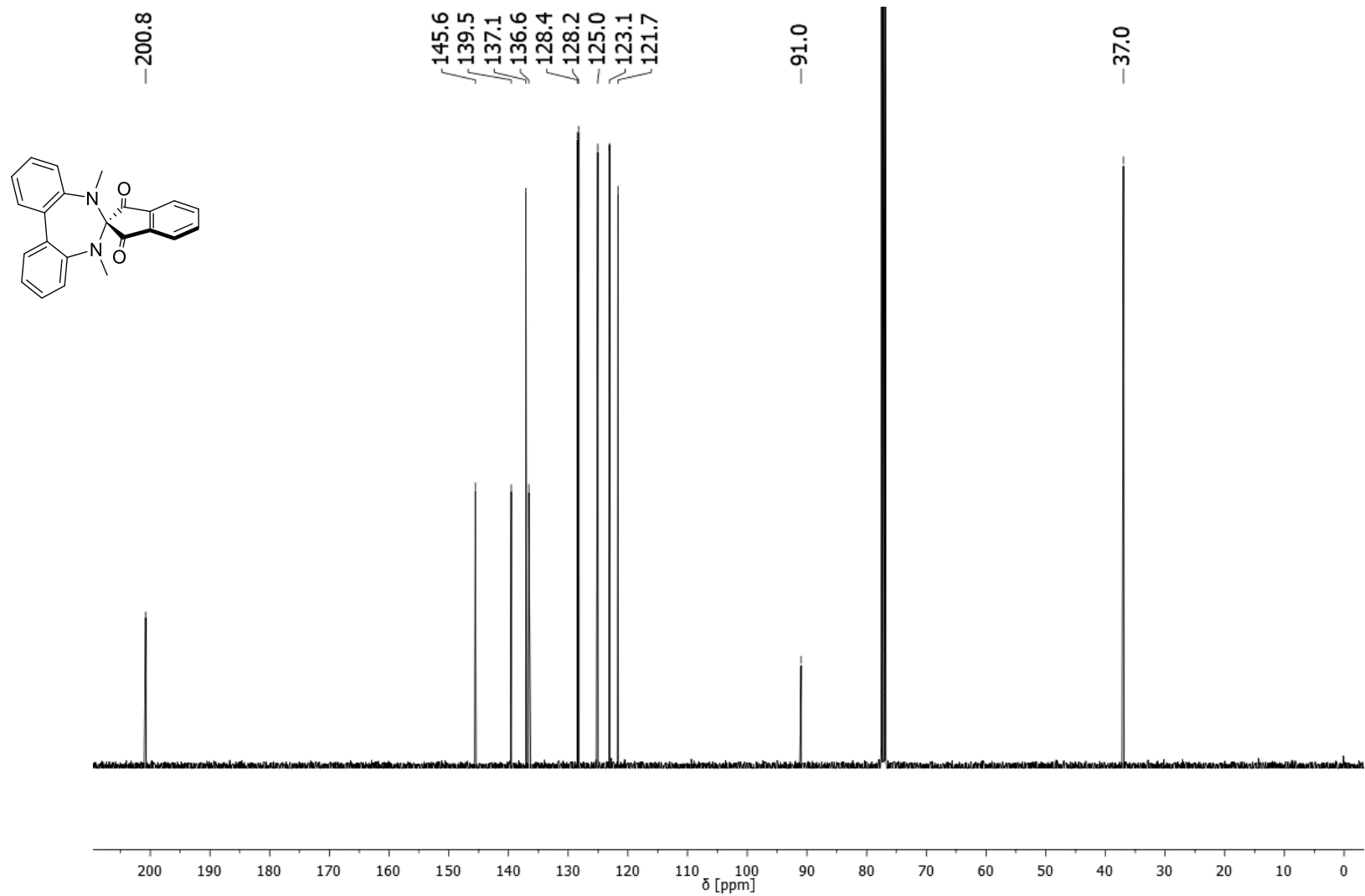


Figure S70: ^{13}C NMR-spectrum of 5 in CDCl_3 (101 MHz).

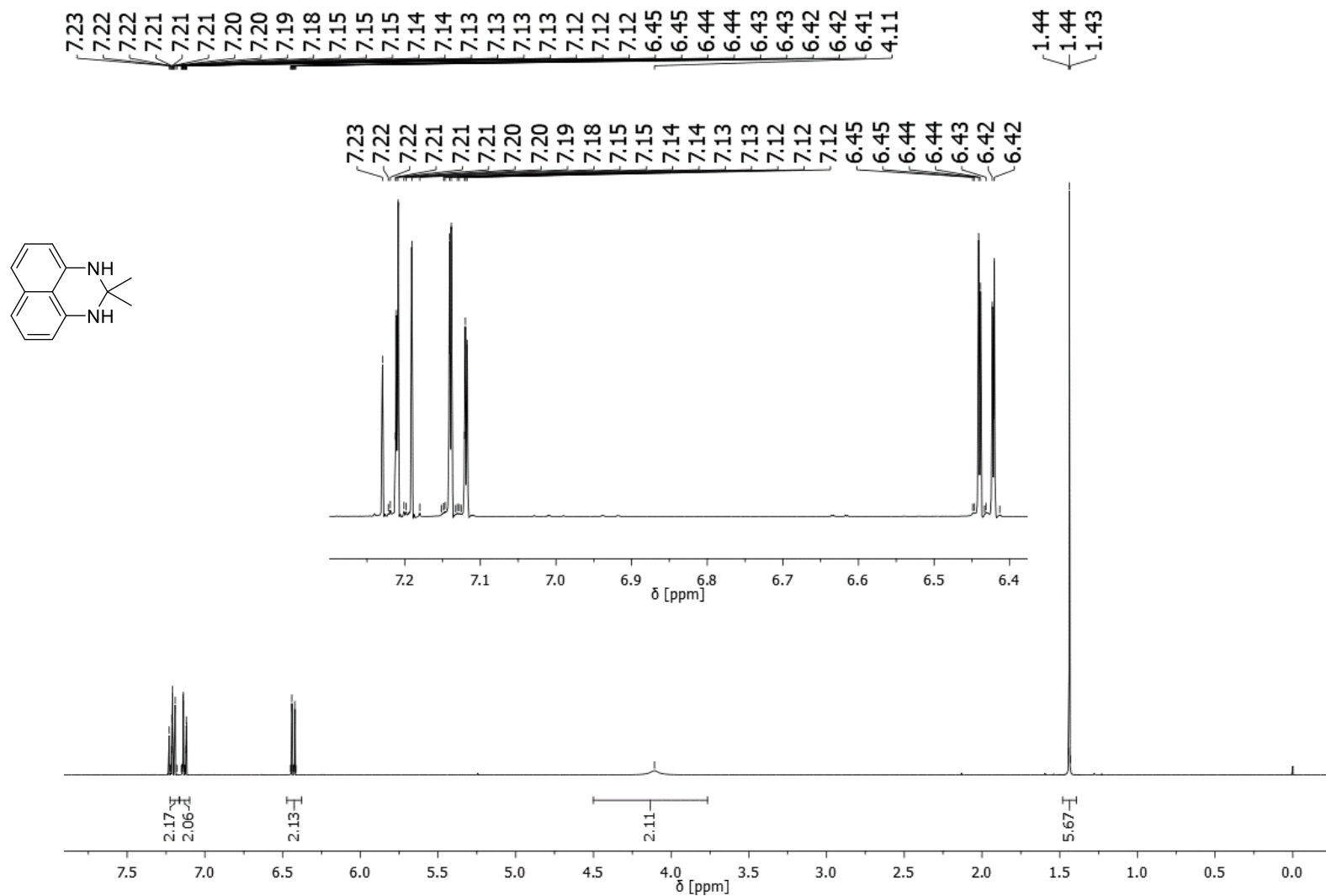


Figure S71: ¹H NMR-spectrum of **33** in CDCl₃ (400 MHz).

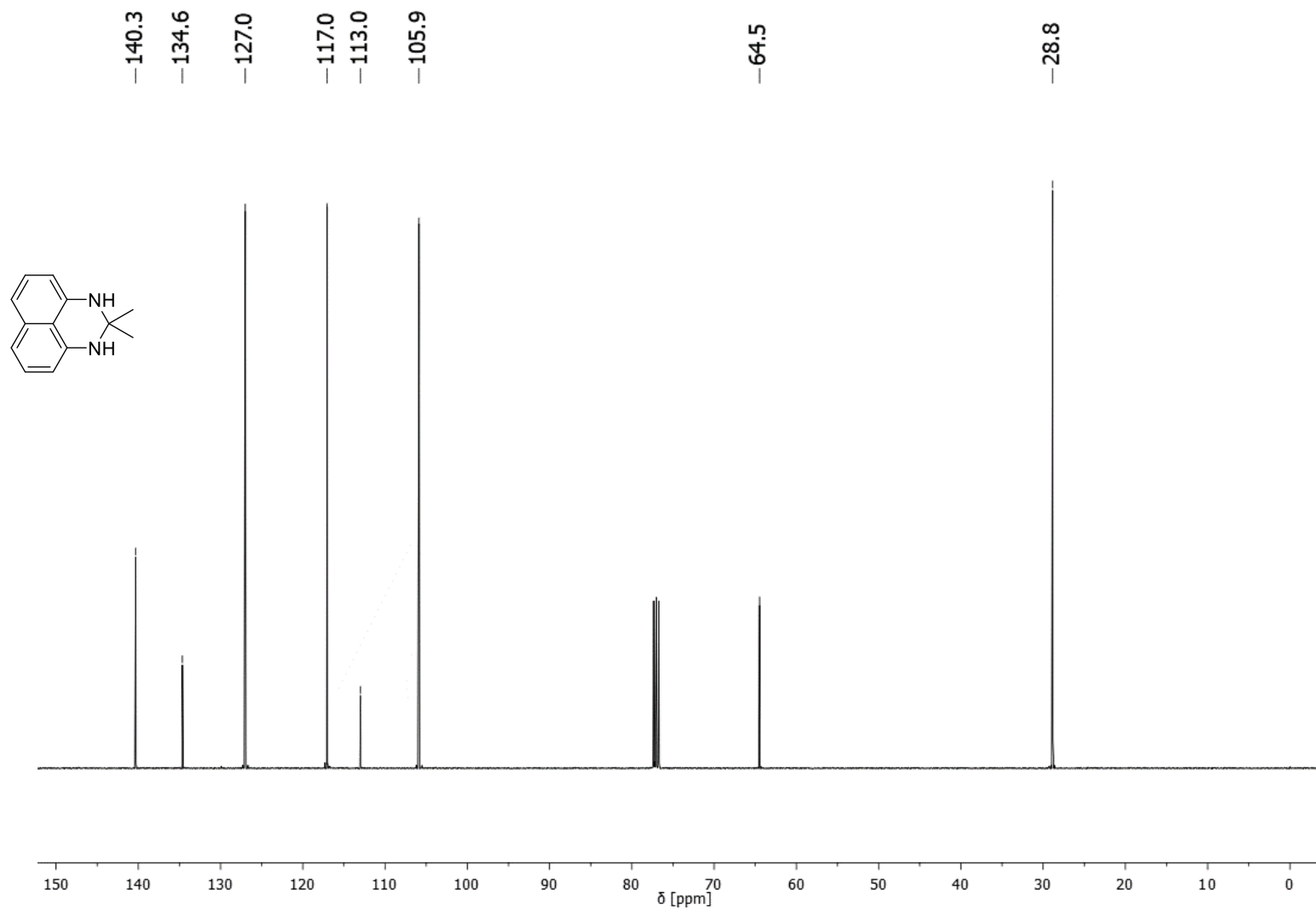


Figure S72: ¹³C NMR-spectrum of **33** in CDCl₃ (101 MHz).

S117

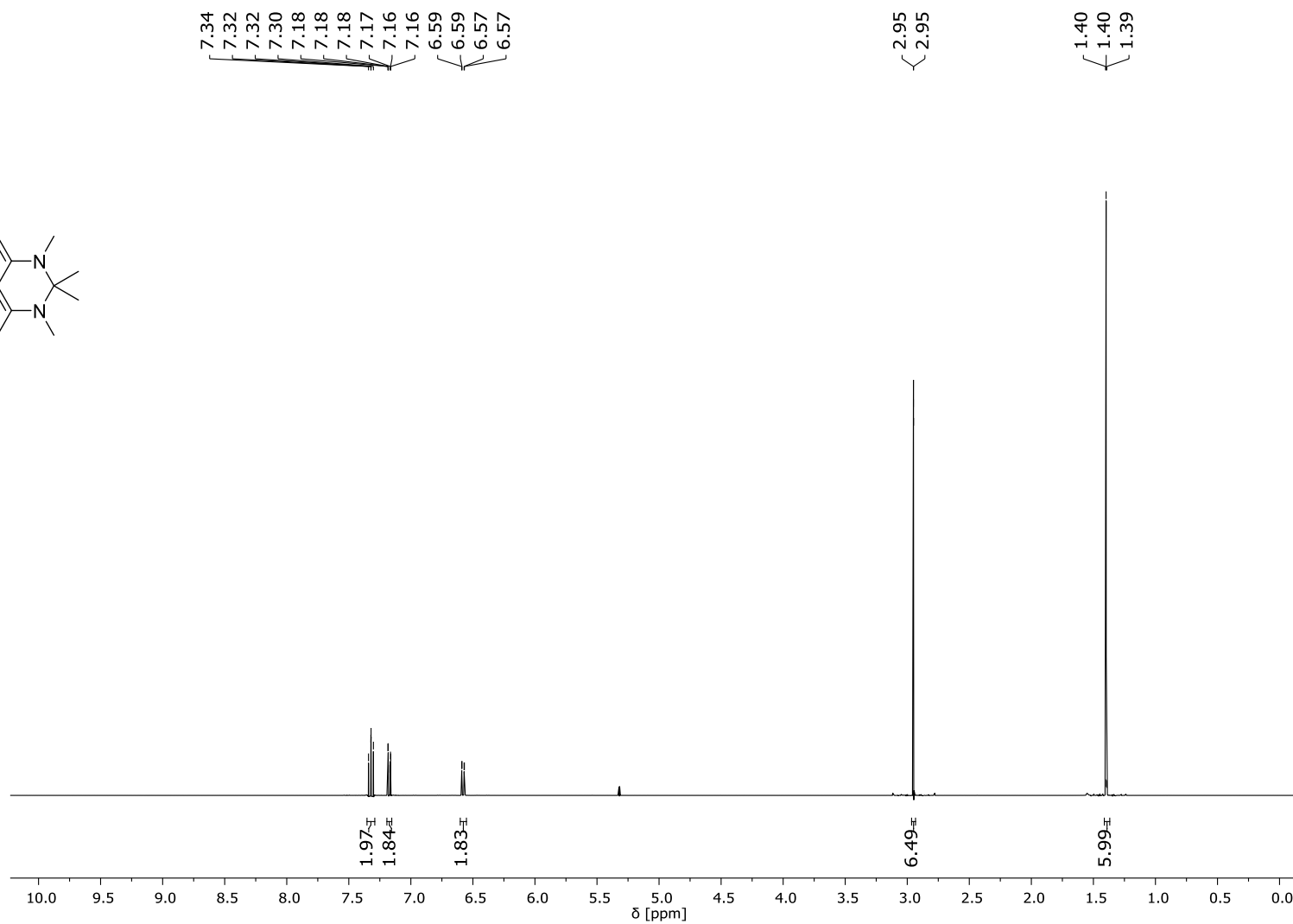
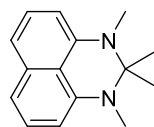


Figure S73: ^1H NMR-spectrum of **12** in CD_2Cl_2 (400 MHz).

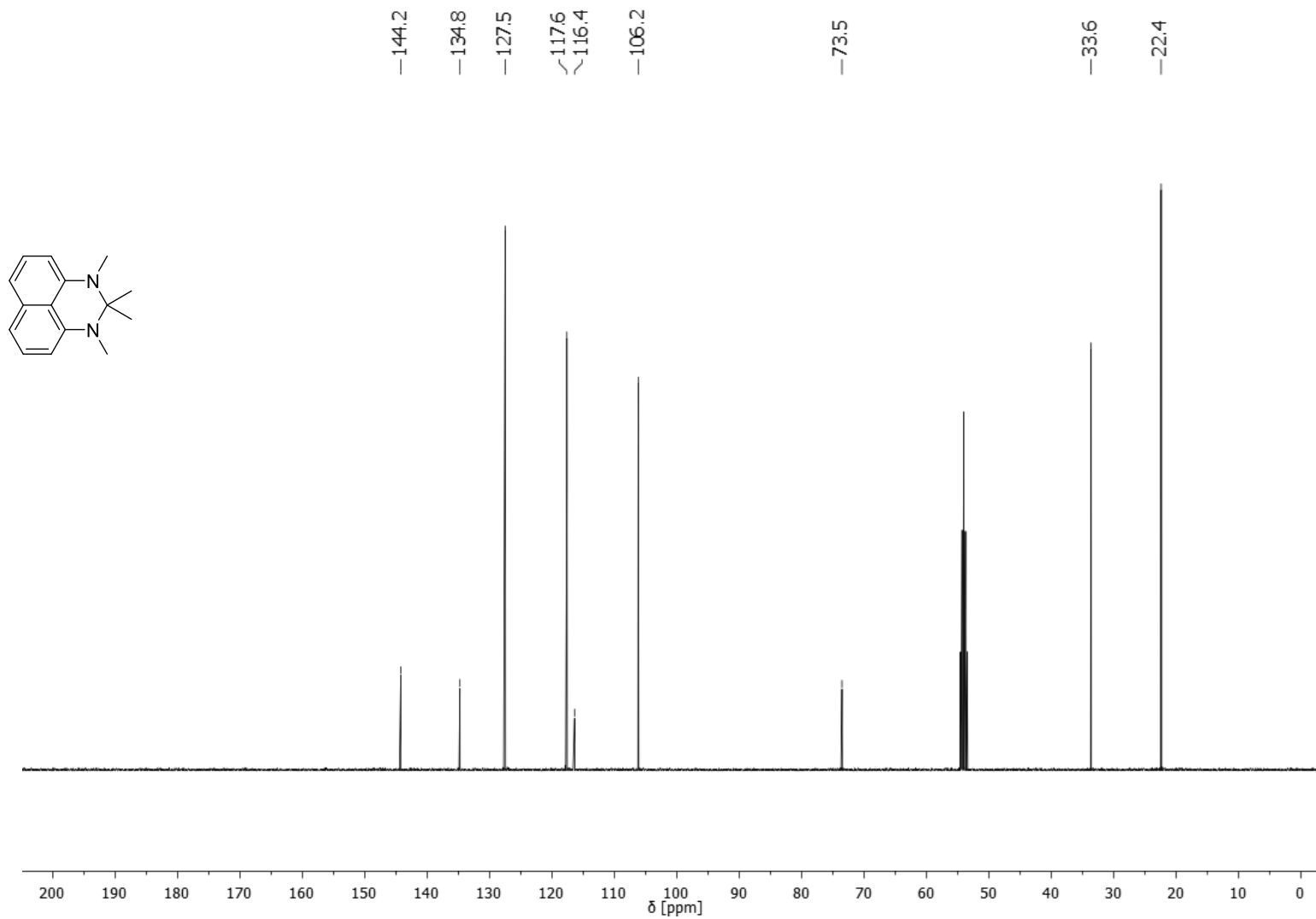


Figure S74: ¹³C NMR-spectrum of **12** in CD₂Cl₂ (101 MHz).

S119

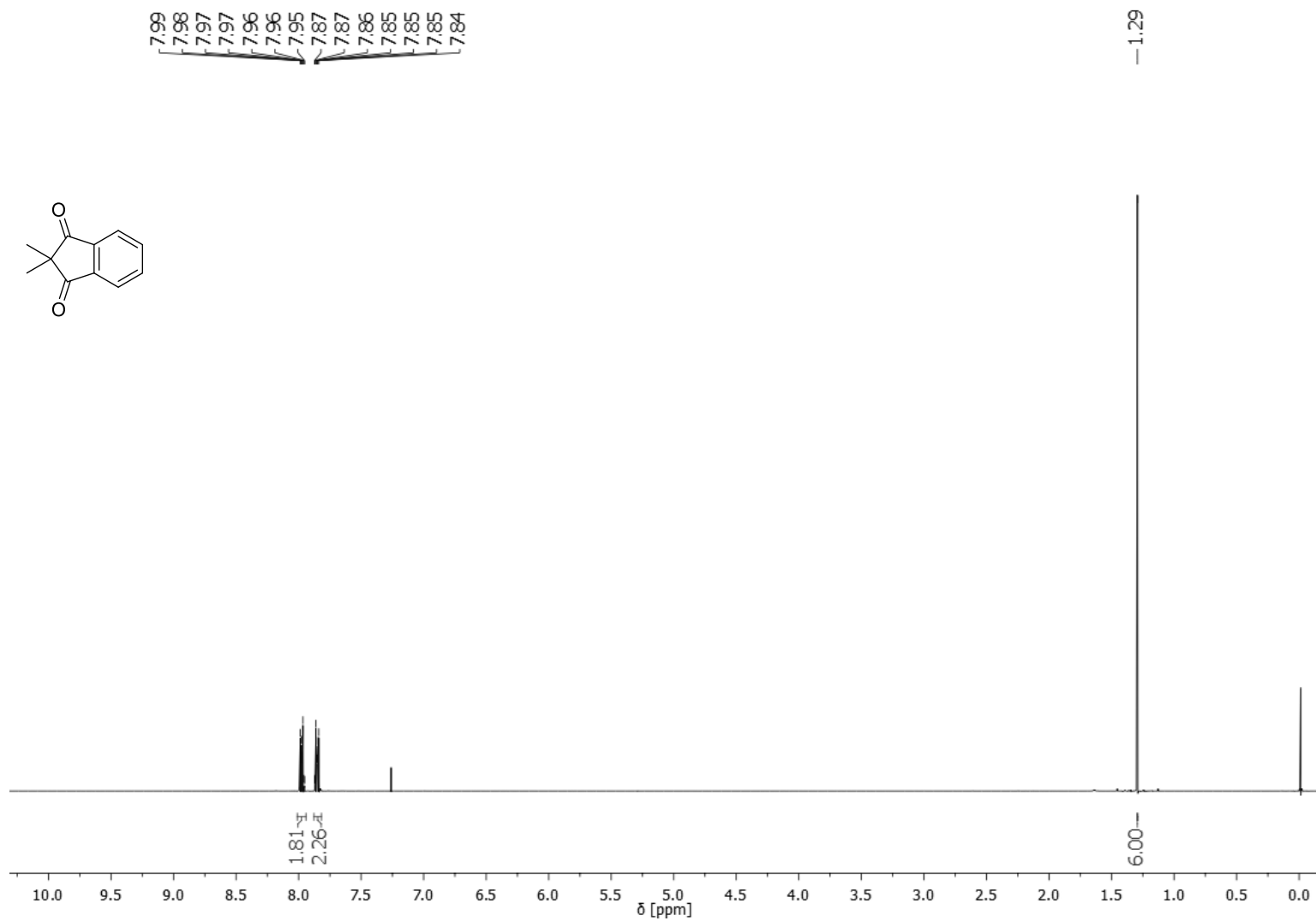


Figure S75: ¹H NMR-spectrum of **13** in CDCl₃ (400 MHz).

S120

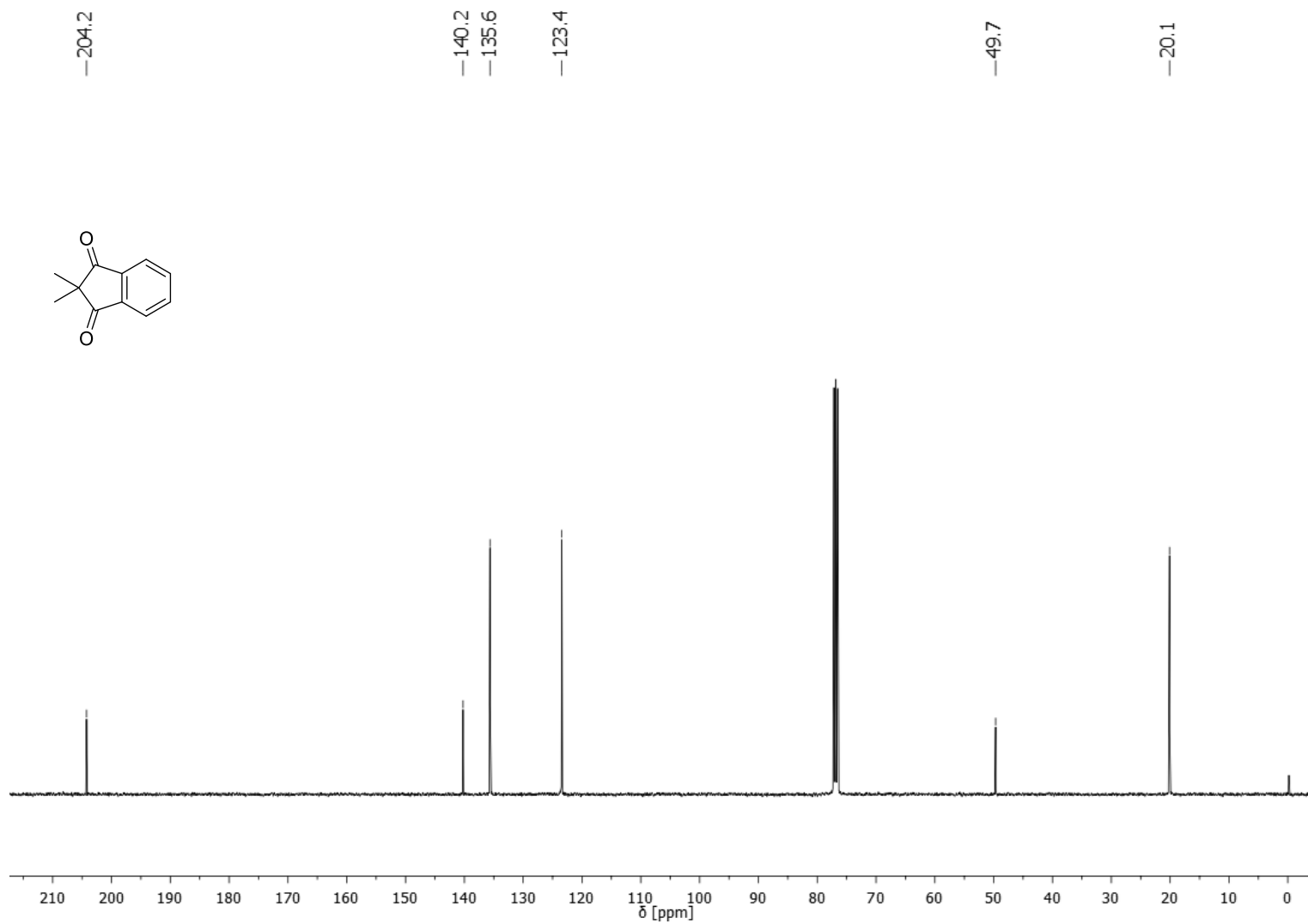


Figure S76: ¹³C NMR-spectrum of **13** in CDCl₃ (101 MHz).

S121

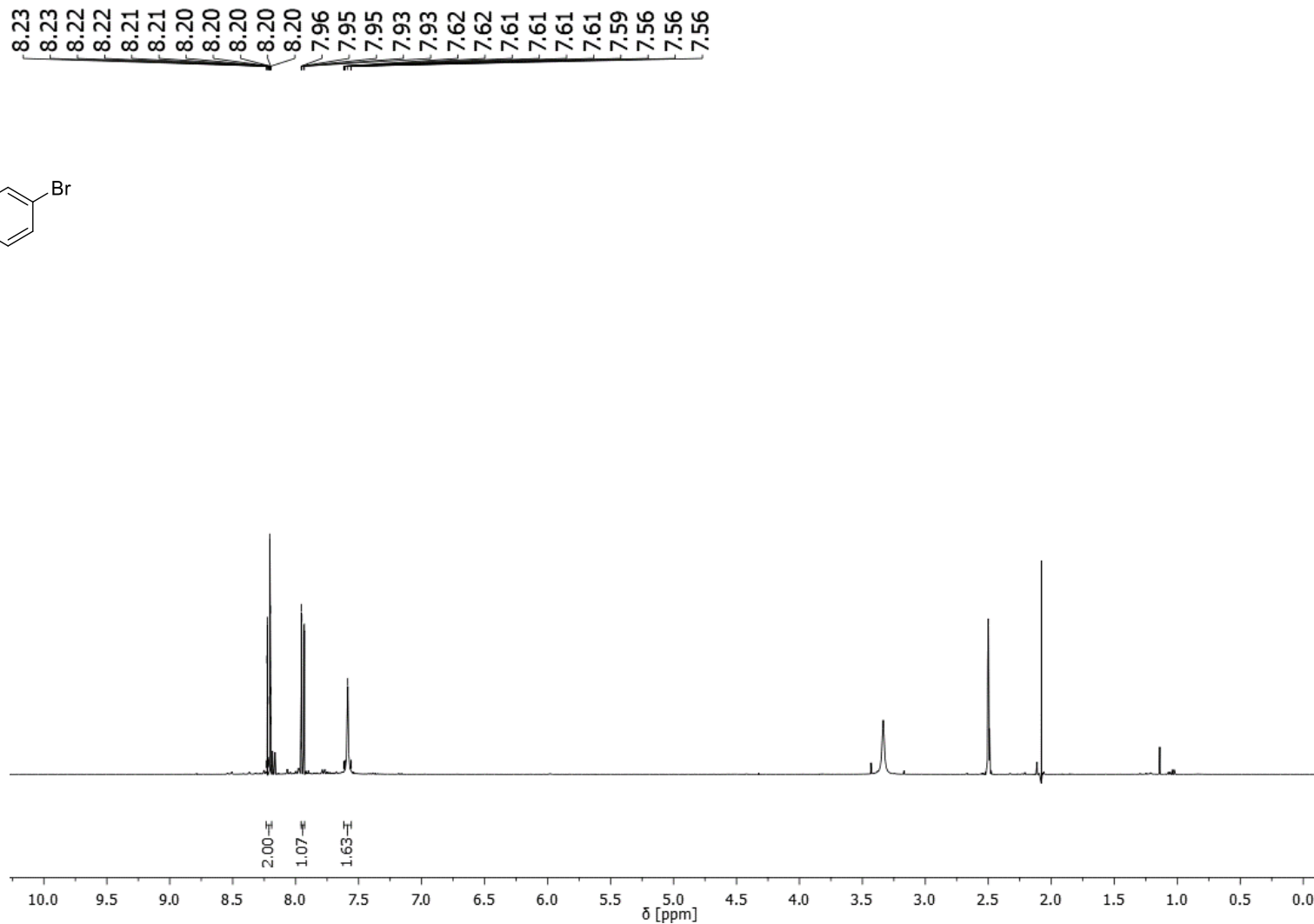
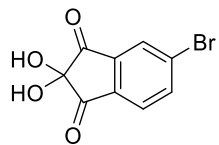


Figure S77: ^1H NMR-spectrum of **19** in $\text{DMSO-}d_6$ (400 MHz).

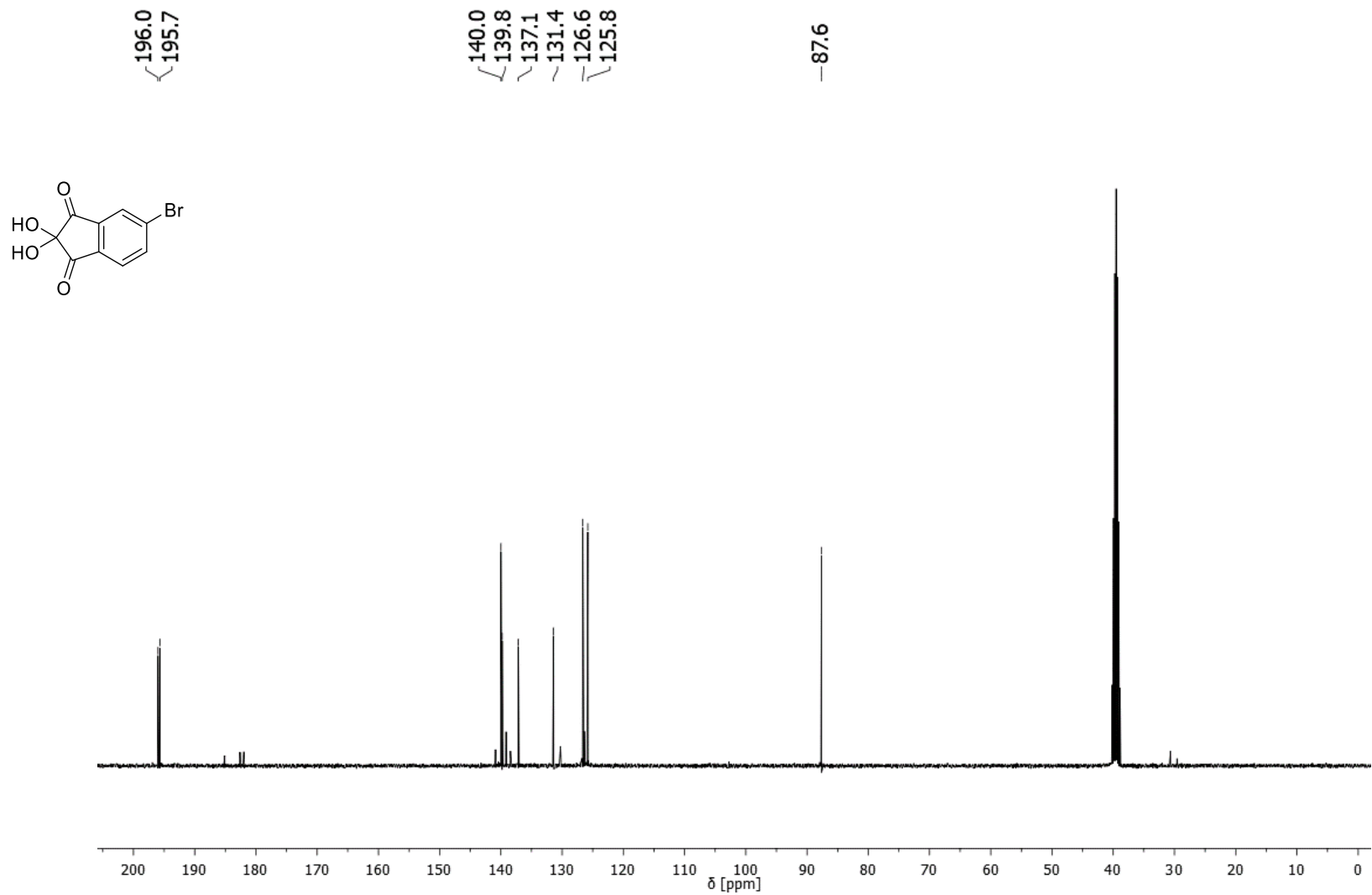


Figure S78: ¹³C NMR-spectrum of 19 in DMSO-*d*₆ (101 MHz).

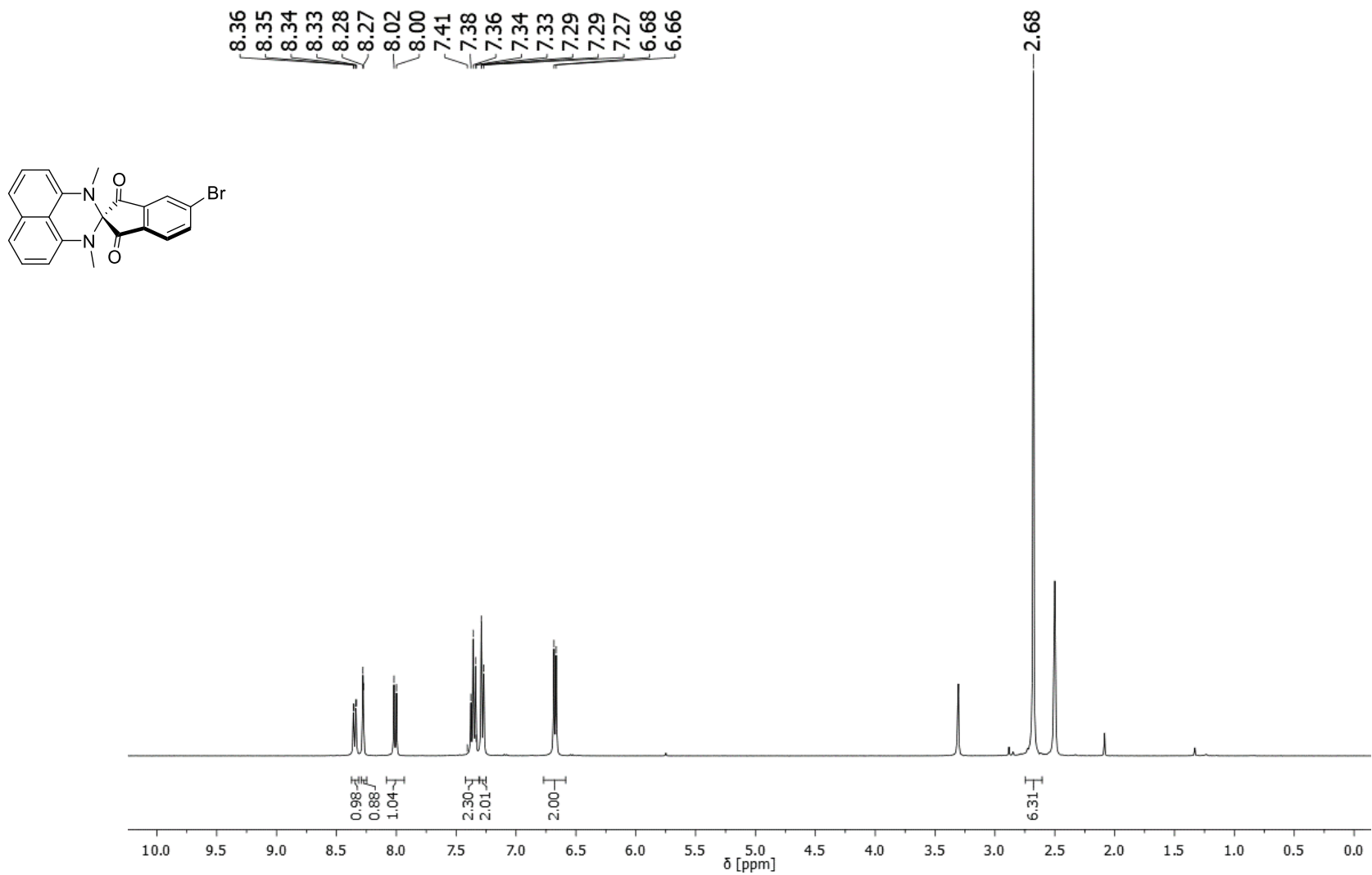


Figure S79: ¹H NMR-spectrum of **21** in DMSO-*d*₆ (400 MHz).

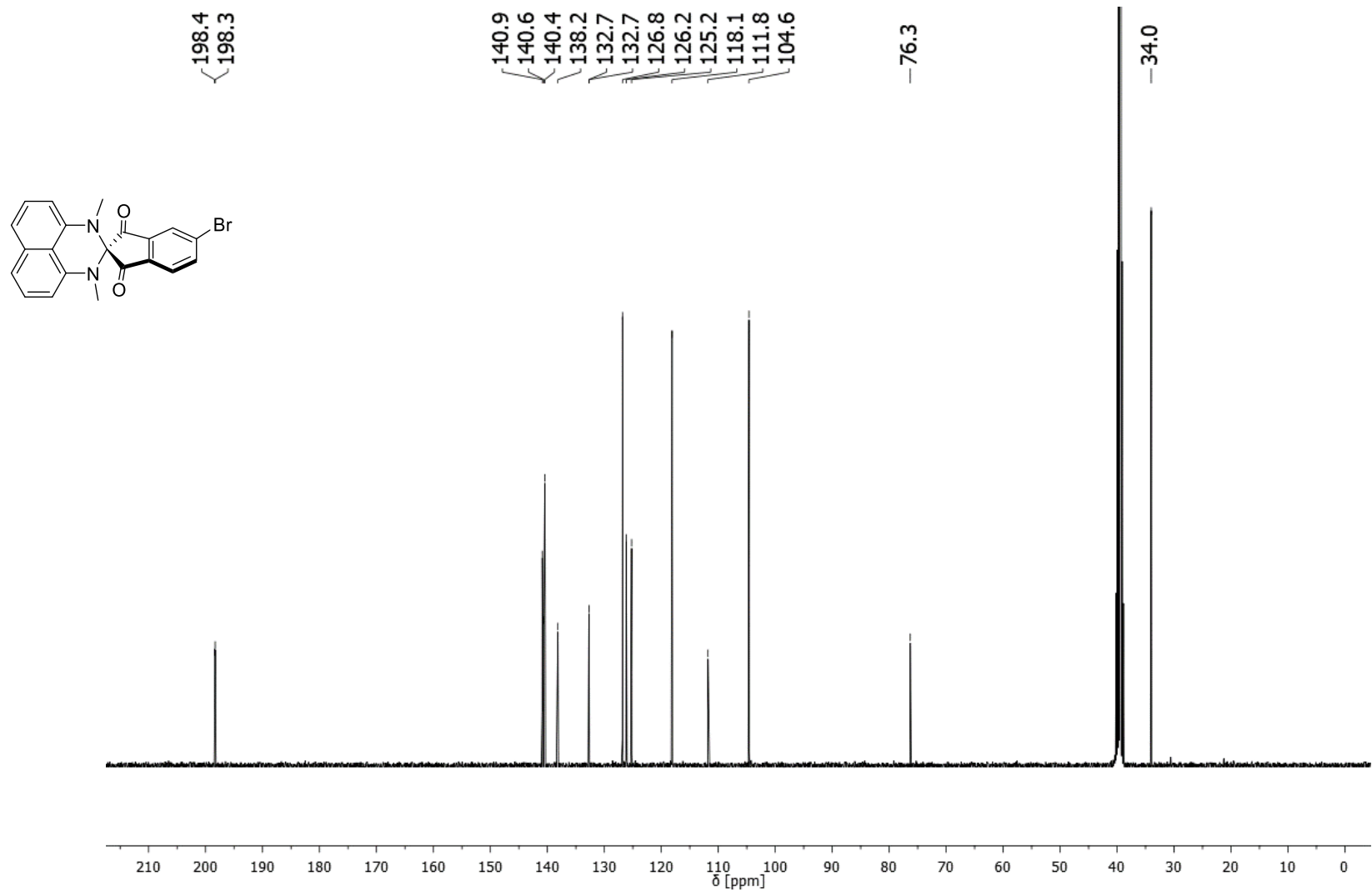


Figure S80: ^{13}C NMR-spectrum of **21** in $\text{DMSO-}d_6$ (101 MHz).

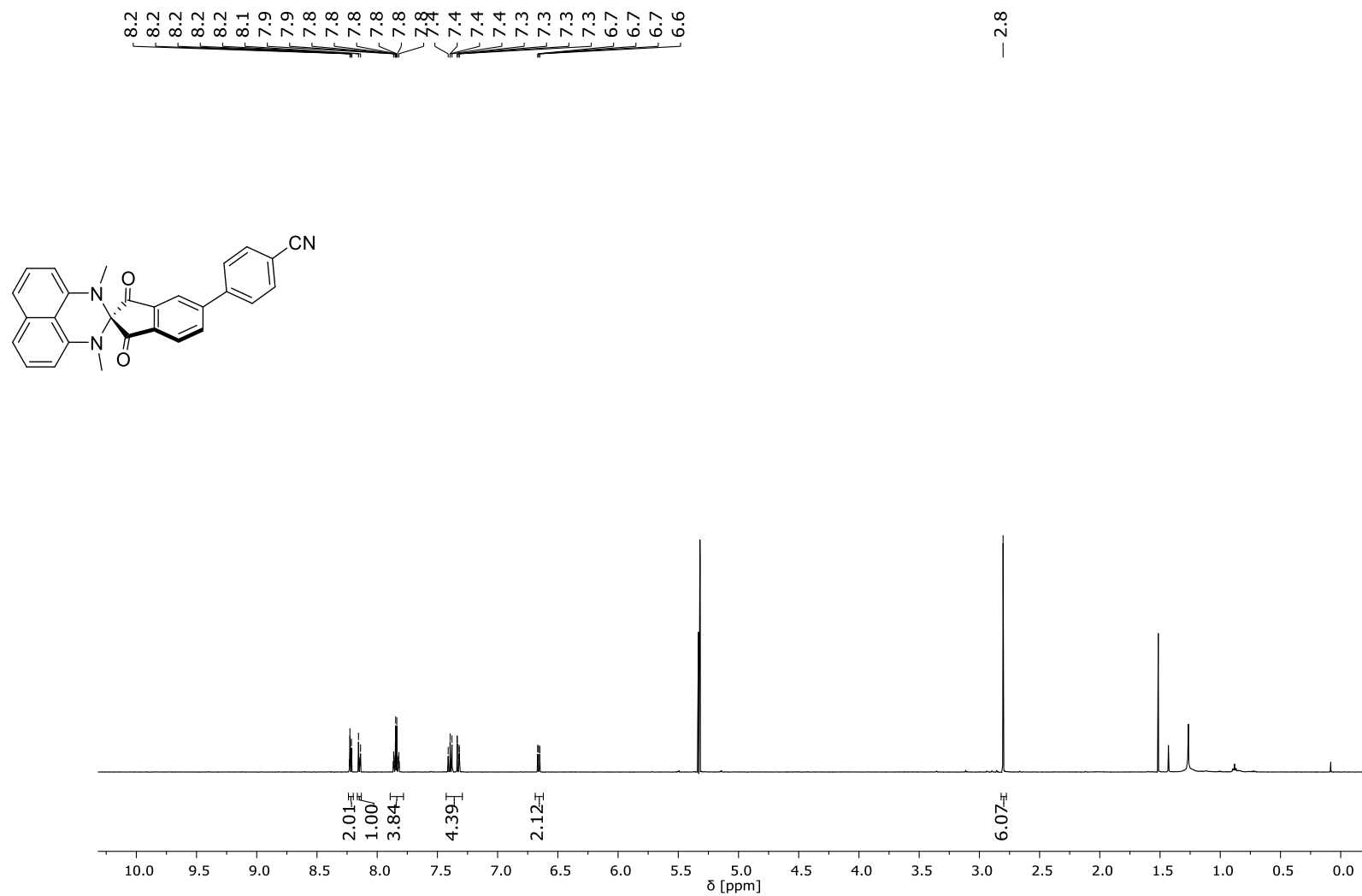


Figure S81: ^1H NMR-spectrum of **15** in CD_2Cl_2 (500 MHz).

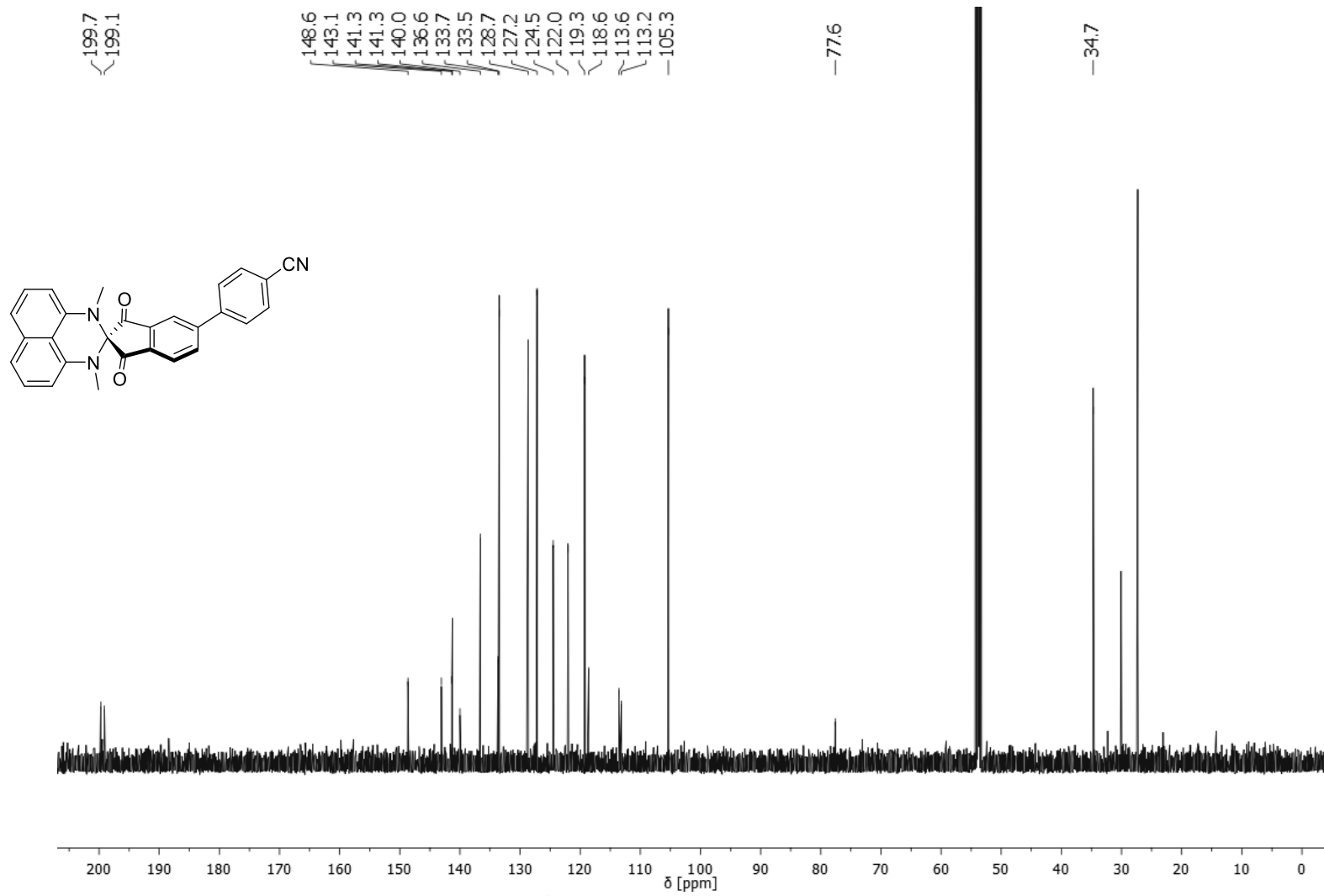


Figure S82: ^{13}C NMR-spectrum of **15** in CD_2Cl_2 (126 MHz).

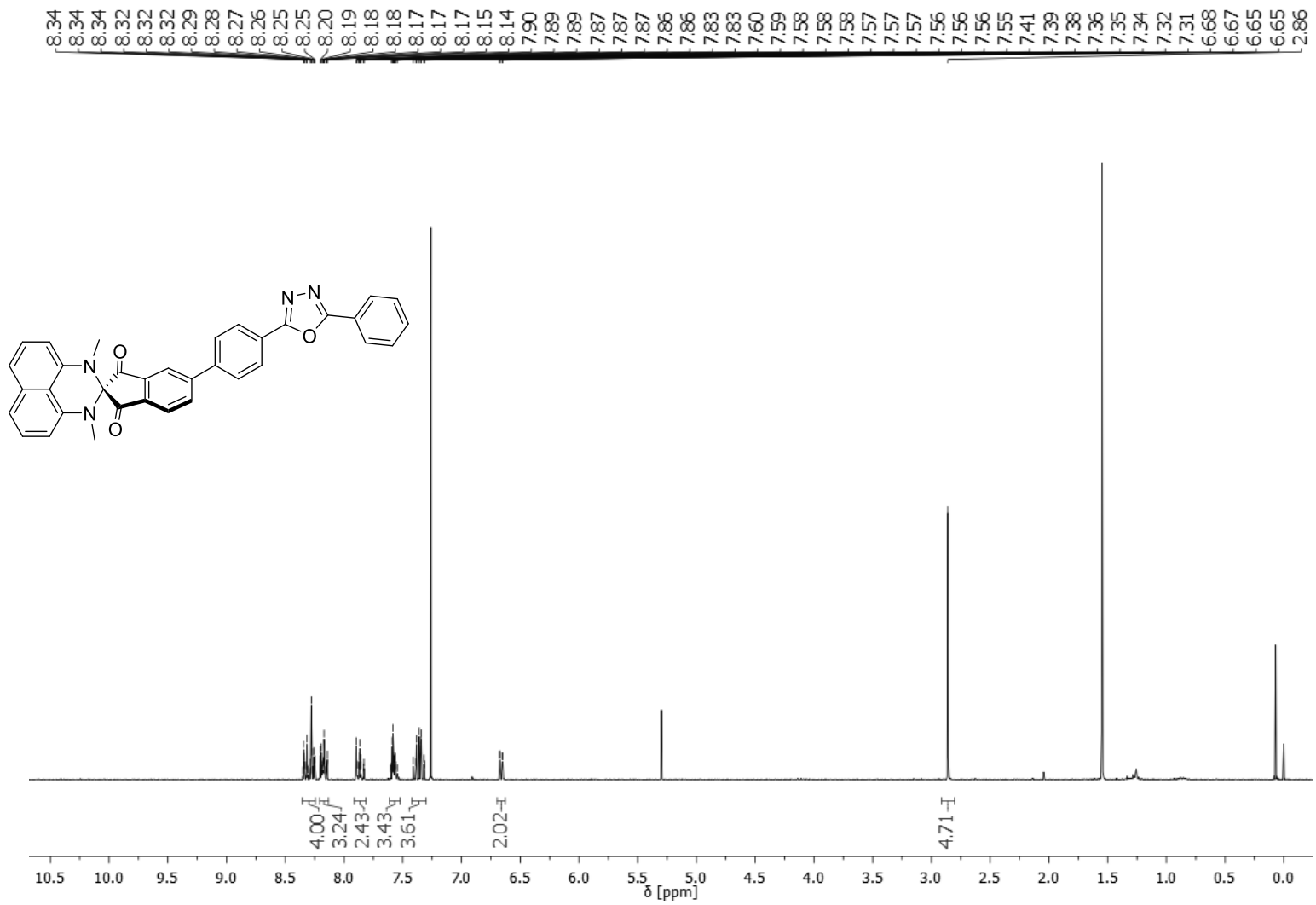


Figure S83: ¹H NMR-spectrum of **14** in CDCl₃ (300 MHz).

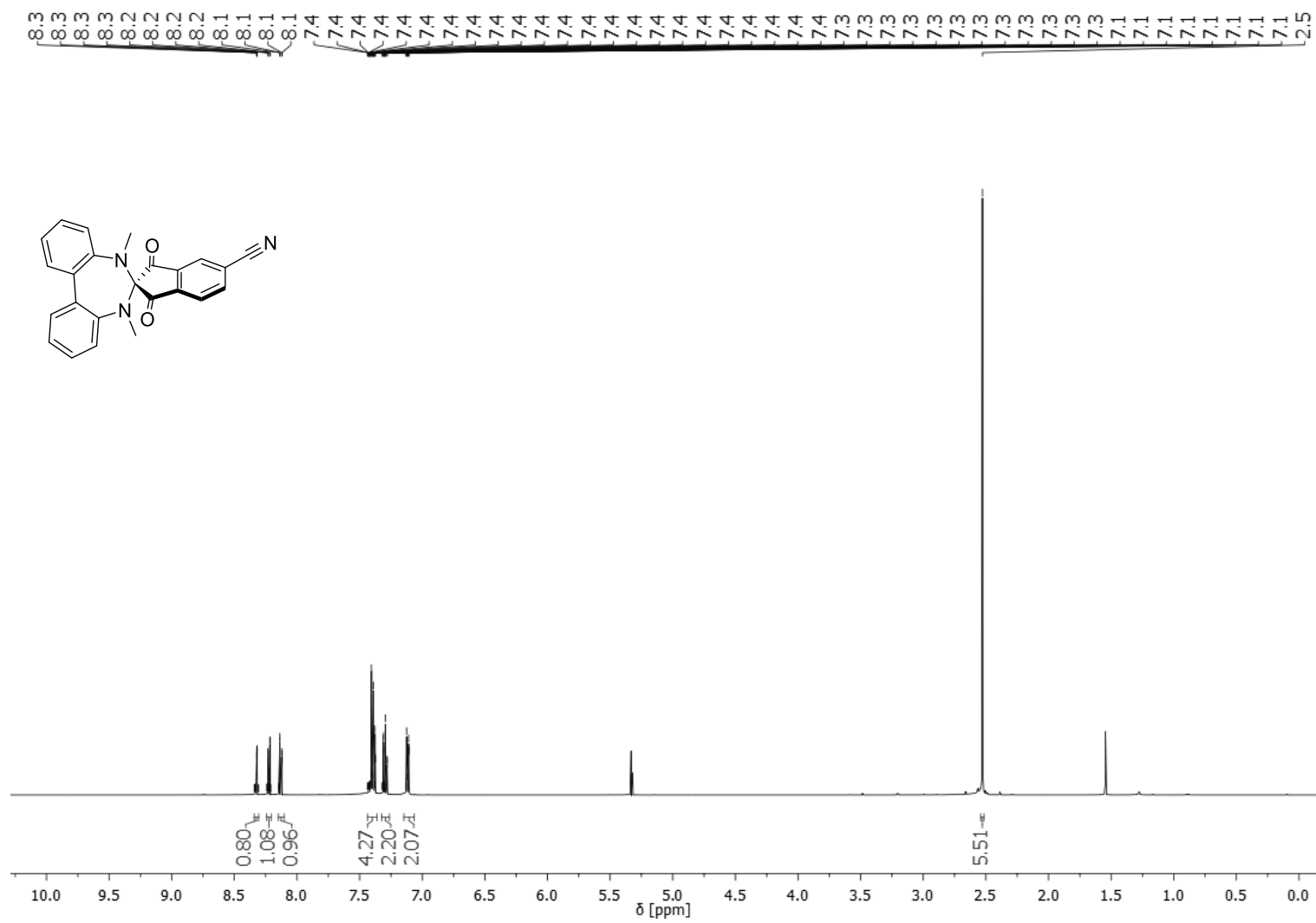


Figure S84: ¹H NMR-spectrum of **17** in CDCl₃ (400 MHz).

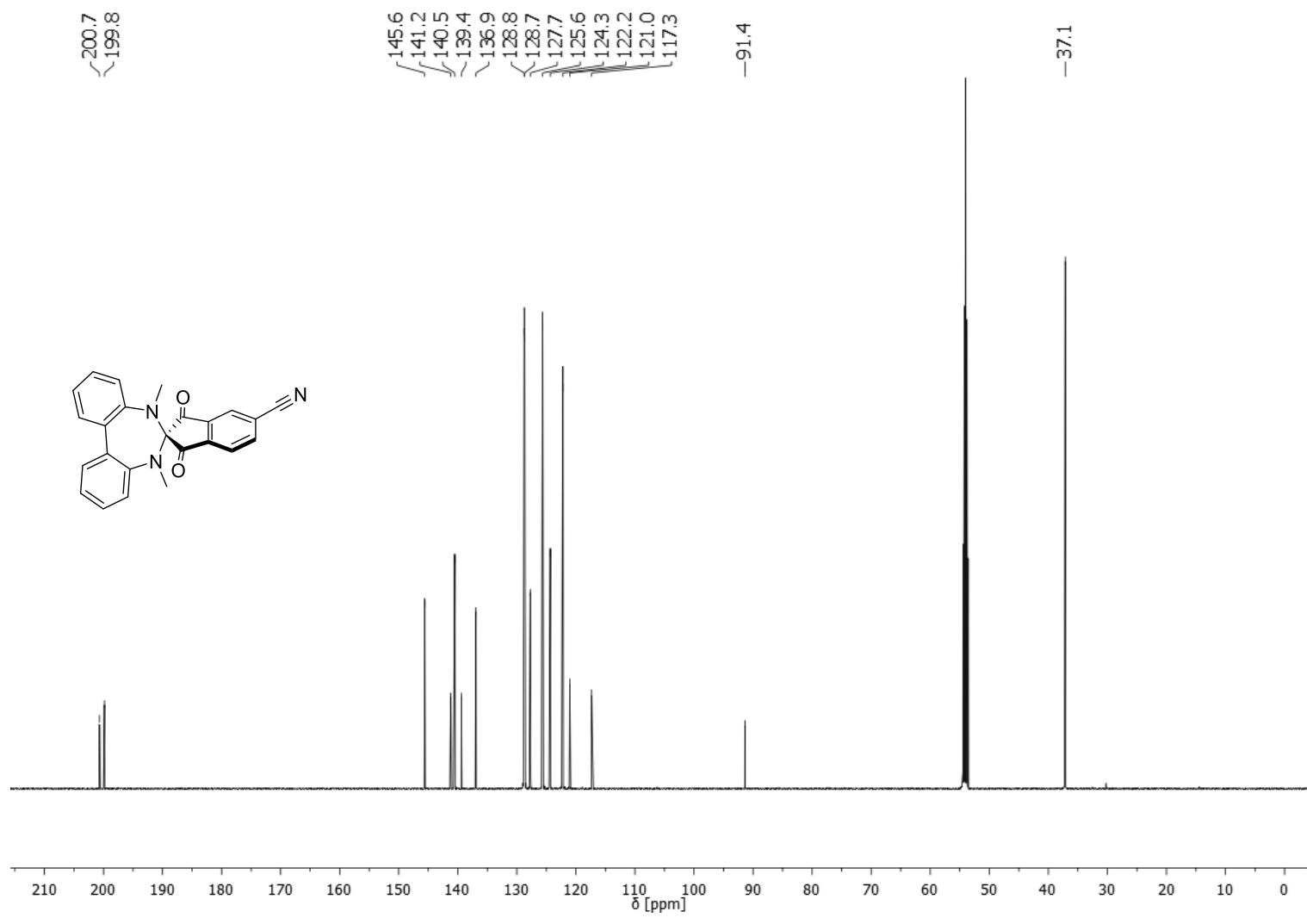


Figure S85: ^{13}C NMR-spectrum of **17** in CDCl_3 (101 MHz).

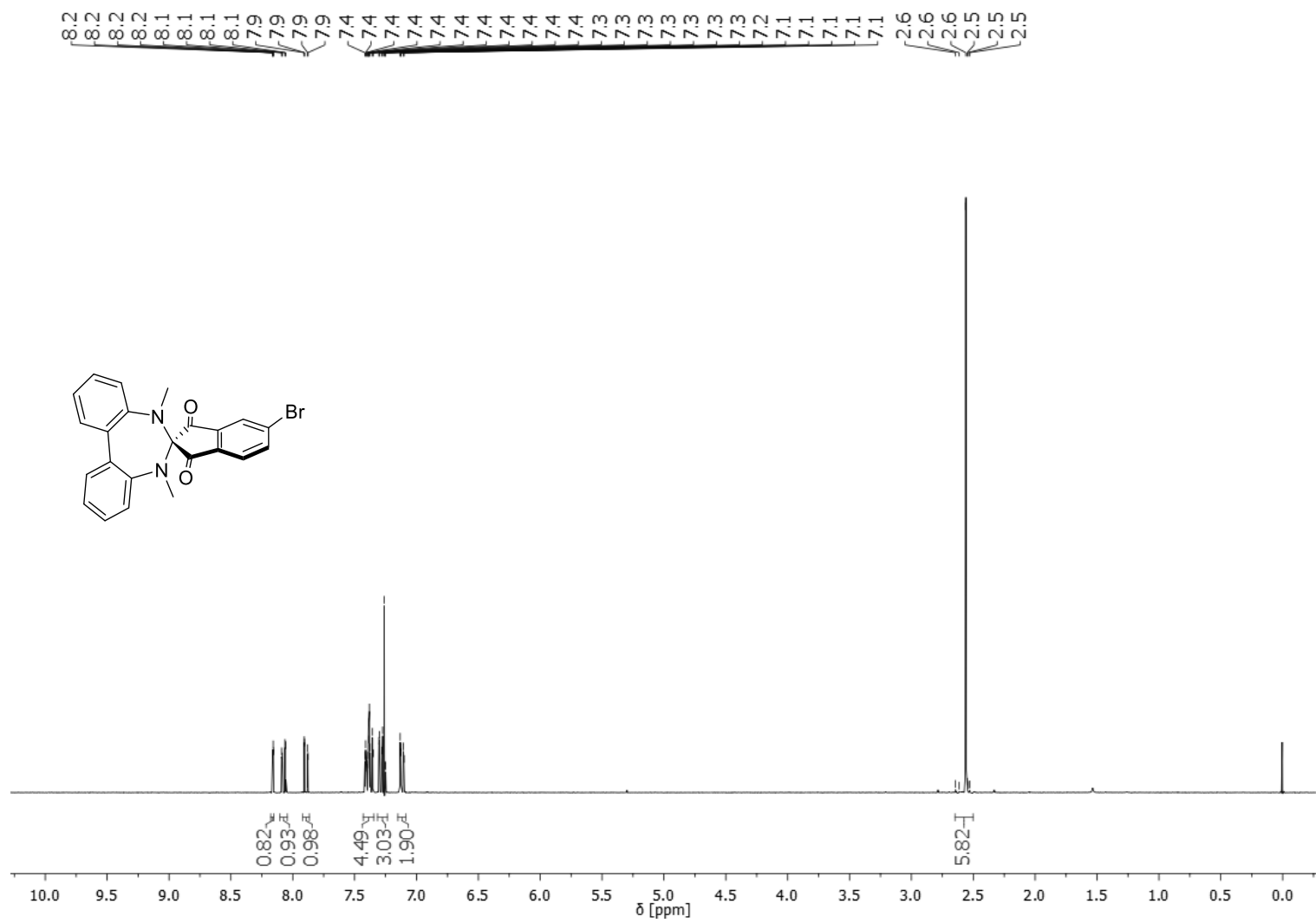


Figure S86: ¹H NMR-spectrum of **21** in CDCl₃ (300 MHz).

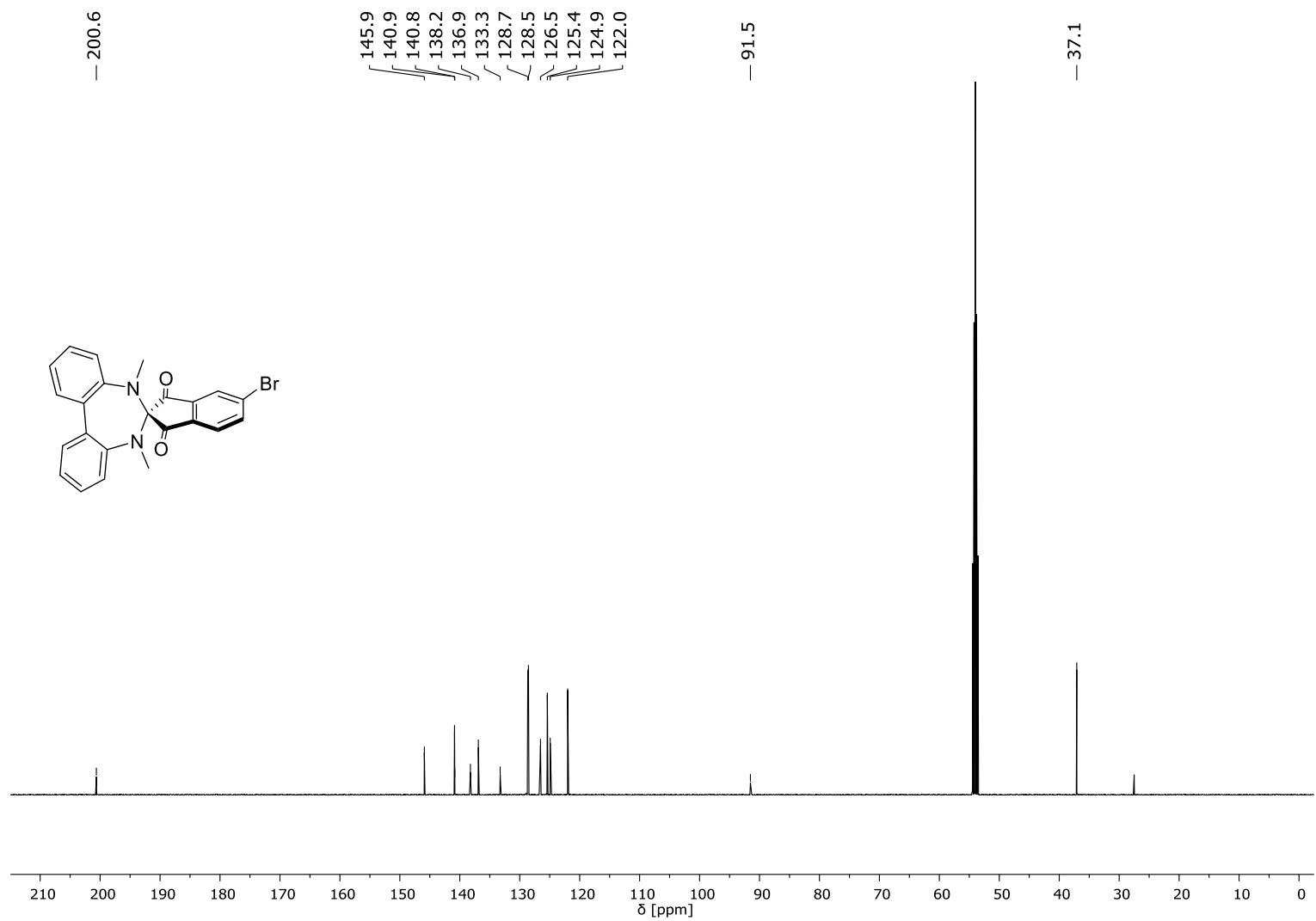


Figure S87: ^{13}C NMR-spectrum of **21** in CD_2Cl_2 (126 MHz).

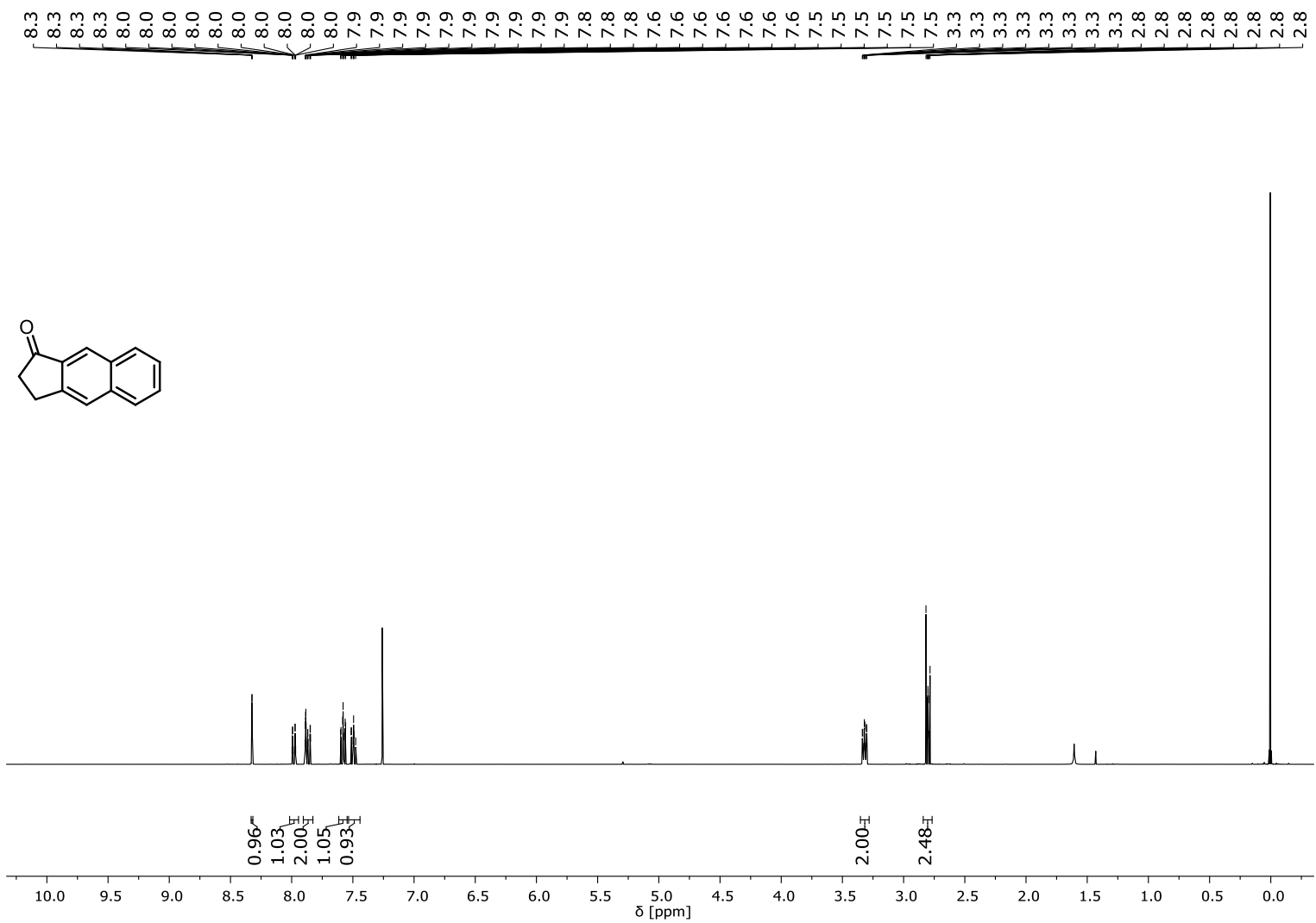


Figure S88: ¹H NMR-spectrum of **25** in CDCl₃ (400 MHz).

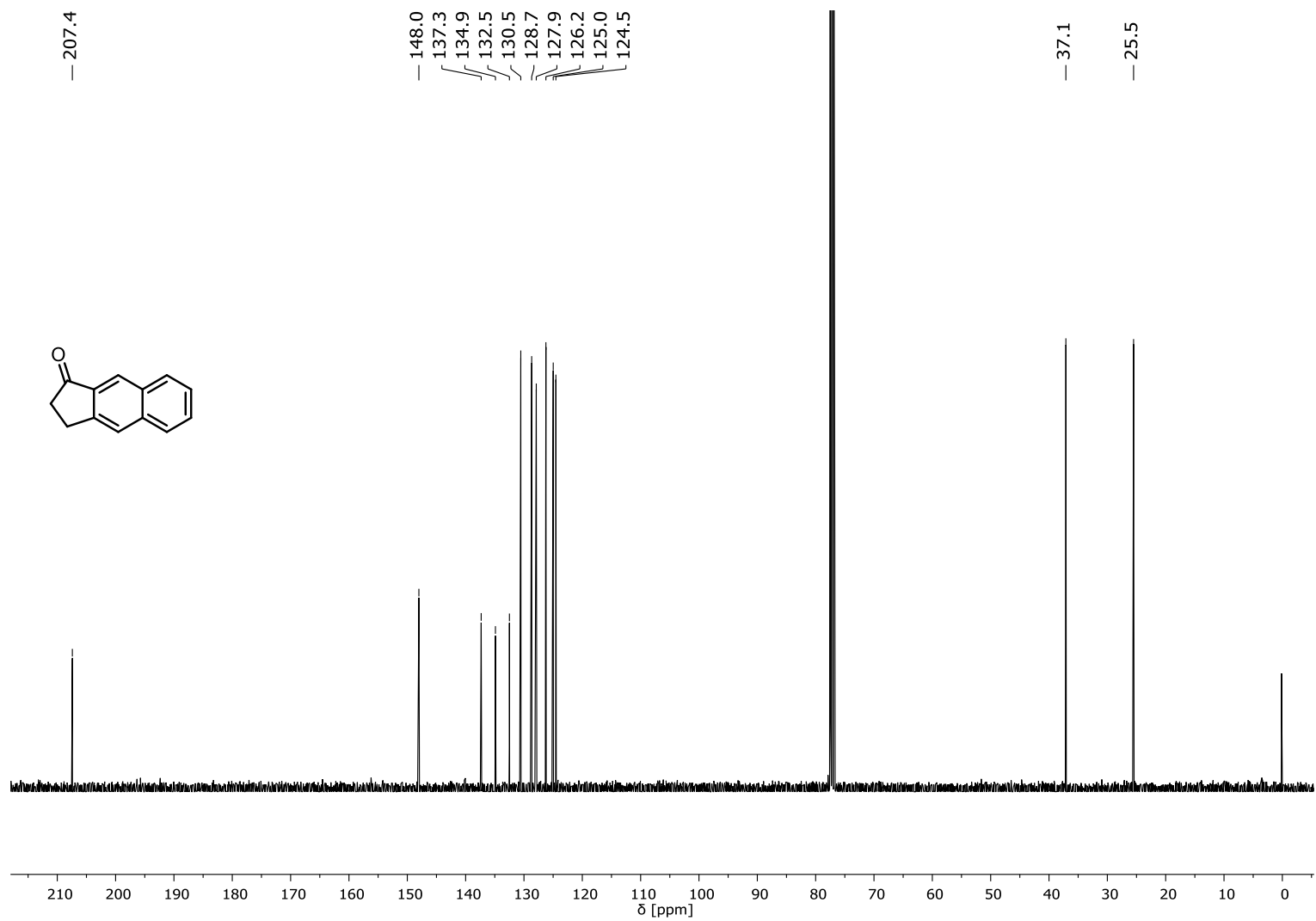


Figure S89: ^{13}C NMR-spectrum of **25** in CDCl_3 (101 MHz).

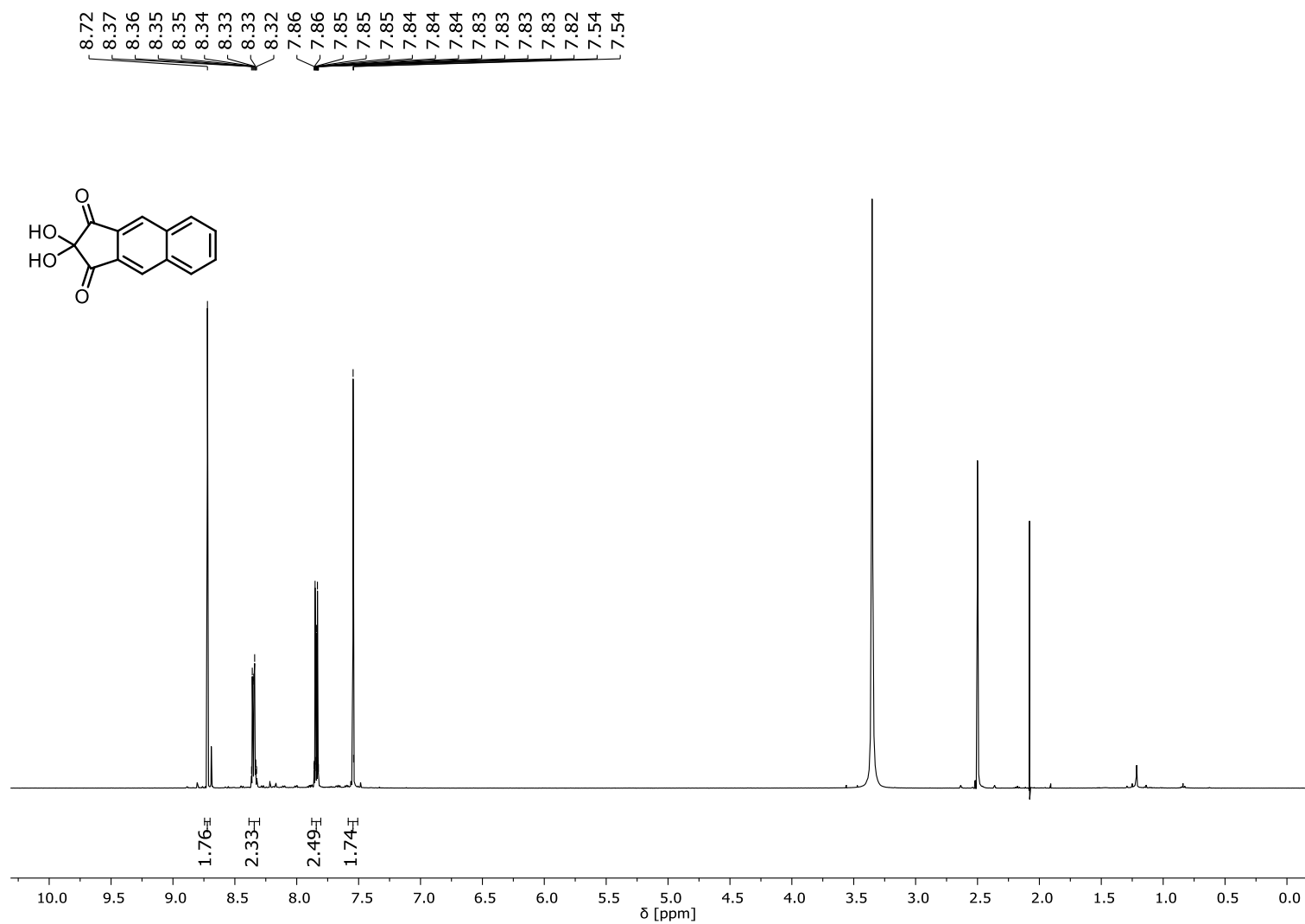


Figure S90: ¹H NMR-spectrum of **26** in DMSO-*d*₆ (500 MHz).

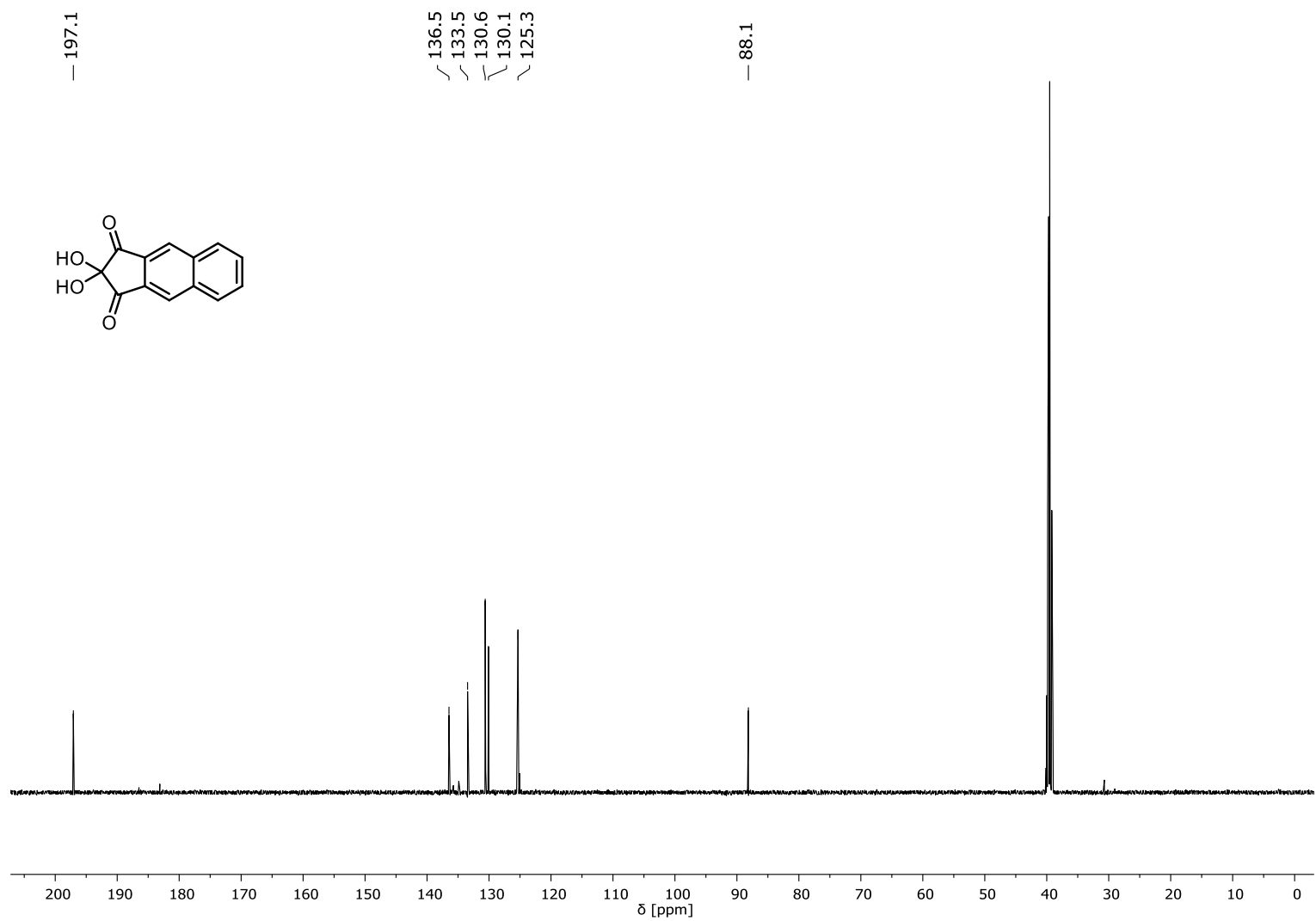


Figure S91: ^{13}C NMR-spectrum of **26** in $\text{DMSO-}d_6$ (126 MHz).

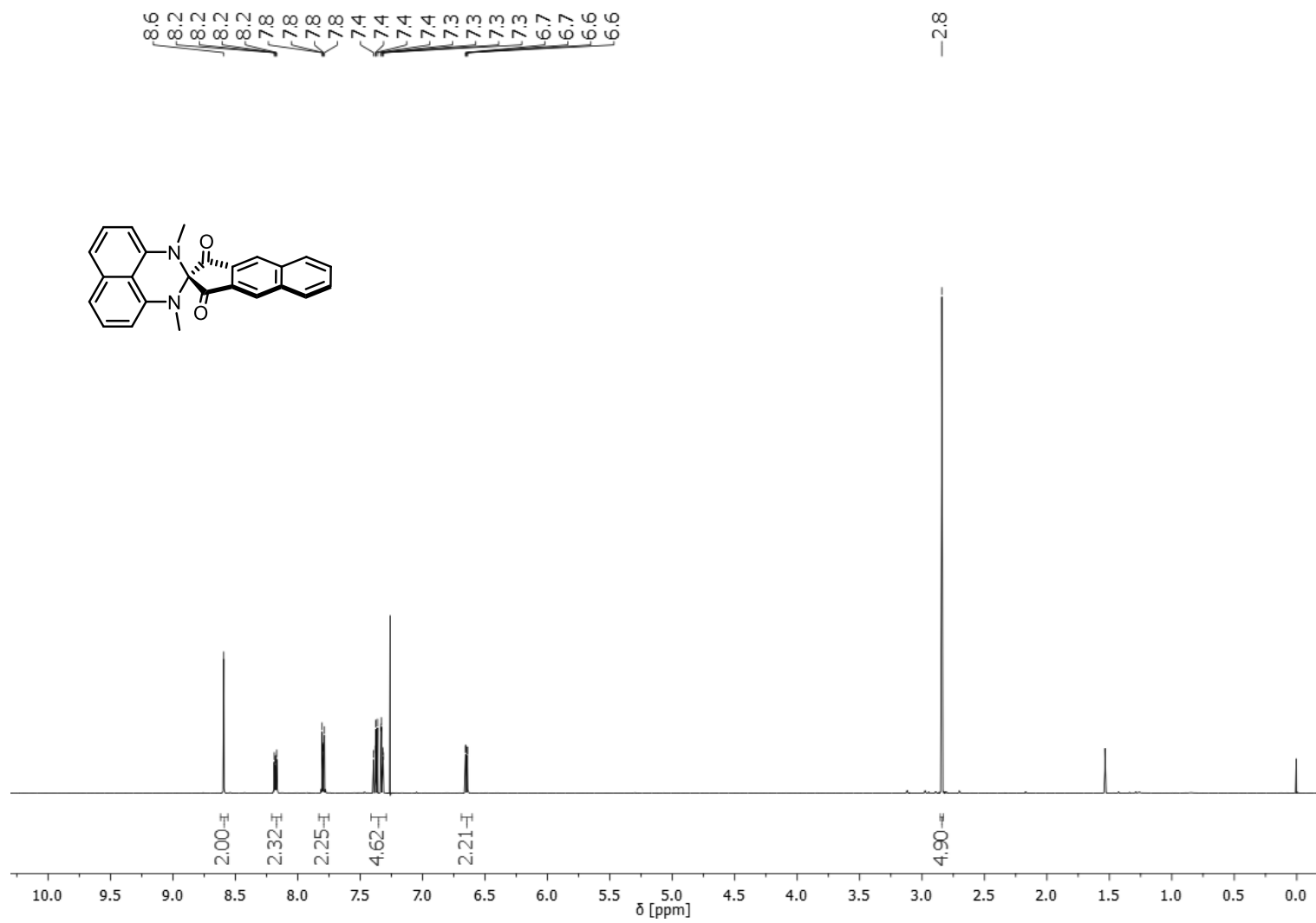


Figure S92: ¹H NMR-spectrum of **16** in CDCl₃ (500 MHz).

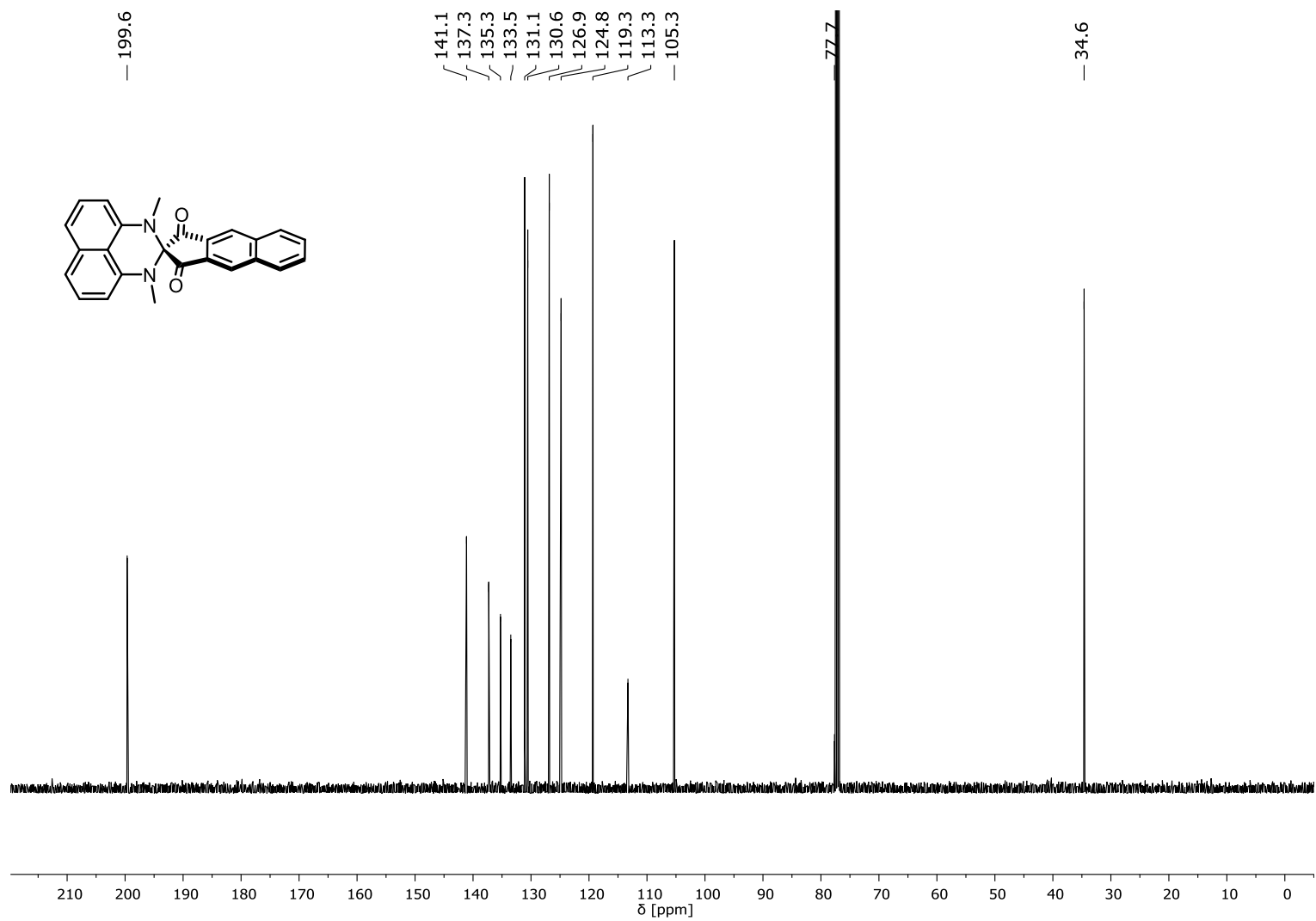


Figure S93: ^{13}C NMR-spectrum of **16** in CDCl_3 (126 MHz).

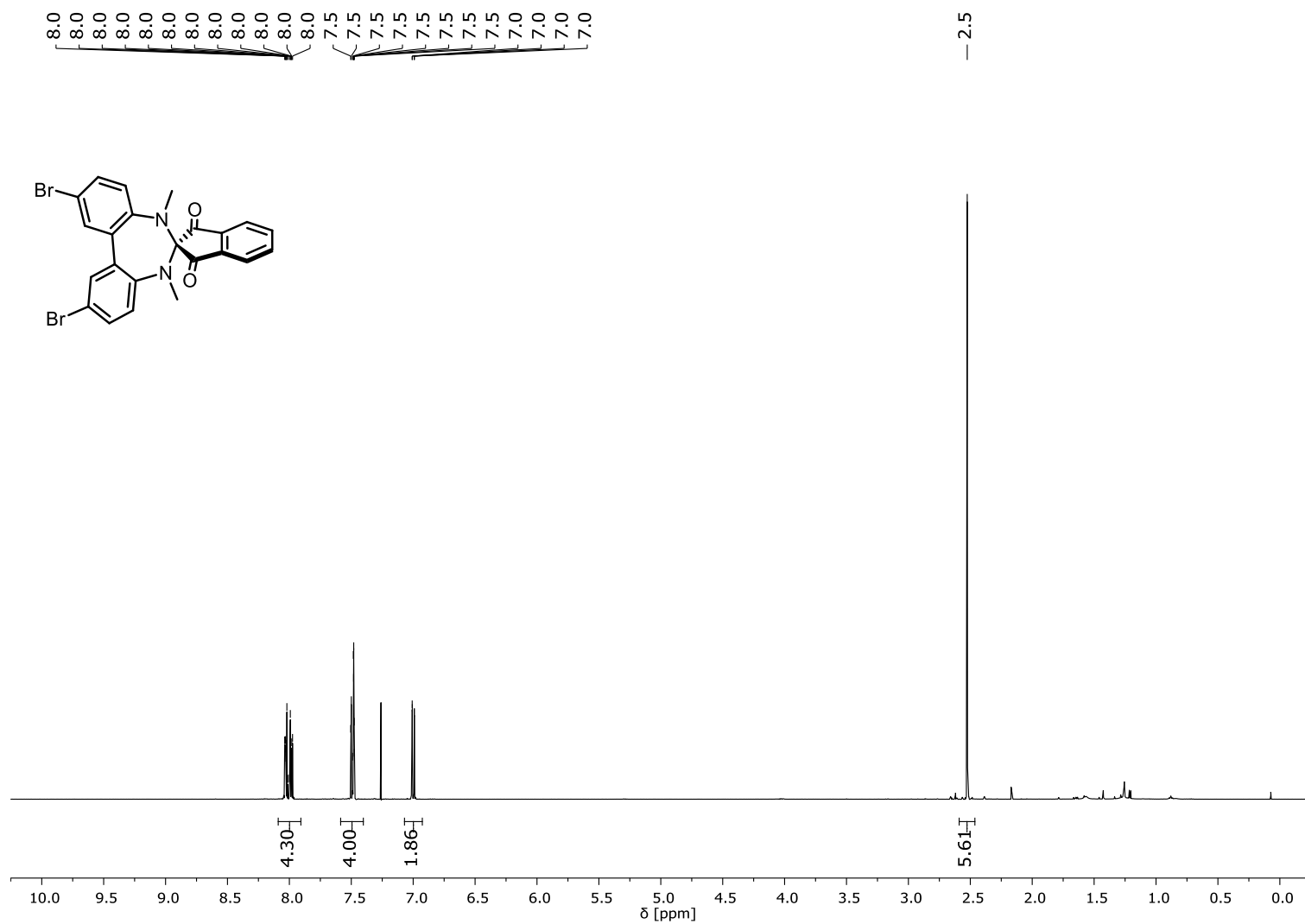


Figure S94: ¹H NMR-spectrum of **27** in CDCl₃ (500 MHz).

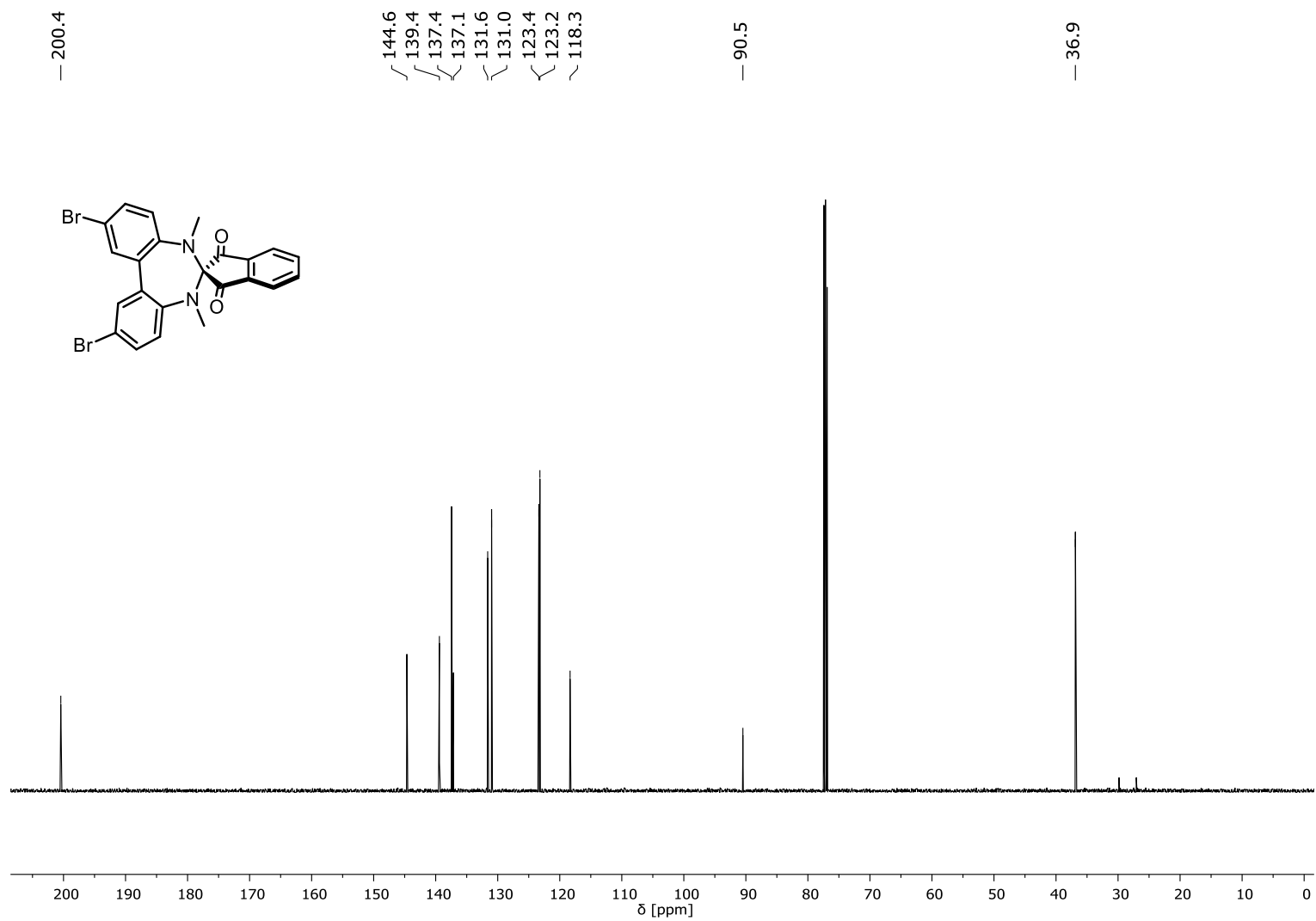


Figure S95: ^{13}C NMR-spectrum of **27** in CDCl_3 (126 MHz).

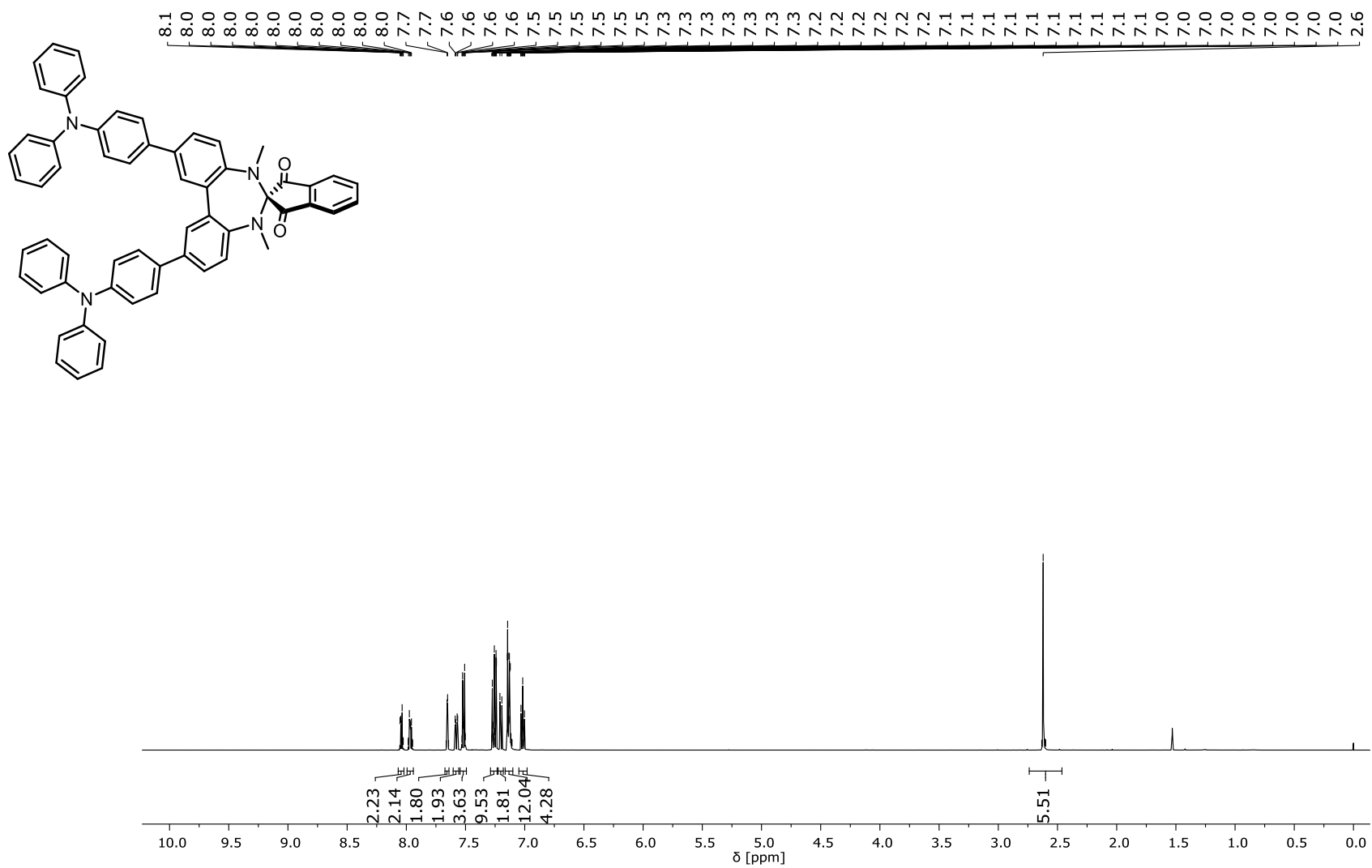


Figure S96: ¹H NMR-spectrum of **29** in CDCl₃ (500 MHz).

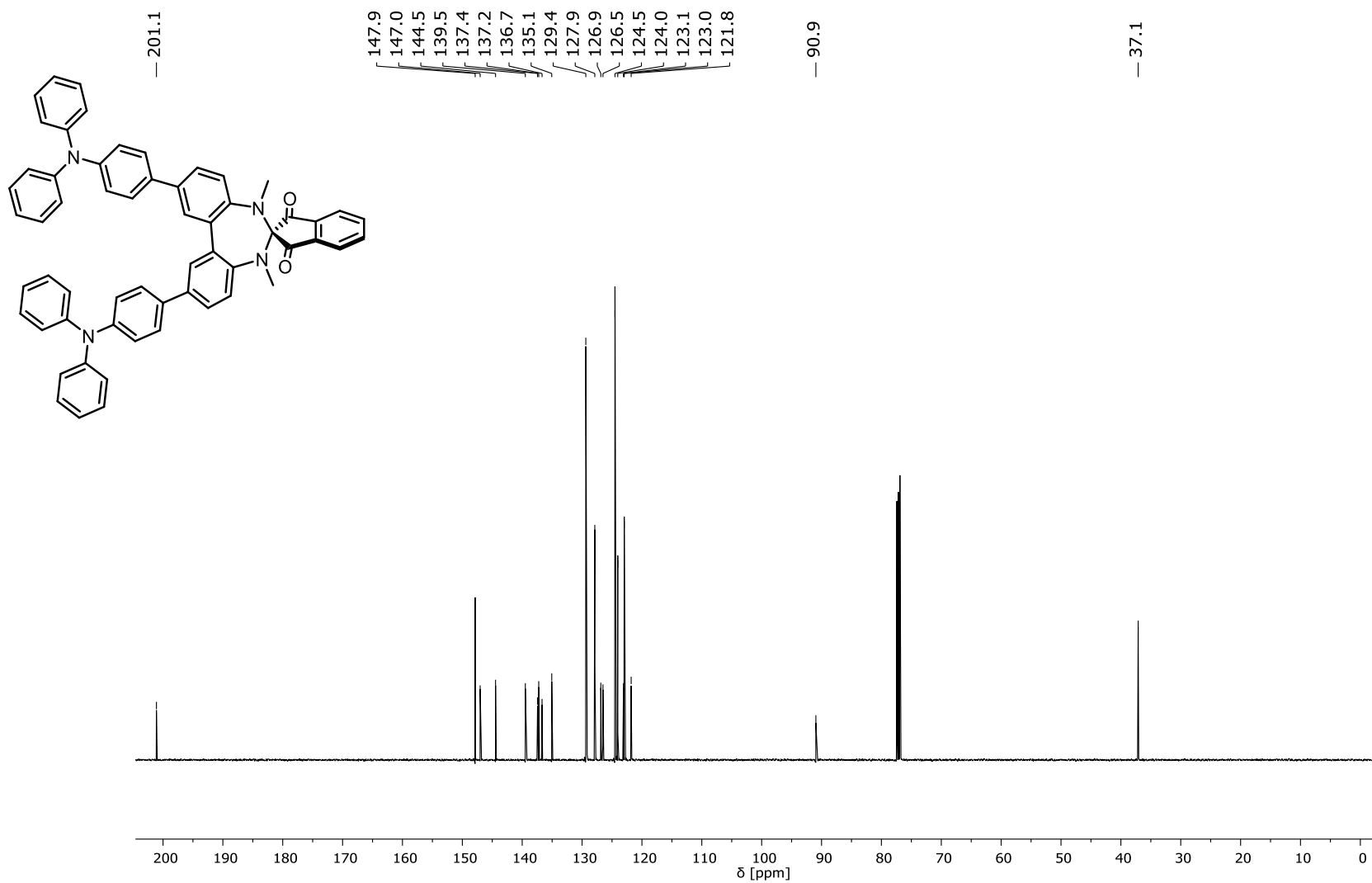


Figure S97: ¹³C NMR-spectrum of **29** in CDCl₃ (126 MHz).

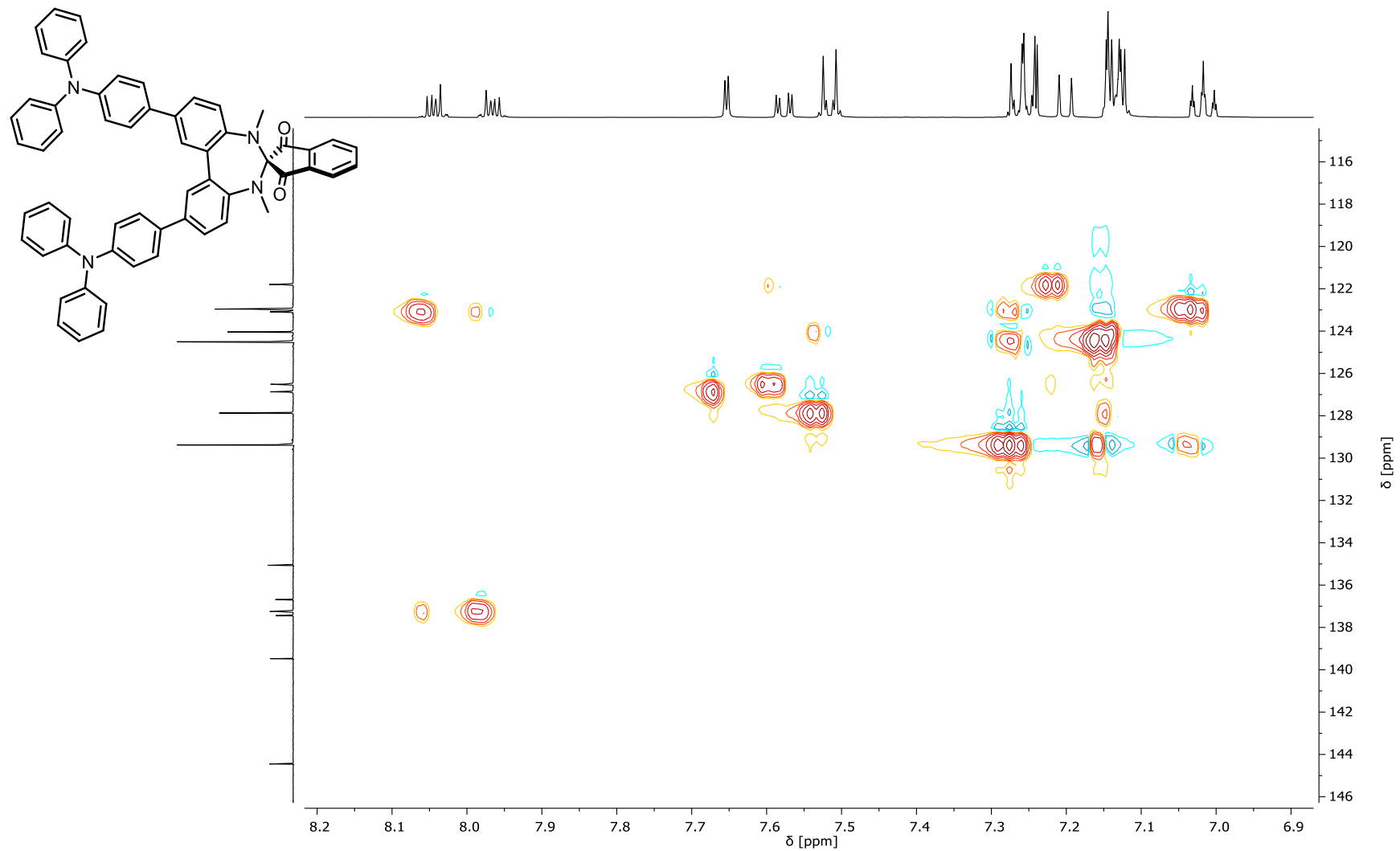


Figure S98: HSQC-spectrum of **29** in CDCl₃ (500 MHz).

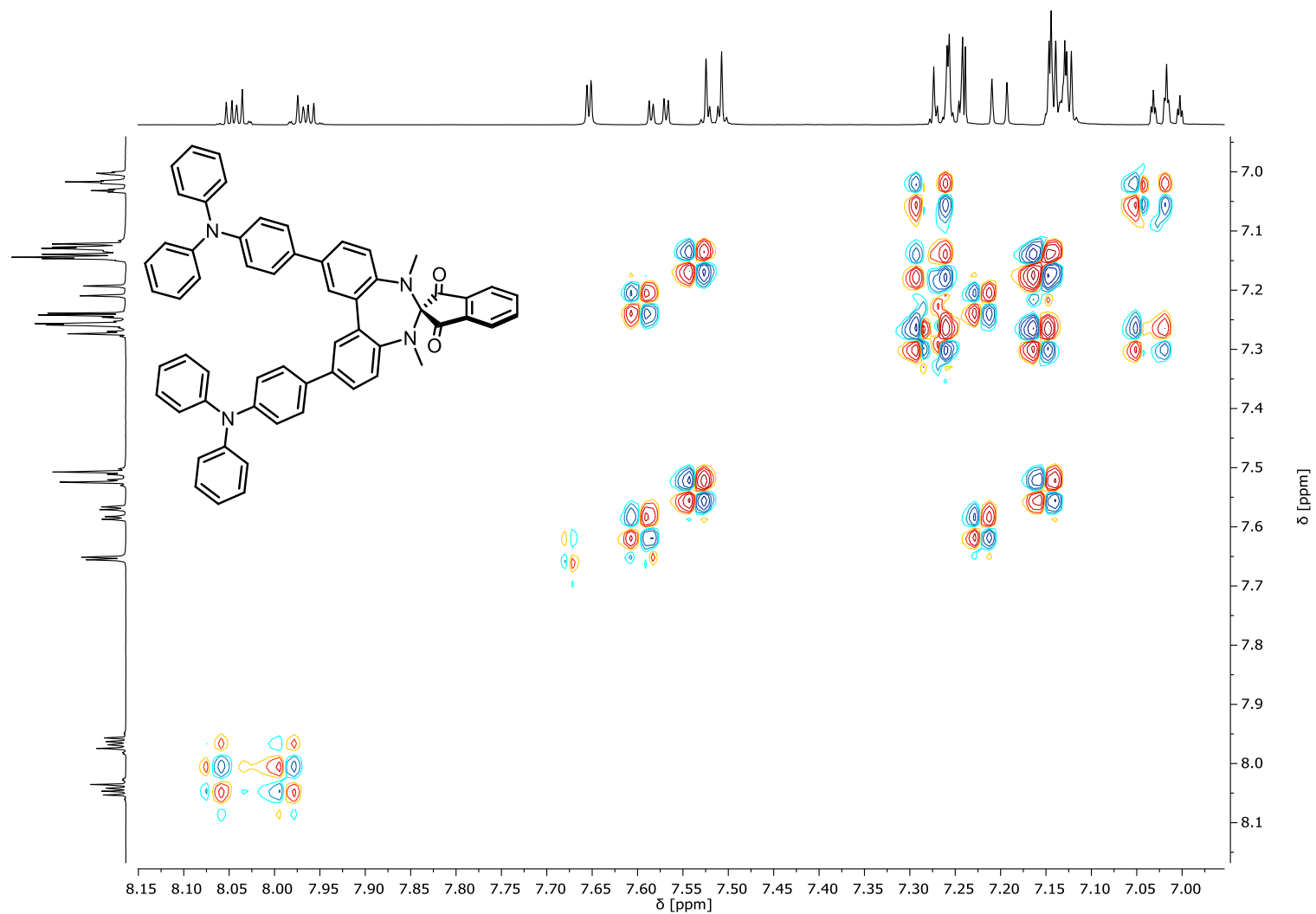


Figure S99: DQF-COSY-spectrum of **29** in CDCl_3 (500/126 MHz).

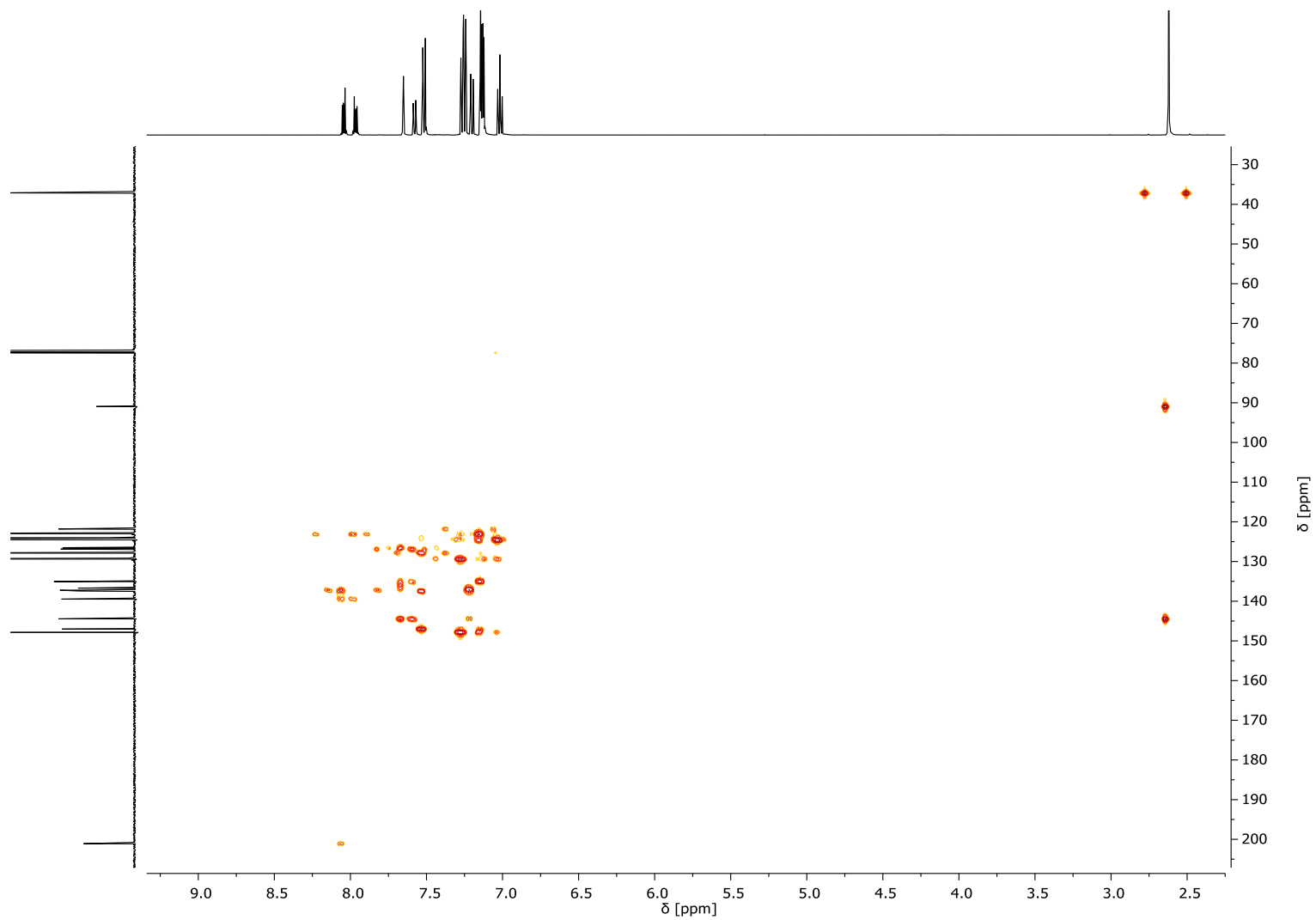


Figure S100: HMBC-spectrum of **29** in CDCl₃ (500/126 MHz).

11. References

- [1] P. Maslak, A. Chopra, C. R. Moylan, R. Wortmann, S. Lebus, A. L. Rheingold, G. P. A. Yap, *J. Am. Chem. Soc.* **1996**, *118*, 1471–1481.
- [2] G. Iannucci, A. Iuliano, *J. Organomet. Chem.* **2016**, *806*, 88–94.
- [3] J. C. M. Kistemaker, P. Štacko, D. Roke, A. T. Wolters, G. H. Heideman, M.-C. Chang, P. van der Meulen, J. Visser, E. Otten, B. L. Feringa, *J. Am. Chem. Soc.* **2017**, *139*, 9650–9661.
- [4] V. A. Ozeryanskii, E. A. Filatova, V. I. Sorokin, A. F. Pozharskii, *Russ. Chem. Bull.* **2001**, *50*, 846–853.
- [5] C. Marminon, A. Nacereddine, Z. Bouaziz, P. Nebois, J. Jose, M. Le Borgne, *Tetrahedron Lett.* **2015**, *56*, 1840–1842.
- [6] R. Hahn, F. Bohle, W. Fang, A. Walther, S. Grimme, B. Esser, *J. Am. Chem. Soc.* **2018**, *140*, 17932–17944.
- [7] S. N. Sanders, E. Kumarasamy, A. B. Pun, M. L. Steigerwald, M. Y. Sfeir, L. M. Campos, *Angew. Chemie Int. Ed.* **2016**, *55*, 3373–3377.
- [8] O. V. Dolomanov, L. J. Bourhis, R. J. Gildea, J. A. K. Howard, H. Puschmann, *J. Appl. Crystallogr.* **2009**, *42*, 339–341.
- [9] G. M. Sheldrick, *Acta Crystallogr. Sect. A Found. Adv.* **2015**, *71*, 3–8.
- [10] G. M. Sheldrick, *Acta Crystallogr. Sect. C Struct. Chem.* **2015**, *71*, 3–8.
- [11] TURBOMOLE V6.2 2010, 1989-2007 Forschungszentrum Karlsruhe GmbH, since 2007; available from TURBOMOLE GmbH, <http://www.turbomole.com>., **n.d.**
- [12] K. Eichkorn, O. Treutler, H. Öhm, M. Häser, R. Ahlrichs, *Chem. Phys. Lett.* **1995**, *240*, 283–290.
- [13] F. Weigend, *Phys. Chem. Chem. Phys.* **2006**, *8*, 1057.
- [14] S. Grimme, J. Antony, S. Ehrlich, H. Krieg, *J. Chem. Phys.* **2010**, *132*, 154104.
- [15] E. R. Johnson, A. D. Becke, *J. Chem. Phys.* **2006**, *124*, 174104.

- [16] S. Grimme, J. G. Brandenburg, C. Bannwarth, A. Hansen, *J. Chem. Phys.* **2015**, *143*, 054107.
- [17] A. Schäfer, C. Huber, R. Ahlrichs, *J. Chem. Phys.* **1994**, *100*, 5829–5835.